보건학박사학위논문

Exposure Assessment of Nanoparticles at the Workplaces -Characterization, Statistical Analysis and Instrument Comparison

사업장에서의 나노입자 특성규명 및 노출평가

2015년 8월

서울대학교 대학원

보건학과 환경보건학 전공

함 승 헌

Abstract

Seunghon Ham

Department of Public Health (Environmental Health)

Graduate School of Public Health

Seoul National University

Since the 1990s, nanotechnology (NT) has rapidly grown in Korea, which has become one of the world's leading nations for the technology. Despite the bright outlook for the future of NT, concern remains human exposure to engineered nanoparticles may lead to significant adverse health effects. Workers could be intentionally and unintentionally exposed to engineered nanoparticles during routine work or during research and development. In 2008, the number of researchers and workers involved in NT was estimated to be about 400,000 worldwide. This number is expected to grow to six million by 2020. Therefore, nanoparticle exposure assessments are important for the protection of workers.

The purposes of the study were as follows: (1) to compare the exposure characteristics of nanoparticles produced in laboratory (LAB), engineered nanoparticles (ENP), and unintended nanoparticle emissions (UNP) in workplaces; (2) to develop an exposure assessment method using a task-based approach for ENP and UNP in workplaces; (3) to suggest possible data interpretation methods for real-time nanoparticle monitoring data by comparing statistical models, such as classical regression and first-

order autoregressive (AR(1)) and autoregressive integrated moving average (ARIMA) models, and then investigate the effect of different averaging times on autocorrelation using field data; and (4) to determine the relationships among three nanoparticle monitoring devices, i.e., scanning mobility particle sizer (SMPS), condensation particle counter (CPC), and surface area monitor (SAM), and to compare two widely used SMPSs for harmonization.

In Chapter 1, the concentrations and characteristics of nanoparticle exposure by size and type of nanoparticles for ENP and UNP are reported. The concentration and characteristics of nanoparticles at nine workplaces where the three types of workplace (LAB, ENP, and UNP) are produced were compared using real-time monitoring instruments (SMPS, CPC, and SAM) and a gravimetric method. The concentrations of UNP were higher than those of LAB and ENP for all of the metrics measured. Geometric means and geometric standard deviations of LAB, ENP, and UNP for the total number concentration measured using a SMPS were 8,458 (1.41), 19,612 (2.18), and 84,172 (2.80) particles/cm^3, respectively. The concentrations of LAB, ENP, and UNP measured by a CPC were 6,143 (1.45), 11,955 (2.42), and 38,886 (2.61) particles/cm^3, respectively. The surface area concentrations of LAB, ENP, and UNP were 32.79 (1.46), 93.68 (2.60), and 358.41 (2.74) $\mu m^2/cm^3$, respectively. The exposure characteristics and size distributions differed among workplaces. Some tasks or processes producing LAB, such as sonication and reaction (LAB-B), produced higher concentrations than those found at workplaces producing ENP or UNP. Local exhaust ventilation (LEV) could be an effective control measure for ENP. Therefore, different exposure characteristics for LAB,

ENP, and UNP were observed, and different risk management strategies were required.

In Chapter 2, an exposure assessment method based on a task-based approach is presented. Unlike time-weighted average (TWA) concentrations collected during shift sampling, measurement of activities of workers who perform a task that is believed to cause concentration fluctuations can precisely reflect actual exposure variations. Most of the NT industry has used batch processing rather than continuous production, making it difficult to generalize. Task-based exposure assessment is potentially appropriate for the ENP manufacturing industry because of the use of irregular processes in the workplace. Two ENP and two UNP workplaces were selected for exposure assessments. Real-time devices were used to characterize the concentration profiles and size distributions of airborne nanoparticles. Filter-based sampling was performed to measure time-weighted average (TWA) concentrations, and using an electron microscope. Workplace tasks were recorded by researchers to determine the concentration profiles associated with particular tasks. This study demonstrated that exposure profiles differed greatly in terms of concentrations and size distributions according to the tasks. The size distributions of emissions produced during tasks were different from those during periods with no activity and from the background. The airborne concentration profiles of the nanoparticles varied according to both the type of workplace and the concentration metrics. The results of this study suggest that a task-based exposure assessment could provide useful information regarding the exposure profiles of nanoparticles and can therefore be used as an exposure assessment tool.

In Chapter 3, appropriate statistical models for autocorrelation were compared. Real-time monitoring is necessary for nanoparticle exposure assessment to characterize the exposure profile, but the data are autocorrelated due to the short measurement intervals. Two methods have been proposed to deal with autocorrelation in data analysis. One is a statistical approach, and the other entails changing the averaging time. This study identified possible data interpretation methods for nanoparticle monitoring data by comparing the results of statistical methods with the effect of averaging time on the reduction of the autocorrelation using field data. The classical regression model was compared with AR(1) and ARIMA. The AR(1) and ARIMA models are alternative statistical methods that remove autocorrelation effects in real-time monitoring data. Three real-time monitoring data sets were used. The first data set was for engineered nanoparticles (ENP; Fe_2O_3, Ti) measured at a LAB workplace, and the second data set was from an ENP (Cu, Ni) manufacturing facility. The third data set, for welding fumes, was for UNP. An SMPS with a 1-minute sampling interval was used to obtain the data. The results of a classical regression, the AR(1) model, and the ARIMA model with averaging times of 1, 5, and 10 minutes were compared. The classical regression model overestimated all of the tasks or processes due to autocorrelation. Of the three statistical methods, the AR(1) and ARIMA models had a similar capacity to adjust the autocorrelation of real-time nanoparticle data. Because of the non-stationary characteristics of real-time monitoring data in the field, the ARIMA model, which incorporates a differencing term (I) is more appropriate. When using the AR(1) model, transformation into a stationary form is necessary. Changing the averaging time did not influence the autocorrelation effect. The results of this study suggest that an ARIMA

model could be used to process real-time monitoring data, especially for non-stationary data, and the use of different averaging times (within 10 minutes) had no effect on the autocorrelation with a specific statistical model. Therefore an averaging time could be used based on the instrument measuring time of one cycle in the workplace, and this was flexible depending on the data interval required to capture the effects of a series of processes for occupational and environmental nanoparticle measurements.

In Chapter 4, the relationships of a portable (P)-SMPS with the CPC and SAM instruments, which are measurement devices with different metrics, were investigated, and two widely used SMPSs were compared to harmonize the measurement protocols. Nanoparticles were measured by several sampling devices. It is necessary to understand the relationship among these measurements because devices produced by different manufacturers are based on different techniques and principles. For LAB and ENP, there was a good correlation among the (P)-SMPS, CPC, and SAM. However, the correlation among (P)-SMPS, CPC, and SAM was only fair in UNP workplaces. This was partly explained by the fact that the particles were not spherical, although the calibration of the sampling instruments was performed using spherical particle; additionally, the concentration of UNP in workplaces was very high, allowing aggregates to form easily. A chain-like particle morphology was identified using the scanning electron microscope (SEM) for workplaces with UNP. The CPC or SAM instrument could be used as an alternative to an SMPS in workplaces handling ENP. In workplaces producing UNP where the concentration is high, real-time instruments should be used with caution. Electron microscope images can be used to confirm the morphology of nanoparticles.

There were significant differences between the two SMPSs. A TSI SMPS indicated a concentration about 20% higher than that produced by a Grimm SMPS in all workplaces. Several factors are responsible for these differences between the two SMPSs: 1) instabilities in the aerosol, 2) the scanning sequences, and 3) the sampling time interval. Therefore, caution is required when comparing data from different SMPSs.

In summary, the applying of different control strategies is required because the concentration profiles and characteristics were different among LAB, ENP and UNP workplaces. The nanoparticle concentrations varied depending on the tasks performed and working status (working or off-duty). Task-based exposure assessments could provide useful information regarding nanoparticle exposure profiles and could be used as nanoparticle exposure assessment tools in place of traditional full-shift measurements. For real-time monitored data, the ARIMA model is the most suitable for the analysis because it accounts for autocorrelation and the stationary nature of the data. Using the ARIMA model, averaging times of 1, 5, and 10 minutes gave almost identical results. Flexible time averaging is suggested because it can be used with a research-grade sampling device, which in this study was a full-size SMPS that had a sampling interval longer than one minute. The CPC or SAM with electron microscope imaging are suitable alternative instruments for nanoparticle exposure assessment, rather than the SMPS, which is a relatively expensive device. Caution is required when interpreting the results and comparing the exposure monitoring field data using different SMPSs.

Key words: Engineered nanoparticle, Nanoparticle exposure assessment, Unintended, Occupational health, SMPS, Autocorrelation

Student Number: 2010-30681

Table of Contents

List of Tables

List of Figures

Chapter 1. Comparison of nanoparticle exposure levels based on facility types—small-scale laboratories, large-scale manufacturing workplaces, and unintended nanoparticle-emitting workplaces

This chapter was published in Aerosol and Air Quality Research 2015

Introduction

Three types of nanoparticle source are classified as: naturally occurring (e.g., volcano ash and forest fires), unintended emission of nanoparticles (UNP) (e.g., welding, smelting, and diesel exhaust), and engineered nanoparticles (ENP) (Oberdörster *et al.,* 2005). Recently, the application of engineered nanoparticles has increased rapidly in various industries. Accordingly, the number of workers with nanotechnology is increasing, and is estimated to be approximately 2 million worldwide in 2023 (Schulte *et al.,* 2008).

Ramazzini implied at his publication ("De Morbis Artificum Diatriba" [Diseases of workers], "noxios alitus ac tenues particulas" [noxious vapors and very fine particles]) very fine particles may affect to adverse health effect to human lungs and skin penetration (Chung 1990). Based on the probable health hazards of nanoparticles and exposure concerns via inhalation and skin absorption, risk management including traditional control strategies in industrial hygiene; i.e., elimination, substitution, isolation, engineering control, administrative control, and personal equipment, have been reported. Moreover, exposure levels may differ throughout the life cycle of nanoparticles due to handling size; i.e., research, development, and production/manufacturing (Paik *et al.,* 2008; Schulte *et al.,* 2008). To implement appropriate strategies, it is important to examine the exposure level. However, data on nanoparticle exposure assessment at laboratories and ENP manufacturing workplaces are insufficient.

Workers in workplaces such as ENP manufacturing, UNP workplaces, and laboratories (LAB) are exposed to nanoparticles. For example, the exposure levels of workers at ENP manufacturing workplaces varied according to the task performed; e.g., handling, use, research, and development. Levels of UNPs such as welding fumes and diesel exhaust were reported to be high (Ham *et al.,* 2012; Lehnert *et al.,* 2012; Zimmer 2002). The exposure levels of university students and researchers in the laboratory varied according to the process type and amount of nanoparticles used during experiments (Demou *et al.,* 2009; Lehnert *et al.,* 2012).

To our knowledge, no study has compared simultaneously nanoparticle exposure at three workplace types: small-scale laboratories (LAB), engineered nanoparticle manufacturing workplaces (ENP), and unintended nanoparticle-emitting workplaces (UNP). It is important to compare the nanoparticle concentration and characteristics based on workplace type to ensure that the appropriate exposure assessments and management strategies are applied. Researchers in a laboratory could be exposed irregularly due to intermittent and short handling durations during experiments and the development process. At UNP workplaces, workers might be exposed continually during the production process due to repetition of the same task over a long period. Nanoparticle exposure to workers at ENP workplaces may be variable according to the type and amount of nanoparticle, and handling tasks and processes performed. Thus, comparison of the exposure level at LAB, ENP, and UNP is important to implement appropriate control strategies. The aims of this study were to investigate the concentrations and characteristics of nanoparticle exposure at LAB, ENP, and UNP workplaces.

Materials and Methods

Sampling Site Facility

Workplaces were classified into three types: laboratory (LAB), engineered nanoparticle (ENP) workplace, and UNP-emitting workplaces (Table 1-1). Measurements at each type of workplace were performed at three locations. Therefore, a total of nine workplaces were investigated. Three laboratories at a university were investigated. LAB-A was an earth environment laboratory, and the primary nanoparticle was Al_2O_3. Two workers performed experiments of transfer to the crucible, transfer from the crucible to a vial, and weighing. LAB-B was involved with development of new materials, with the primary nanoparticles used being Fe_2O_3 and TiO_2. Primary experiments were weighing, sonication, and reaction. Seven workers performed the experiments. LAB-C dealt with graphene for space aviation. DIP-coating processes to fabricate graphene were the primary experiments performed; together with spraying the base of the DIP coater for cleaning by five workers. A natural ventilation system and a fume hood were installed in all laboratories.

Three ENP manufacturing workplaces participated in this study. ENP-D manufactured Ti and Zn powder for cosmetic sunscreen. Reaction, dehydration, mixing, drying, and bagging were the main processes at ENP-D. The reaction was performed at 120 °C and 3 atm, and dehydration was applied at 60 °C. There was a natural ventilation system without local exhaust ventilation (LEV). The production rate at ENP-D was 10 tons for TiO_2 and 50 tons for ZnO per year. ENP-E dealt with metallic nanopowders such

as copper, nickel, and silver. Nanopowders were produced using the high-voltage pulsed-wire evaporation (PWE) method, and the main products were copper-nickel alloy and nickel nanopowders for use as additives in automobile engines. The main processes were collecting and sieving. Manufacturing equipment for PWE was isolated in a cabinet equipped with a LEV system. Production rates for Ni and Cu-Ni alloy were 100 kg per year. During the manufacturing process, the glass door was closed. Amorphous silica was manufactured at ENP-F and all processes were automated. Amorphous silica was used for abrasive materials that were applied in the chemical mechanical polishing (CMP) process in the semiconductor industry. The main process was packaging of a 10 kg bag. A total of 9,000 tons of amorphous silica was manufactured annually at ENP-F. A natural ventilation system and LEV were installed during the bagging process. Forklifts were used at ENP-D and F.

Three UNP-emitting workplaces were sampled. UNP-G manufactured heat exchangers and steel structures, such as the H-beam; arc welding and stainless steel welding were the main processes and a total of 100 workers performed welding. The main product of UNP-H was bodyframes for the back hoe and forklift. Welding and grinding were the primary processes at UNP-H. Sampling was performed at the arc welding process on the first day and at the stainless steel welding process on the second day. A total of 30 workers were active. UNP-I manufactured automobile engine parts, which involved smelting and welding. Sampling was performed during the smelting process on the first day and during the welding process on the second day. There were two shifts with 15 workers per shift, and three welders worked on one shift. A natural

ventilation system but no LEV was installed at the UNP workplaces. Forklifts were operated at all UNP workplaces.

Sampling and analysis

To determine the distribution of particle sizes, an SMPS (Nanoscan, Model 3910, TSI Inc., USA) with a detectable size range from 10 to 420 nm and a concentration range of 0 to 10^6 particles/cm^3 was used. The inlet flow rate was 0.75 L/min and the sample flow rate was 0.25 L/min. A flow check was performed in the laboratory prior to taking measurements. The sampling time of the SMPS was one minute per averaging time, and particle sizes from small to large were measured using 13 sequence channels. A cyclone was used to remove the larger particles. The particles were collected from the inlet and passed through the aerosol neutralizer using a unipolar charger. Particles were separated using a mobility diameter with a radial differential mobility analyzer (RDMA) before being counted using an isopropanol-based CPC. An external isopropyl reservoir was used.

A CPC (P-Trak Model 8525, TSI Inc., USA) was used to measure the number concentration of particles of 20 to 1,000-nm diameter with a 0.1 lpm sample flow rate. The capable concentration range was 0–500,000 particles/cm^3. Isopropyl alcohol (Sigma Aldrich, USA) was used for particle condensation, which increases the particle size to enable optical detection. One sampling averaging time was set as 1 min. The zero calibration was performed using a HEPA filter before sampling.

To measure the surface area concentration, a surface area monitor (SAM) (AeroTrak Model 9000, TSI Inc., USA) was used. One averaging time was set as 1 min. The

measuring particle size range was 10–1,000 nm and the aerosol concentration ranged from 1–10,000 μm^2 /cm^3 for the alveolar deposition method. A cyclone was installed on the inlet to prevent the entry of particles larger than 1 μm. The flow rate of the aerosol sample branch was 1.5 lpm. Zero calibration of the electrometer was performed before sampling. The sampled particles were mixed with ions in the chamber of the device and the particles were charged. The charged particles were passed along the electrometer, and the charges of the ions were measured and converted to surface area metrics.

Integrated sampling using filter media was performed for gravimetric analysis. Sampler (2 lpm, Escort ELF, MSA, USA) with an open-faced three-piece cassette was used to capture airborne nanoparticles. Sampling was performed during a full working shift. Filters were pre- and post-equilibrated before weighing in an environmentally controlled weighing room that was maintained at a temperature of 20 °C ± 1 °C and a relative humidity of 50% ± 5%. After sampling, the cassettes were sealed tightly using silicon tape and transported in a clean box. Weighing was performed using a microbalance. A transmission electron microscope (TEM) (JEM-3010, JEOL, Japan) grid (Q225-CR1, 200 mesh copper, EMS, USA) was used to analyze particle sizes and morphologies.

The height of the inlets ranged between 1.2 and 1.5 m for all measuring devices. In this study, researchers observed and recorded the TAD for all tasks during the sampling time, except during off-duty periods.

Statistical analysis

Descriptive statistics was performed to show the concentration level. Analysis of variance (ANOVA) tests were performed to compare both workplace types and individual workplaces of the same type. Scheffe's *post hoc* analysis was performed to identify significant differences between means. Data analysis was performed using SPSS (version 20.0, IBM, USA).

Results

Table 1-1 summarizes the general characteristics of workplaces investigated based on the type of workplace, emitted or source of nanoparticles, ventilation type, processes or tasks, size of workplaces, number of workers, and other possible sources. Two LABs were dealing with metal and one LAB handled graphene. Two ENPs manufactured metal nanoparticles and one ENP manufactured fumed silica. All UNP workplaces performed welding, and UNP-I also undertook smelting processes.

All LABs had natural ventilation (NV) and a fume hood. For ENP workplaces, ENP-D had NV. Local exhaust ventilation (LEV) and isolated cabinets for facilities were installed at ENP-E. NV and LEV were installed at the ENP-F workplace. Only NV was installed at the UNP workplaces in this study.

There were two, seven, and five workers at the LAB workplaces. Six to twelve workers were engaged at the ENP workplaces. One hundred, thirty, and three welders were employed at the UNP-G, UNP-H, and UNP-I workplaces, respectively. At the UNP-I workplace a total of 30 workers participated in two shifts, each of which comprised 15 workers.

Table 1-1. General characteristics of workplaces

Workplace		Emitted / source of nanoparticles	Ventilation type	Task****	Production rate	Workplace Area (m^2)	No. of workers / NP handling workers	Sampling duration
LAB*	A	Al_2O_3	NV, Fume hood	Transferred to crucible, Transferred from crucible to vial, Weighing	-	120	2	One shift + One off-duty time
	B	Fe_2O_3, TiO_2	NV, Fume hood	Weighing, Sonication, Reaction	-	78	7	One shift + One off-duty time
	C	Graphene	NV, Fume hood	Spraying air using compressor, DIP-coater	-	90	5	One shift + One off-duty time
ENP**	D	TiO_2, ZnO	NV	Reaction, Dehydration, Mixing, Drying, Bagging, Lunch	TiO2: 10 ton/year ZnO: 50 ton/year	1,400	10	Two day shifts + One night shift
	E	Cu-Ni alloy, Ni	LEV and Isolation	Collecting, Sieving, Lunch	Ni: 100 kg/year Cu-Ni: 100 kg/year	97	6	One shift
	F	Fumed silica	LEV, NV	Packaging, Meal (Lunch, dinner), Break time, Night shift - No works, Outdoor, Warehouse	9,000 ton/year	3,500	12	Two day shifts + One night shift
UNP***	G	Welding (Arc, SUS)	NV	Arc Welding, SUS Welding, Break time, Lunch	-	Arc: 10,000 SUS: 820	100	Two day shifts
	H	Welding (Arc)	NV	Arc Welding, grinding (Day shift, Night shift), Lunch	-	2,017	30	Two day shifts + One night shift
	I	Smelting process, Welding (Arc)	NV	Smelting, Welding, Break time, Lunch	-	11,000	Smelting: 15/shift * 2 Welding: 3	Two day shifts + One night shift

* Laboratory; ** ENP: Engineered nanoparticle manufacturing workplace; *** UNP: Unintended nanoparticle-emitting workplace
**** Contextual information such as meal (lunch, dinner) time, break time, no working, outdoor, and warehouse are not tasks.

Table 1-2 shows descriptive statistics of workplaces measured using SMPS, CPC, SAM, and gravimetric sampling. In addition, it shows the concentration levels among groups (LAB, ENP, and UNP) and homogeneous subsets among workplaces.

The geometric mean for LAB was lower than those of ENP and UNP workplaces for all metrics. UNP workplaces were highest concentration among the workplaces. Table 1-2 shows the differences in nanoparticle exposure levels among LAB, ENP, and UNP workplaces. The total number concentrations, number concentrations below 100 nm, CPC, and SAM differed significantly among LAB, ENP, and UNP workplaces ($p<0.01$).

Homogenous workplaces in terms of exposure level were observed (Table 1-3). For example, LAB-A, LAB-B, LAB-C, ENP-E, and ENP-F showed similar low exposure levels in terms of the total number concentration, particles greater than 100 nm in diameter, and SAM ($p<0.01$). The concentrations of particles less than or equal to 100 nm in diameter were similar among LAB-A, LAB-B, and LAB-C, and ENP-E and ENP-F ($p<0.01$). LAB-A, LAB-B, and ENP-E were categorized as homogeneous in terms of number concentration measured based on CPC ($p<0.01$).

Exposure levels within UNP workplaces varied markedly compared to the LAB and ENP workplaces. GSD of UNP ranged from 2.61 to 3.23, while it was less than 1.49 in LAB workplaces and 2.00-2.60 in ENP workplaces, regardless of the exposure metric. In addition, UNP workplaces were classified as non-homogenous with other workplaces. For example, the exposure level at each UNP workplace (A, B, and C) was non-homogenous in terms of the total number concentration and surface area (SAM).

By gravimetric sampling, mass concentration at LAB workplaces was low (mean; 0.025 mg/m^3, range; 0.020-0.028 mg/m^3), followed by (in order): ENP workplaces (mean; 0.122 mg/m^3, range; 0.031-0.120 mg/m^3) and UNP workplaces (mean; 1.122 mg/m^3, range; 0.146-2.834 mg/m^3).

Table 1-2. Descriptive statistics of workplaces measured using SMPS, CPC, SAM, and gravimetric sampling

Workplace		GM (GSD) [5th-95th percentile]					Gravimetric Sample (mg/m^3)
		SMPS ($particles/cm^3$)			CPC ($particles/cm^3$)	SAM ($\mu m^2/cm^3$)	
		Total number concentration	≤ 100 nm	> 100 nm			
LAB	A (N=1,727)	6,998 (1.30) [4,777-10,704]	4,549 (1.39) [2,756-7,834]	2,385 (1.23) [1,695-3,258]	5,221 (1.39) [3,477-9,849]	42.33 (1.27) [28.65-62.20]	0.020
	B (N=1,625)	8,351 (1.85) [3,062-20,735]	6,423 (1.86) [2,238-15,229]	1,806 (2.15) [570-6,054]	8,808 (1.58) [4,444-18,908]	33.71 (3.13) [4.20-164.50]	0.028
	C (N=399)	9,652 (1.37) [4,725-15,442]	6,733 (1.47) [2,691-11,568]	2,866 (1.20) [2,077-4,024]	-	30.07 (1.43) [16.42-50.26]	0.026
LAB-Sub*		**8,458 (1.41) [3,695-16,668]**	**5,879 (1.49) [2,600-13,328]**	**2,521 (1.30) [665-4,196]**	**6,143 (1.45) [3,613-16,209]**	**32.79 (1.46) [7.94-98.51]**	**0.025**
ENP	D (N=1,200)	22,107 (2.08) [6,520-62,619]	16,902 (2.22) [4,537-49,618]	4,498 (1.86) [1,543-11,206]	15,456 (2.14) [4,584-50,502]	-	0.120 0.031 0.023
	E (N=413)	11,394 (1.22) [8,232-14,814]	9,516 (1.23) [6,707-12,638]	1,864 (1.21) [1,373-2,474]	7,348 (1.25) [4,988-11,307]	37.06 (1.24) [25.13-50.42]	0.093
	F (N=1,851)	10,572 (2.12) [4,953-45,717]	6,885 (2.26) [2,331-31,072]	3,373 (2.04) [1,373-15,289]	7,173 (2.15) [3,201-34,126]	83.33 (2.12) [23.05-261.36]	0.345
ENP-Sub*		**19,612 (2.18) [5,152-54,428]**	**14,969 (2.18) [3,047-43,294]**	**4,643 (2.00) [1,421-12,089]**	**11,955 (2.42) [3,575-58,153]**	**93.68 (2.60) [24.57-549.09]**	**0.122**
UNP	G (N=812)	33,958 (3.08) [3,633-153,302]	22,744 (2.82) [2,730-90,512]	7,035 (4.73) [772-80,077]	19,838 (2.71) [2,443-67,427]	179.87 (3.21) [25.93-1,148.85]	0.146
	H (N=1,867)	88,416 (2.60) [16,693-339,069]	56,770 (2.64) [12,041-266,503]	29,049 (2.66) [4,562-101,145]	44,322 (2.63) [6,728-144,979]	481.83 (2.80) [65.34-1,689.77]	0.423
	I (N=1,875)	119,908 (2.24) [39,741-554,124]	102,063 (2.39) [32,550-493,494]	13,791 (2.28) [4,693-59,397]	50,826 (1.93) [12,420-131,653]	356.71 (2.01) [120.01-1,207.64]	1.085 2.834
UNP-Sub*		**84,172 (2.80) [14,249-369,765]**	**61,167 (2.94) [10,667-315,822]**	**16,539 (3.23) [2059-91,790]**	**38,886 (2.61) [6,039-134,751]**	**358.41 (2.74) [61.37-1,514.03]**	**1.122**

* ***Significant difference between groups at $p < 0.01$***

Table 1-3. Homogeneous subset by post hoc test for workplaces

Workplace		**Homogeneous Subset *Post hoc* test *(p < 0.01)*** SMPS				
		SMPS			**CPC**	**SAM**
		Total number concentration	**≤ 100 nm**	**> 100 nm**		
LAB	**A**	1	1	1	1	1
	B	1	1	1	1 2	1
	C	1	1	1	- - - - -	1
ENP	**D**	2	2	1	3	- - - - -
	E	1 2	1	1	1	1 2
	F	1 2	1	1	2	2
UNP	**G**	3	2	2	4	3
	H	4	3	3	5	4
	I	5	4	2	5	5

Note: same number refers the same homogenous group

The total number concentrations by task or process for each workplace as determined using SMPS are shown in Figure 1-1 for LAB (a), ENP (b), and UNP (c). The concentrations varied according to the task or process. In general, tasks such as welding or smelting in UNP workplaces emitted a higher concentration of nanoparticles compared to the LAB and ENP workplaces. Although the geometric mean concentration in LAB was lower than those at ENP and UNP workplaces (Table 1-2), some tasks—such as sonication and reactions at LAB-B, spraying, and DIP-coating at LAB-C—resulted in high levels of exposure.

Background (BG) concentration as a continuous and stable period at each workplace was selected to compare processes and tasks with the lowest concentration during measurement. Compared to the BG, processes and tasks were higher. In addition, BG levels differed among the workplaces. Unlike LAB and ENP workplaces, the concentrations during a break or lunch at UNP workplaces were relatively high because tasks such as welding or smelting emitted a high concentration of particles, and NV in the absence of LEV did not result in exhausting of particles.

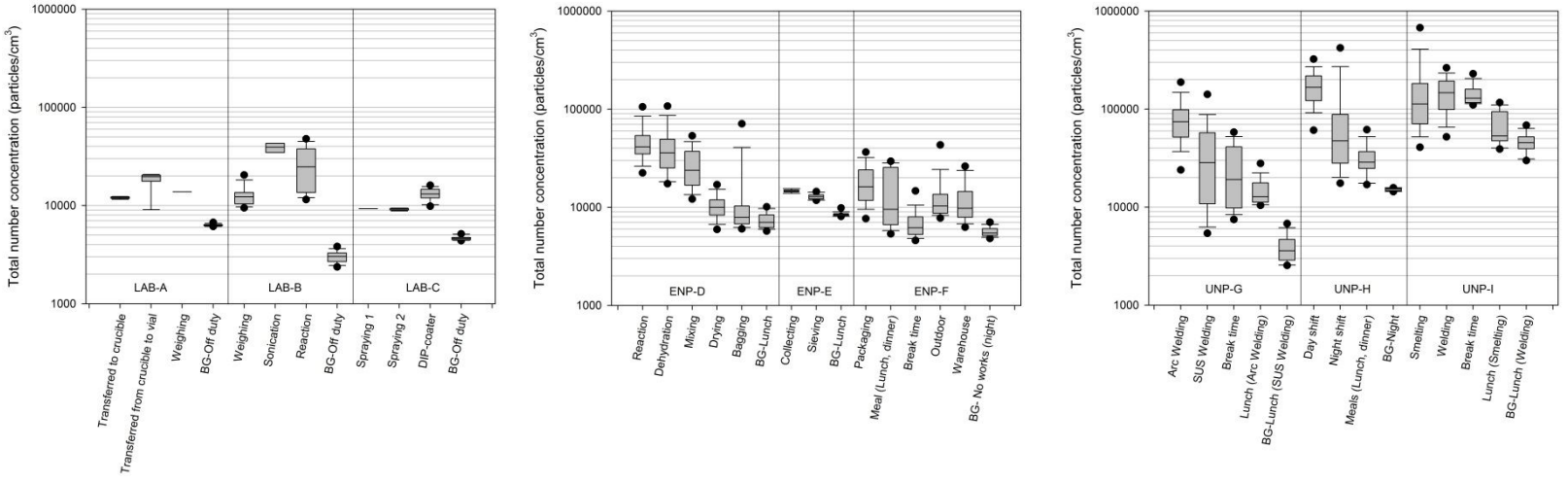

(a) (b) (c)

Figure 1-1. Boxplot of total number concentrations based on the type of workplace. (a) LABs, (b) ENPs, and (c) UNPs. BG is the background concentration for each workplace and was selected as continuous and stable time to compare with processes and tasks with the lowest concentrations during measurement. Upper and lower whiskers represent the 5th and 95th percentiles, respectively. The boxes show the 25th and 75th percentiles. The median is indicated by the solid line inside the box.

Figure 1-2 shows the nanoparticle concentration based on size distribution at the workplaces. Figure 1-2 (a), (b), and (c) show the concentrations at LAB. The majority of concentrations at LAB did not exceed 4,000 particles/cm^3 for each size channel. However, sonication and reaction processes at LAB-B were associated with concentrations of over 6,000 particles/cm^3 of ~100-nm diameter (Figure 1-2 (b)). Size distributions for ENP workplaces are shown in Figure 1-2 (d), (e), and (f). The dehydration process at ENP-D emitted over 6,000 particles/cm^3 of 20 to 50-nm diameter. In addition, the reaction and mixing process at ENP-D emitted slightly over 4,000 particles/cm^3 (Figure 1-2 (d)).

UNP workplaces showed that emissions of over 10,000 particles/cm^3 during major processes such as welding and smelting (excluding stainless steel welding) at UNP-G (Figure 1-2 (g)). Size distributions and number concentrations varied widely among workplaces. The majority of processes—such as transferring from a crucible to a vial at LAB-A, dehydration process for ENP-D, and the smelting process at UNP-I—showed a bimodal distribution (Figure 1-2).

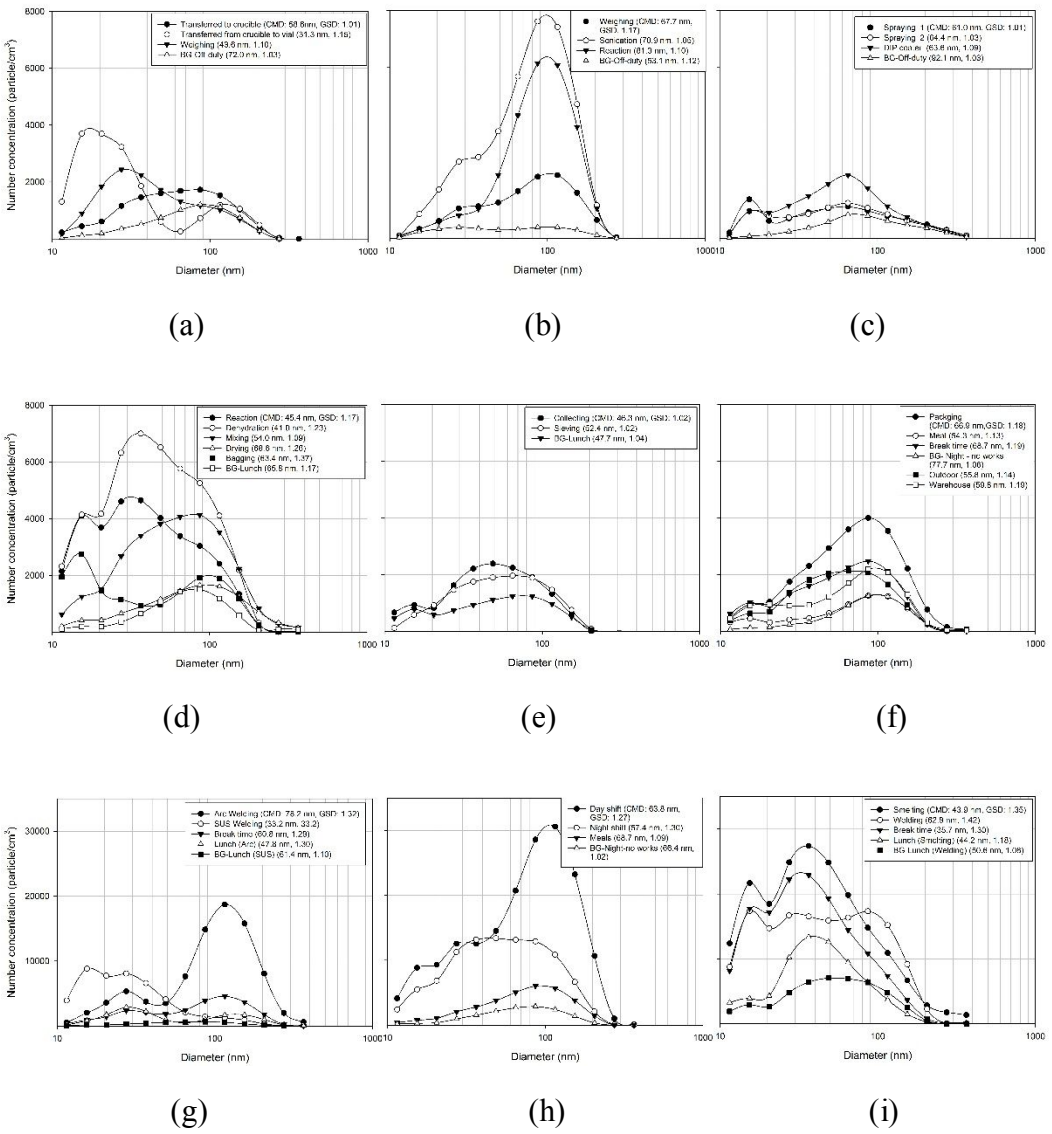

Figure 1-2. Size distribution at a nanometer scale based on the concentration in nine workplaces categorized into three types. LAB - (a) A, (b) B, (c) C, ENP - (d) D, (e) E, (f) F, and UNP - (g) G, (h) H, (i) I.

Figure 1-3 shows the geometric mean of total number concentration (particle/cm^3) measured using SMPS, together with the percentage of particles of less and greater than 100 nm diameter. The percentage of nanoparticles less than or equal to 100-nm diameter was over 65% at all workplaces, regardless of type of workplace.

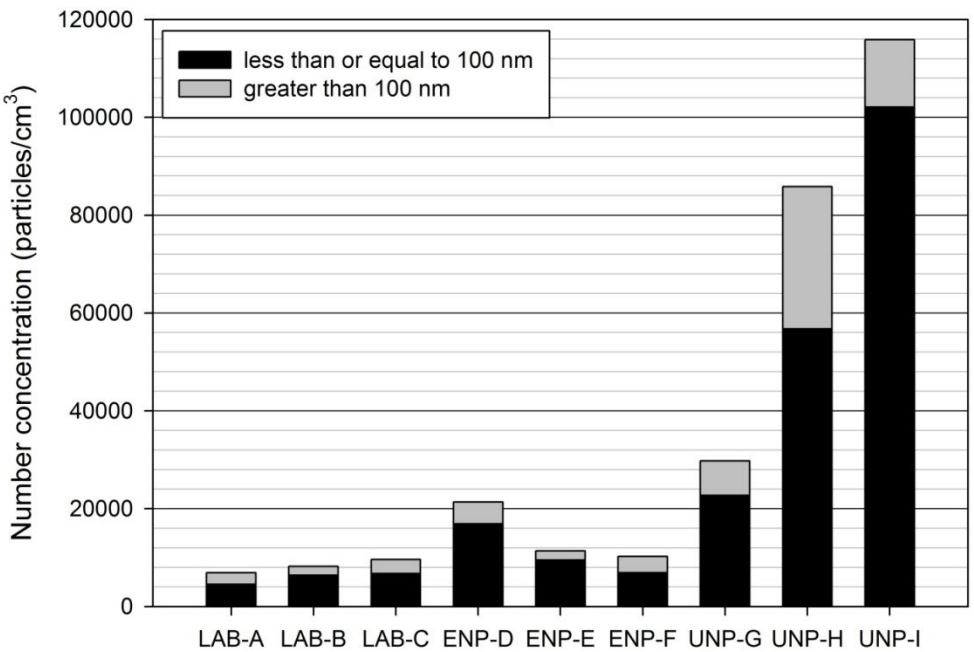

Figure 1-3. Nanoparticle (less than or equal to 100 nm) fraction (given as a percentage of total number concentration) and concentration as measured by SMPS for all workplaces.

Figure 1-4 shows TEM images of particles collected, including the primary particle size, shape, and agglomeration of particles. Manufactured primary particles at ENP-D were about 100 nm (a) in diameter. The primary particle size at ENP-F was ~7–40 nm, and those particles were agglomerated (b). At UNP-G, chain-like particles were detected (c) and (d).

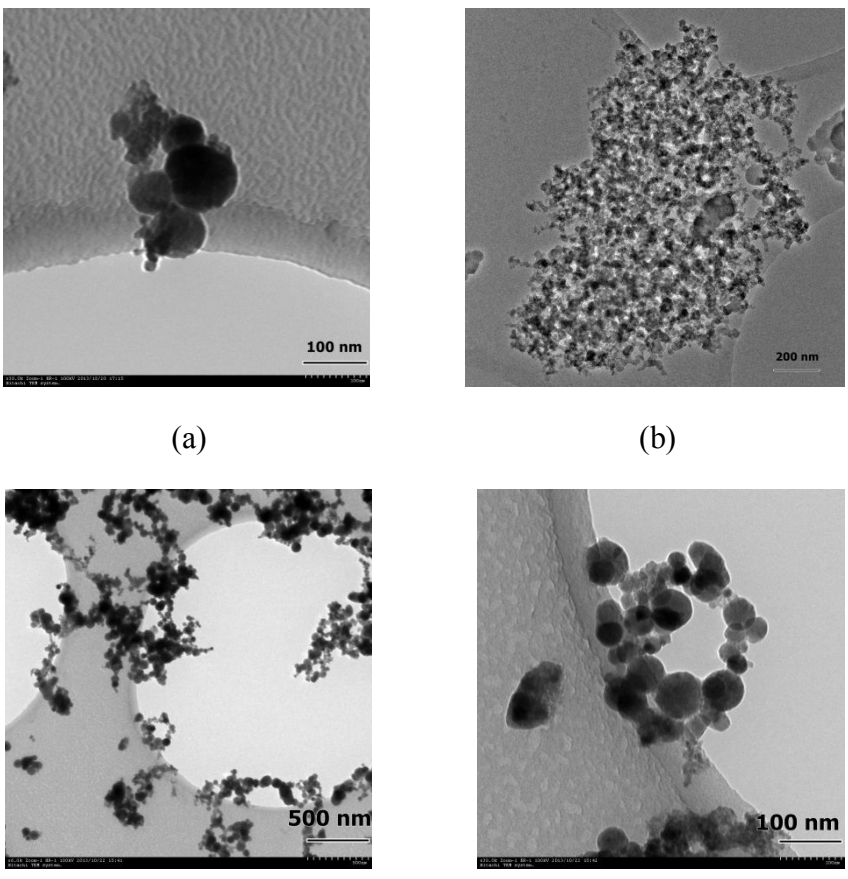

(a) (b)

(c) (d)

Figure 1-4. Transmission electron microscopy (TEM) images at (a) ENP-D (30,000×), (b) ENP-F (6,000×), (c) UNP-G (10,000×), (d) UNP-G (30,000×).

Discussion

This study compared the concentrations and characteristics of nanoparticles at nine workplaces categorized as three types (LAB, ENP, and UNP) to examine nanoparticle exposure based on real-time data and gravimetric sampling. A major challenge in comparing nano-related workplaces of various sizes is implementation of control strategies (Schulte *et al.,* 2008). No previous reports have compared three types of workplace simultaneously.

The exposure levels at LAB differed from those at ENP and UNP workplaces. Although the geometric mean at LAB was low (Table 1-2), exposure levels for some tasks could be high (Figure 1-1).

For example, at LAB-B two tasks emitted high concentrations of nanoparticles; namely, sonication and reaction (Figure 1-1 (a), Figure 1-2 (b)). These showed similar concentration levels to those at dehydration processes ENP-D and were higher than those of mixing, drying, and bagging (Figure 1-1 (b), Figure 1-2 (d)). Characteristics of LAB were: (1) intermittent performance of experiments, (2) the possibility of exposure to high nanoparticle concentrations in a short time period, (3) the existence of many unknown risks, and (4) difficulty in determining the exposure history due to the lack of an exposure assessment record. Engineered nanoparticle workplaces (ENP) showed higher concentrations than LABs and lower concentrations than UNP workplaces. The packaging process showed the highest nanoparticle concentration at ENP-F. Unintended

nanoparticle release occurred at ENP-D and F because a forklift was used to transport pallets of product to the truck or warehouse. UNP workplaces showed the highest concentration for all measured metrics, which differed significantly compared to those at LAB and ENP ($p<0.01$). Welding is a well-known source of nanoparticles, and welding fumes could lead to adverse health effects (Donaldson *et al.,* 2005; Yoon *et al.,* 2003). Smelting showed the highest nanoparticle concentration (CPC: 50,826 particles/cm^3) in this study. In previous reports, aluminum smelting processes to manufacture battery parts showed a mean concentration from 70,000 to 144,000 particles/cm^3 as determined using the same CPC device as in our study. The study reported higher concentrations than our results (Table 1-2) (Debia *et al.,* 2012). Exposure assessment and control strategy based on time-weighted average (TWA) approaches may not be appropriate, especially at LAB, because it may not reflect variation among tasks. Therefore, task-based exposure assessment strategies may be a feasible method of evaluating nanoparticle exposure (Cena and Peters 2011; Ham *et al.,* 2012; Peters *et al.,* 2008).

According to the hierarchy of controls for general industrial hygiene (Halperin 1996) and nanoparticle risk management (Schulte *et al.,* 2008), elimination, substitution, isolation, engineering controls, administrative controls, and personal protective equipment are required for control measures. Fume hoods had been installed and were in operation at all LABs but all experiments sampled were performed at the table outside of the fume hoods. At LAB-B, sonication, reactions, and weighing processes were performed outside of the fume hood. This might have increased the nanoparticle concentration in the air (Figure 1-1 (a), Figure 1-2 (b)). In addition, transfer of

nanoparticles from a crucible to a vial, to a crucible, and weighing were performed outside of the fume hood. This might have increased the concentration, as shown in Figure 1-1 (a) and Figure 1-2 (a). In a previous report, it was shown that laboratory nanoparticle experiments should be performed inside the fume hood using the smallest quantity possible and the least energetic handling (Tsai *et al.,* 2009). Thus, it is important to handle nanoparticles in a well-controlled environment such as an LEV or fume hood. At the ENP-E workplaces, an isolation cabinet equipped with an LEV system to exhaust the emitted nanoparticles from the facility during the collecting process. In addition, there was an LEV system was installed for the sieving process (Figure 1-1 (b)). Isolation and engineering control measures, such as LEV systems, could mitigate exposure to nanoparticles. At the ENP-F workplace an LEV system was involved in the packing process. At the ENP-F workplace all processes were automated, with the exception of the packaging process. Therefore, there are fewer possibilities for exposure to nanoparticles during regular processes, excluding the packaging process. No control measures were installed at the ENP-D workplace because natural ventilation, which opens the entrance door of factory building, was present. The nanoparticle concentration was higher for the reaction, dehydration, and mixing processes than the other processes. There was no LEV at UNP workplaces, and welding and smelting processes generated higher nanoparticle concentrations than those at the LAB and ENP workplaces. Welding fumes generated by stainless steel welding, which contains hexavalent chromium, is known to cause lung cancer (Yoon *et al.,* 2003), and manganese is a cause of manganese-induced parkinsonism (Olanow 2004). In addition, respiratory symptoms such as asthma and lung function decline have been reported in the smelting industries (Søyseth *et al.,* 2013). In a

previous report, efficient use of LEV was shown to lead to a significant reduction in exposure to welding fumes (Ashby 2002; Lehnert *et al.,* 2012). In addition, portable LEV is a feasible control method for welding because welding process is not always performed at fixed point (Meeker *et al.,* 2007). At the UNP-I workplace a lid with a ventilation system was installed for smelting processes, but its purpose was to exhaust heat from the factory and it does not have sufficient capacity to capture the nanoparticles emitted during the smelting process. Therefore, this process emitted a high concentration of nanoparticles. Thus, LEV system should be installed at UNP workplaces. Engineering controls such as facilities, process design changes, and ventilation could be effective for reducing nanoparticle exposure. Control measures, such as isolation of the process or worker, should be applied during the initial design prior to construction of the production facilities, because modifying the facilities thereafter is difficult. LEV systems are effective for capturing airborne nanoparticles. According to Schulte *et al.,* (2008), 1–300-nm particles and fine dusts can be captured by diffusion using the LEV system. However, microscale particles are moved by inertia, which results in them crossing streamlines of moving air and so avoiding capture. Overall, LEV systems could be appropriate control measures to reduce nanoparticle concentrations.

SMPS was applied to investigate the size distribution of collected particles. SAM, CPC, and gravimetric sampling are incapable of obtaining information on size distribution. Size distribution based on the number concentration was varied depending on the situation. A bimodal size distribution according to nanoparticle concentration was observed during this investigation (Figure 1-2), similar to previous reports (Dasch and

D'Arcy 2008; Pfefferkorn *et al.,* 2010; Zimmer *et al.,* 2002). As shown in Figure 1-2 (g), (h), and (i), welding processes showed a bimodal nanoparticle size distribution. Two peaks occurred at 5,366 and 18,730 particles/cm^3 at 27 and 116 nm, respectively, at UNP-G (Figure 1-2 (g)). Smelting processes also showed a bimodal nanoparticle size distribution at the UNP-I workplace (Figure 1-2 (i)). The concentrations at 15 and 37 nm were 21,698 and 27,398 particles/cm^3, respectively, during the smelting process at the UNP-I workplace. In contrast, the nanoparticle size distribution was unimodal during the welding process at the UNP-H workplace (Figure 1-2 (h)). A unimodal size distribution was also reported for gas metal arc welding processes (Zhang *et al.,* 2013). In addition, bimodal size distributions were detected during some tasks at LAB and ENP. The transfer of nanoparticles from a crucible to a vial at LAB-A, sonication at LAB-B and spraying at LAB-C showed a bimodal distribution. In addition, the majority of processes and tasks showed bimodal distributions.

The contents of particles less than or equal to 100-nm diameter was higher than that of those greater than 100 nm (Figure 1-3). Over 65% of particles were of less than 100-nm diameter at all workplaces. A similar finding (60.7%) was reported during gas metal arc welding (Zhang *et al.,* 2013). Nano-sized particles have a large surface area. However, this characteristic of airborne nanoparticles could change upon their agglomeration after emission into the air. Although terms such as agglomeration and aggregation are defined to differentiate the strength of adherence (ISO 2008), measuring or differentiating nanoparticles existing as individual particles, agglomerations, or aggregates in the air remains challenging. Concentrations measured using SMPS and

CPC in ENP-E and ENP-F were similar, but the surface area concentration and mass concentration were higher at the ENP-F workplace (Table 1-2), while the percentage of particles less than 100 nm was greater at the ENP-E workplace. This is partly due to the difference in adherence. As shown in Figure 1-4, particles at (a) ENP-E (ca. 100 nm) showed larger primary particle sizes than those at (b) ENP-F (7 to 40 nm). Based on the number concentration, surface area concentration, and SEM images, particles confirmed at ENP-F were present as agglomerates rather than individually. During the welding process, particles in chain-like formations were detected; Figure 1-4 (c) and (d), as have been reported previously (Antonini *et al.,* 2007; Zimmer and Biswas 2001). However, there are still controversial issues for exposure assessment strategy as well as toxicology studies (Brouwer *et al.,* 2012). Toxicology researches have reported that nanoparticles are more biologically active and possibly hazardous compared with the unit mass of larger particles of the same composition; however, this remains controversial (Wittmaack 2007). Thus, mass based occupational limits should be re-evaluated to enhance worker protection. Lower occupational exposure limits might need to be established for nanoparticles by mass based metric; alternatively, occupational exposure limits might need to be considered using the number or surface area concentration of nanoparticles, which better explains the dose-response relationships for particles with same chemical composition (Oberdörster *et al.,* 2007; Schulte *et al.,* 2008). Thus, mass, number, and surface area concentration measurements should be performed prior to setting of the occupational exposure limit.

Background (BG) concentration measurements are important for exposure

assessment to distinguish particles emitted by the process itself from those with other sources. Background concentration was measured using the near-field method in the same place at different times (i.e., off-duty, during lunch, or continuously stable time during sampling duration) (Figure 1-1). The majority of BG concentrations were lower compared to other tasks performed at workplaces because the BG was selected as constantly stable. However, the BG concentration of UNP workplaces was higher than that at other workplaces, except at lunch time during stainless steel welding processes at UNP-I because the production rate was lower than that during arc welding. In some cases, lunch-time levels were not lowest and so could not be used as a background. During non-working periods, such as off-duty time or lunch, no air circulation occurred because there was only natural ventilation through windows and doors. Therefore, many factors affect background concentrations; e.g., task, time, stability, other possible sources, and measured concentrations.

There is no single instrument that could characterize nanoparticles perfectly. Therefore, several instruments have been used to measure nanoparticles (Ham *et al.,* 2012; Methner *et al.,* 2012; Peters *et al.,* 2008). The SMPS could characterize the size distribution of nanoparticles as well as concentration with several channels but it is expensive and heavy. The CPC is portable and cheaper than SMPS but it needs to refill the isopropyl alcohol (IPA) regularly (8 hours in manual but shorter than 8 hours) and could not measure size distribution. The SAM could measure lung deposited surface area concentration but it is heavy and measures integrated size range (10-1,000 nm). All these instruments are not for personal monitoring but for area sampling. The point of view for

industrial hygiene, portable and inexpensive measurement devices are required.

ANOVA revealed a limitation in the auto-correlation, and autocorrelation was not considered in this study. The real-time monitored data are highly auto-correlated between samples. ARIMA model could be used to account for the effects of autocorrelation for real-time data (Brouwer *et al.,* 2012; Ham *et al.,* 2012). Time activity diary was recorded as forklift was operated. However, the effect of fork lift could not considered in quantitatively because it is difficult to distinguish the nanoparticles between intended and unintended.

Conclusion

Comparison of the concentration and investigation of the characteristics of nanoparticles at nine workplaces categorized into three types were performed. UNP workplaces generated the highest concentration for all measured metrics. The nanoparticle concentration at LAB workplaces was lower than those at other workplaces. In addition, the characteristics of exposure and size distributions differed according to workplace. Some tasks or processes at LAB showed higher concentrations than at ENP or UNP workplaces, despite the short exposure period. The LEV system may be appropriate for reducing exposure to nanoparticles at ENP workplaces. UNP workplaces emit high levels of nanoparticles, and exposure to workers should be reduced. Therefore, the characteristics of exposure differ at LAB, ENP, and UNP workplaces, and different risk management strategies are required.

Chapter 2. Task Based Exposure Assessment of Nanoparticle in the Workplace

This chapter was published in Journal of Nanoparticle Research 2012; 14: 1126

Introduction

Three types of nanoparticles have been identified: naturally occurring nanoparticles (e.g., volcanic ash), unintentional nanoparticles (e.g., internal combustion engines), and engineered nanoparticles (ENPs) (Oberdörster *et al.,* 2005). Recently, applications for ENPs have increased in various industries, such as medicine, engineering, and cosmetics. The number of workers involved with nanotechnology, including the use of ENPs and manufacturing, is increasing, and estimates indicate that around two million such workers will be employed worldwide in 2023 (Schulte *et al.,* 2008).

However, concern about the potential health hazard of nanoparticles is also increasing (Oberdörster 2010). Many factors, including the size, morphology, and exposure route, have been known to influence the toxic effects of nanoparticles. For example, nanoparticles possessing the same crystal structure but a smaller particle size are more toxic than are larger-sized particles (Oberdörster *et al.,* 1994).

Compared with the number of studies regarding the toxicity of nanoparticles, exposure-monitoring studies are limited, and most only provide information about the status of nanoparticle emissions (Bello *et al.,* 2009; Schmoll *et al.,* 2010; Tsai *et al.,* 2011), mapping (Heitbrink *et al.,* 2009; Park *et al.,* 2010; Peters *et al.,* 2006), and factors influencing the concentration profiles (Methner *et al.,* 2010; Tsai *et al.,* 2009).

A recent controversial issue in nanoparticle exposure assessments has involved the standardization of sampling strategies. A standardized sampling strategy, incorporating a

task-based approach, could potentially ensure that all collected data are compatible and allow for comparisons among different exposure situations (Brouwer *et al.,* 2012; Brouwer *et al.,* 2009; Ramachandran *et al.,* 2011).

Task-based sampling is different from full-shift sampling. Unlike time-weighted average (TWA) concentrations collected during shift sampling, measurement of the activity of a worker performing a given task that is believed to cause concentration fluctuations precisely reflects real exposure variations, which can lead to adoption of appropriate controls. The advantages of task-based exposure assessment are most significant for jobs that have a high degree of variability in the time spent performing individual tasks on a daily basis (Seixas *et al.,* 2003). The definition of a task is an important aspect of a task based approach and lack of standardized task definition can make it difficult to compare results among studies (Virji *et al.,* 2009). Most of the nanotechnology industry is utilizes batch processing rather than continuous mass production, which is difficult to generalize. Task-based exposure assessment is potentially appropriate for the engineered nanoparticle manufacturing industry because of the irregular processes in the workplace. However, very little data on task-based sampling for nanoparticle exposure assessment in such workplaces have been published.

The purposes of this study were to compare nanoparticle concentrations during a task and during periods of no activity using a task-based approach and to describe the concentration profiles of an engineered nanoparticle manufacturing workplace (ENP) and an unintended nanoparticle-emitting workplace (UNP).

Materials and Methods

Manufacturing Facilities

A total of four workplaces, i.e., two ENPs and two UNPs (welding fume generation workplaces), participated in this study. Sampling was conducted from July to August in 2009.

In ENP-J, the floor area was 176 m^2, and titanium dioxide and aluminum ENPs were manufactured by one worker. Natural ventilation was available throughout the measurement. Personal protective equipment was not worn by the worker. The worker performed several tasks occasionally. Titanium dioxide was extracted from titanium tetrachloride for the photocatalyst material. The liquid-phase titanium dioxide was synthesized using low-temperature (i.e., without any heat treatment) homogeneous precipitation methods by the hydrolysis process. Electrolysis was used to manufacture aluminum nanoparticles. There was an intermittent welding process that occurred next door, but the door was closed for most of the working duration. At ENP-K, silver, aluminum and copper nanoparticles were manufactured. The area of the workplace was 97 m^2. The four workers wore only poly gloves to reduce their exposure to the environment. The manufacturing in the ENP facilities was enclosed with sashes and included a ventilation system. Additionally, natural ventilation was installed. The workplaces were separated by walls among the processes. The nano metals (Ag, Al, and Cu) were generated by eight well-contained booth-type facilities that used a pulsed wire evaporation method. The parent metal wire was evaporated by 30 kV pulse power and

was condensated into the cyclone, where very fine particles were collected. During the process, all side walls were closed and a flexible duct that was connected to the upper part of the booth-type facilities was operated.

Gas metal arc welding (GMAW) on mild steel was performed at UNP-L and UNP-M such that welding fumes, or unintended nanoparticles, were generated. In UNP-L, 20 out of a total of 35 employees were responsible for welding, and the area was 2,017 m^2. A diesel-fueled forklift carried the final products to the warehouse, and natural ventilation was available through the doors and windows in the walls of UNP-L. The main products of UNP-L were the various body parts of backhoes. In UNP-M, 23 workers constructed steel bobbins for electrical wire that were 3 meters in diameter. The floor area was 2,420 m^2. Two workers produced one bobbin on each side. The bobbin was located on a roller to allow it to rotate easily. Steel sheets were cut by plasma and bent by a 200-ton press during the preparation process. There was an intermittent plasma cutting process taking place next door. The welding rods consisted of iron, manganese, silicon and copper. During the survey, the temperature ranged from 26.5 to 30.7 °C, and the relative humidity was 61.5 to 65.9%

Measurement strategy

For portability, a sampling cart was used to move the sampling devices. The inlets of each instrument were installed within at least 30 cm of each other to reduce the measurement error. The heights of the inlets were located between 1.2 and 1.5 m. The real-time measurements were performed for two days in ENP-J, ENP-K, and UNP-L and included the work shift of the first day, the night downtime, and the work shift of the second day. Six-hour measurements were performed in UNP-M. Gravimetric sampling was performed during the work shifts of all workplaces. During sampling, the researcher observed the activities of the workers and wrote in a time activity diary (TAD) to record contextual information, which was matched with the concentration profiles obtained by real-time measurement devices. During the night downtime, the sampling devices were operated in the absence of the researcher. At ENP-J, the inlets of the sampling devices were located about 0.5 m from the source. At ENP-K, the inlets were placed about 0.5 m from the ENP manufacturing facilities. At UNP-L and UNP-M, the inlets were positioned about 1 m from the source of the welding fumes. All of the instruments were connected to AC power for electrical power.

Real-time measurements

Several real-time instruments, such as a scanning mobility particle sizer (SMPS), a surface area measuring instrument, a particle number measuring instrument, and a mass measurement instrument, were employed.

To investigate the distribution of particle sizes, an SMPS (Model 3936L75, TSI Inc., Shoreview, MN, U.S.A.) with a detectable size range from 14.6 to 661 nm and a concentration range of 0 to 10^7 particles/cm^3 was used. The sample flow rate was 0.3 liters per minute, and the sheath flow rate was 3 liters per minute for the optimum sample flow rate/sheath flow rate ratio of 1:10. Flow calibrations were performed in the laboratory before any measurements. The sampling time of the SMPS was 135 seconds per averaging time, and it measured the particle size from small to large with 107 sequence channels. The particles were collected from the inlet and passed through the aerosol neutralizer using krypton-85. Particles were separated by mobility diameter using a differential mobility analyzer (DMA) before being counted using a condensation particle counter (CPC).

A condensation particle counter (CPC: P-Trak Model 8525, TSI Inc., Shoreview, MN, U.S.A.) was used to measure the total number concentration of the particles ranged from 20 to 1,000 nm in diameter with a 0.1 lpm sample flow rate. The capable concentration range was 0 to 500,000 particles/cm^3. Isopropyl alcohol (Sigma Aldrich, U.S.A.) was used for particle condensation which increases the particle size to enable optical detection. One sampling averaging time was set as 1 minute. The zero calibration

was performed using a HEPA filter before sampling.

To measure the surface area concentration, a surface area monitor (SAM: AeroTrak Model 9000, TSI Inc., Shoreview, MN, U.S.A.) was utilized. One averaging time was set as 1 minute. The measuring particle size range was 10 to 1,000 nm, and the aerosol concentration range was 1 to 10,000 $\mu m^2/cm^3$ for the alveolar deposition method. A cyclone was installed on the inlet to prevent the entry of particles larger than 1 micrometer. The flow rate of the aerosol sample branch was 1.5 lpm. The zero calibration of the electrometer was performed prior to sampling. The sampled particles were mixed with ions in the chamber of the device, and the particles were charged. Then, the charged particles passed along the electrometer, and the charges of the ions were measured and were converted to surface area metrics.

A portable aerosol spectrometer (PAS, 1.109, Grimm, Germany) was used to measure the masses of aerosols less than 1.0 μm ($PM_{1.0}$). One averaging time was set as 1 minute. The measured mass concentration was corrected with the gravimetric correction factor (*C-factor*). To calculate the C-factor, a PTFE filter (47 mm, 0.5 μm, Toyo Roshi Kaisha Ltd., Japan) was used to adjust the results. The filter was pre- and post-desiccated to obtain its equilibrium weight. An analytical balance (Ultra Microbalance XP2U, METTLER TOLEDO, U.S.A.) in a weighing room (constant temperature and humidity maintained at 20 °C ± 1 °C and 50% ± 5%, respectively) was used.

$$C - factor = \frac{Filter\ weight\ (loaded\ filter - clean\ filter)}{Theoritical\ Weight\ shown\ by\ the\ instrument}$$

Thermo recorder (TR-72U, T&D corp., Japan) was used to measure temperature and relative humidity. One averaging time was set as 1 minute.

Off-line measurements

Integrated sampling using filter media was performed for gravimetric, chemical and electron microscope analysis. A polycarbonate filter (37 mm, 0.8 μm, SKC Inc., USA) was used to capture the airborne nanoparticles using a mass sampler (2 lpm, Escort ELF, MSA, USA) with an open-faced 3-piece cassette. Sampling was performed in full shift of working time. Some samples, for example, aluminum nanopowder grinding, were collected short term during one specific task. Filters were pre- and post-equilibrated prior to weighing in an environmentally controlled weighing room that was maintained at a temperature of 20 °C ± 1 °C and a relative humidity of 50% ± 5%. After the sampling, the cassettes were sealed tightly using silicon tape and carried in a clean box. Weighing was performed using a microbalance.

The sizes, morphologies and elemental compositions of the particles were investigated in detail with a field emission-scanning electron microscope (FE-SEM, JSM-6360F, JEOL, JAPAN) and an energy dispersive spectrometer (EDS, INCA 7582, Oxford, U.K.). The filters were platinum coated for electron microscope analysis. For SEM analysis, the open face sampling technique was used as like asbestos sampling. Filter was cut randomly because the assumption of particles were evenly distributed on the filter.

Time Activity Diary (TAD)

A TAD was recorded by the researcher. Most of the behaviors of the workers and contextual information of the workplace, such as break time, lunch time, and starting or finishing of work, was recorded. Also, task observation, cycle, duration was recorded. Tasks were defined by researcher because there was no defined standard process to manufacture the ENP at the ENP workplaces. There were one task which was welding at the UNP workplaces. During the downtime at night, there were no working activities, and hence records of TAD were off-duty. For data analysis, code of working status, tasks were determined.

Data analysis

Descriptive statistics were used. The geometric mean (GM) and geometric standard deviation (GSD) of the number concentration, surface area concentration, and mass concentration were calculated. Parametric statistics were used to test for relationships between the concentration levels and other factors though some subset data failed goodness of fit test. Most data set were skewed. Analysis of variance (ANOVA) followed by Sheffes's post hoc test were used to determine whether or not there were differences in concentration levels by tasks. All statistical analyses were performed with the SPSS 18.0 software package (SPSS. Inc., Chicago, IL, U.S.A.). A graphical representation was generated using SigmaPlot 10.0 (Systat, Chicago, IL, U.S.A.). The figures shown in this manuscript are from the SMPS only. Data from the SMPS were converted using Aerosol Instrument Manager Software 9.0 (TSI Inc., Shoreview, MN, U.S.A.). Other instruments had their own conversion software to manage the data.

Results

Table 2-1 summarizes the general characteristics of the workplaces in terms of the following variables: nanoparticle type, ventilation status, temperature, humidity, descriptive statistics for the measured metrics (e.g., GM, GSD, and the fifth through the ninety-fifth percentiles of particle-number concentrations measured by SMPS as well as surface area and number particle and mass concentrations. SMPS data were separated according to size.

The highest surface area and total number concentrations measured by SAM and CPC, $PM_{1.0}$ mass concentration, and TWA filter-based mass concentration as well as the number concentration measured by SMPS were measured at the heavy-duty welding UNP-L. The GMs of the surface area concentration, CPC total number concentration, $PM_{1.0}$ mass concentration, and TWA filter-based mass concentration were 403.78 $\mu m^2/cm^3$, 54,476 particles/cm^3, 350.22 $\mu g/m^3$, and 1,058 $\mu g/m^3$, respectively. The lowest concentrations were observed in ENP-K, where the GMs of the surface area concentration, CPC total number concentration, $PM_{1.0}$ mass concentration, and TWA filter-based mass concentration were 30.84 $\mu m^2/cm^3$, 8,471 particles/cm^3, 37.17 $\mu g/m^3$, and 74.62 $\mu g/m^3$, respectively.

Table 2-1. Summary of the general characteristics of the workplaces

Source Type	Work-place	NPs[c]	Ventilation Type	Temp. (RH%)	GM(GSD) [5th-95th percentile]						
					SMPS*			CPC (0.02-1.0 μm) (particles/ cm^3)	SAM (μm^2/ cm^3)	PM $_{1.0}$ (μg/m^3)	Filter-based Mass (μg/m^3)[f]
					Total (particles/cm^3)	14.6-100 nm (particles/ cm^3)	100-661.2 nm (particles/ cm^3)				
ENP[a]	J	TiO_2, Al	NV[d]	28.8 (64.6)	1,032,889(1.73) [464,959-2,468,792]	658,348(1.86) [253,877-1,693,888]	357,207(1.63) [168,897-843,820]	20,830(2.63) [2,493-68,061]	91.38(1.92) [34.63-266.97]	46.09(1.52) [29.35-97.87]	110.97[1)]
	K	Ag, Al, Cu	LEV[e] and Isolation	30.6 (61.5)	152,861(1.35) [93,814-235,780]	111,252(1.40) [64,998-185,747]	40,616(1.32) [26,146-62,572]	8,471(1.43) [4,532-14,295]	30.84(1.34) [30.32-46.69]	37.17(1.32) [26.80-60.20]	74.62[1)] 76.63[2]
UNP[b]	L	Welding fumes	NV	30.7 (62.8)	3,076,614(3.09) [653,259-17,448,199]	2,090,554(2.93) [371,486-9,618,876]	1,545,473(3.45) [278,546-8,675,807]	54,476(2.63) [2,778-233,266]	403.78(1.70) [56.35-2,469.01]	350.22(2.25) [128.06-1057.69]	1058.52[1)] 1191.70[2)]
	M	Welding fumes	NV	26.5 (65.9)	312,855(2.67) [86,802-1,295,592]	203,143(2.68) [57,884-913,673]	100,816(2.98) [29,490-468,327]	34,661(2.59) [10,476-137,333]	193.09(2.93) [51.18-968.55]	202.68(2.39) [55.76-696.86]	484.81[1)]

* Sum of concentrations of each size bin
a: Engineered nanoparticle
b: Unintentional nanoparticle
c: Nanoparticles
d: Natural ventilation
e: Local exhaust ventilation
f: Traditional gravimetric method (One full shift integrated sample);
Sampling duration: J (390 min.), K (421 min.[1)], 465 min.[2)]), L (396 min.[1)], 395 min.[2)]), M (243 min.);
Numbers of samples were 1 in ENP-J and UNP-M, respectively, and 2 in ENP-K and UNP-L, respectively.
[1)] First day; [2)] Second day

Figure 2-1 shows the total number concentration profile measured with the SMPS at ENP-J over a 27-hour period that included two work shifts and one overnight period. At this workplace, the work shifts were from 8:30 to 20:30. As seen in Figure 2-1, the number concentration of the ENPs varied substantially with time, which reflects the different specific tasks being performed. The concentration profile was high during the work shift compared with during the downtime at night, as shown in Figure 2-1. Contextual information collected during the survey permitted us to confirm that the highest peaks were closely related to specific tasks or other episodes, including spills or smoking. The highest peak was defined as an instantaneous concentration. For example, Box 1 in Figure 1 shows an accident in which liquid-phase titanium-dioxide solution was spilled on the floor. After the reaction process, the bottle containing the solution had to be moved to another location, but it was dropped during this activity. Box 2 represents an off-duty period and was designated as the background concentration. Box 3 illustrates the liquid-phase titanium-dioxide pouring process. The pouring task involved movement from the reactor to a large bottle after a reaction involving titanium tetrachloride was complete. Box 4 illustrates cigarette smoking by workers in the workplace, and Box 5 indicates significant concentrations of ENPs after the opening of an aluminum nanopowder grinder. Figures 2-2 and 2-3 show the concentration profiles for the specific tasks numbered in Figure 2-1.

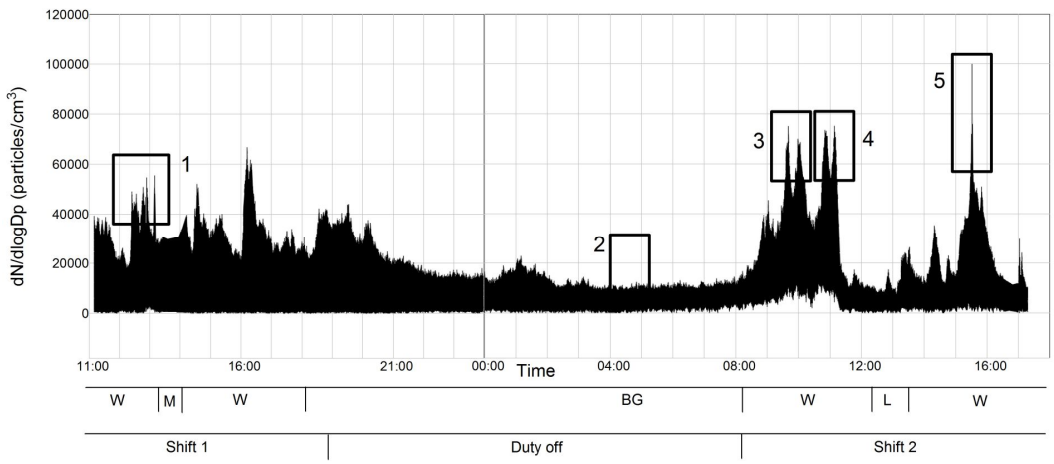

Figure 2-1. Number concentration profiles of nanoparticles measured by SMPS over time at the ENP-J (X axis, time; Y axis, concentration). The numbers above the profile are: 1, liquid-phase TiO_2 accidental spillage; 2, background; 3, liquid-phase TiO_2 regular pouring process; 4, tobacco smoking; 5, aluminum nanoparticle grinding in ENP-J; W, working; M, missing data; BG, background; L, lunch.

The liquid-phase titanium-dioxide pouring process was one of the regular processes in ENP-J (Figure 2-2 (a)). During this process, a worker transports a 2-L bottle of liquid-phase titanium dioxide from the equipment after the reaction was complete.

An accident occurred at 12:47 in ENP-J that involved the breakage of a liquid-phase titanium-dioxide (TiO_2) bottle during its transport to another process (Figure 2-2 (a)), which resulted in a high concentration of airborne ENPs of 44,952 particles/cm^3 at 68.5 nm. After the accidental spillage, the worker poured water on the floor and mopped the floor with a damp rag. A standing-type fan was then employed to dry the floor, and a high concentration of ENPs of 54,629 particles/cm^3 at 241.4 nm was then measured after the spillage. The frequent increases and decreases in the number concentrations in Box 1 of Figure 2-1 indicate that nano-sized titanium-dioxide particles were dispersed into the air by the fan. The median diameter was 67 nm during pouring, but it increased to 162.11 nm 10 minutes after the spillage.

This size was comparable to the size distribution measured during the regular pouring process of the liquid-phase titanium dioxide. The highest concentration during the regular pouring process was 72,489 particles/cm^3 at 57.3 nm. After 20 minutes of pouring, the concentration was 68,036 particles/cm^3 at 145.9 nm. The median diameter increased from 57.6 nm to 120.6 nm after the regular pouring process, which was partly caused by aggregation or agglomeration (Figure 2-2 (b)).

During the work shift, a worker smoked near the sampling instrument on two

occasions. As a result, the peak concentrations increased to 73,554.9 particles/cm^3 at 71 nm at 10:50 and 75,187 particles/cm^3 at 71 nm at 11:08 (Figure 2-2 (c)) during these periods of smoking. Figure 2-2 (d) shows that the background size distribution at ENP-J was constant over time.

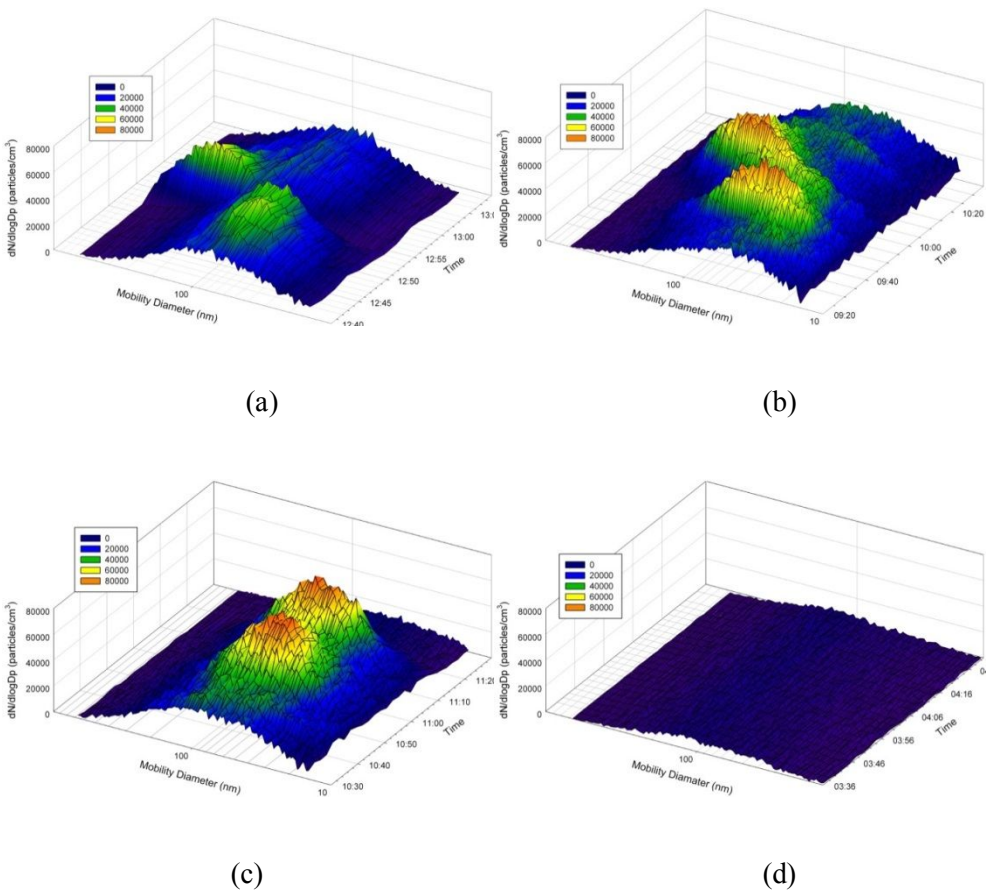

Figure 2-2. Concentration profiles according to specific tasks in ENP-J: (a) during the accidental spillage at 12:47 (Figure 2-1-Box 1), (b) regular pouring process at 9:40 (Figure 2-1-Box 3), (c) tobacco smoking at 10:50 and 11:08 (Figure 2-1-Box 4), and (d) background (Figure 2-1-Box 2).

Figure 2-3 (a) shows the size distribution of aluminum nanoparticles during the grinding process in ENP-J. At 15:25, a worker began to grind a mass of aluminum nanoparticles to produce finer particles prior to packing. The grinding process was necessary to produce particles in a powder state from the semi-cake state resulting from the drying process in the oven. The highest exposure to aluminum nanoparticles during the grinding process, of 99,984 particles/cm^3 at a size of 57 nm, occurred during the opening of the cover of the grinder at 15:51. No local exhaust ventilation (LEV) system removed particles from the workplace. Figures 2-3 (b) and 2-3 (c) show an SEM image and the EDS graph produced during the aluminum grinding process. The SEM image indicates that aluminum nanoparticles with diameters of 50 nm–60 nm formed agglomerates/aggregates after the grinder cover was opened. The EDS graph implies that the particles consisted primarily of aluminum (Figure 2-3 (c)).

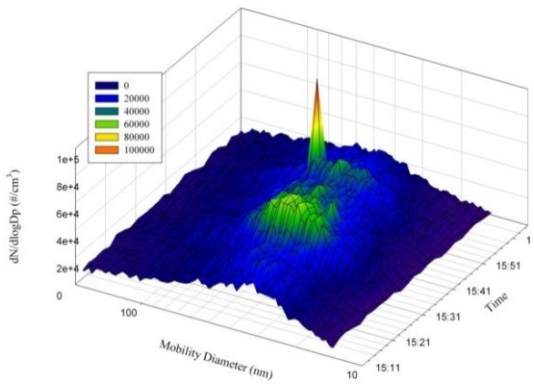

(a)

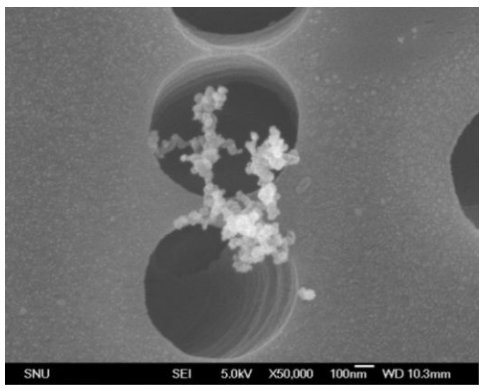

(b)

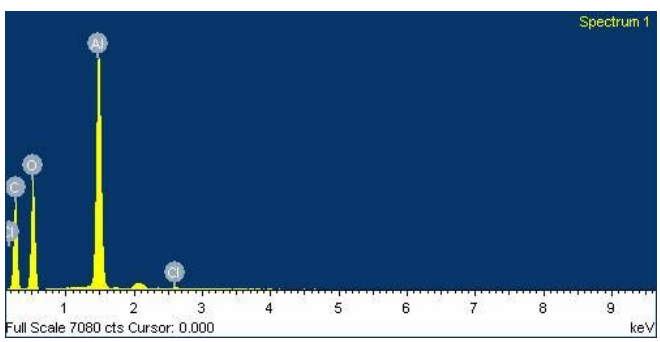

(c)

Figure 2-3. The results of direct reading devices (SMPS) and SEM imaging with EDS peaks in ENP-J: (a) size distribution of nanoparticles during the aluminum nanoparticle grinding process in ENP-J (grinding began at 15:25, and at 15:51, the grinder cover was opened; peak: 57 nm), (b) SEM image to investigate morphology and (c) EDS graph to confirm the chemical composition of sampled nanoparticles during the aluminum grinding process.

Figure 2-4 (a) shows the concentration profile of ENP-K, measured with the SMPS from 10:20 of the first day to 17:12 on the second day (31 hours), which included two work shifts and one overnight period. The work shift was from 8:30 to 17:30 and included a lunch period from 12:30 to 13:30. The number concentrations in this workplace were much lower than were those in ENP-J because all of the generation sources were contained. Furthermore, the concentrations during the downtime overnight were comparable to the concentrations during the work shifts (see Discussion). Concentration fluctuations were also observed in this workplace according to the performance of specific tasks. For example, at 15:35, one of the manufacturing devices was turned off to allow collection of the manufactured ENPs. The concentration was 3,786 particles/cm^3 with a diameter of 33.4 nm during the manufacturing process with the collection panel door closed at 15:05. The operator waited until all of the manufactured ENPs were collected. Simultaneously, the equipment's LEV system was also switched off. The cabinet door was opened to allow access to the collected ENPs at 16:03, and the concentration increased to 10,826 particles/cm^3 with a size of 94.7 nm (Figure 2-4 (b)). Figure 2-4 (c) shows the concentration profile during the off-duty period when no manufacturing processes were occurring. It shows relatively stable concentrations and a similar particle size of 69.3 nm, which was considered to be the background concentration.

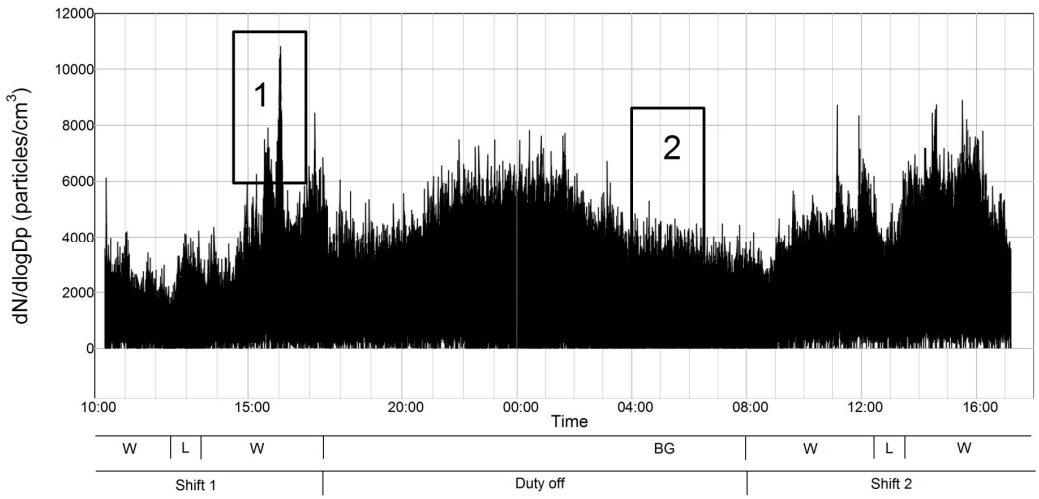

(a)

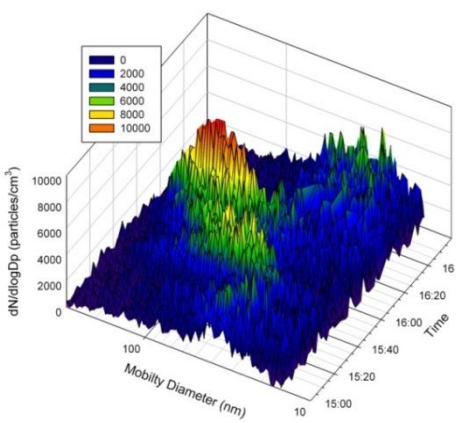

(b)

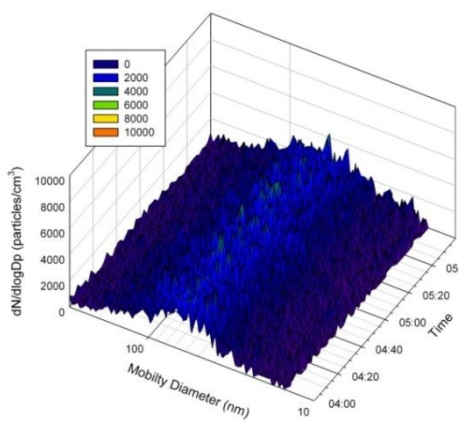

(c)

Figure 2-4. Results of the direct reading device (SMPS) in ENP-K: (a) concentration profiles of nanoparticles by time and concentration in ENP-K (X axis-time, Y axis-concentration), (b) size distribution measured during the opening of the production system isolation cage to remove manufactured nanoparticles and (c) size distribution of background. W, working; L, lunch; BG, background.

Figure 2-5 (a) presents the concentration profile measured with SMPS in UNP-L from 9:44 of the first day to 16:27 of the second day (31 hours), which included two shifts and one overnight period. In this workplace, the work shift was from 8:00 to 17:00, but overtime work was also performed. The lunch break was from 12:00 to 13:00, and an additional break occurred from 15:00 to 15:15. During the break time, the total concentration measured by SMPS was 34,651 particles/cm^3 at 15:10, whereas the concentration was 153,907 particles/cm^3 immediately prior to the break time, at 14:57 (Figure 2-5 (b)). The concentration profile implies that the concentrations during work and break times differed substantially. There was a significant difference from the concentrations measured during the background period (Figure 2-5 (c)).

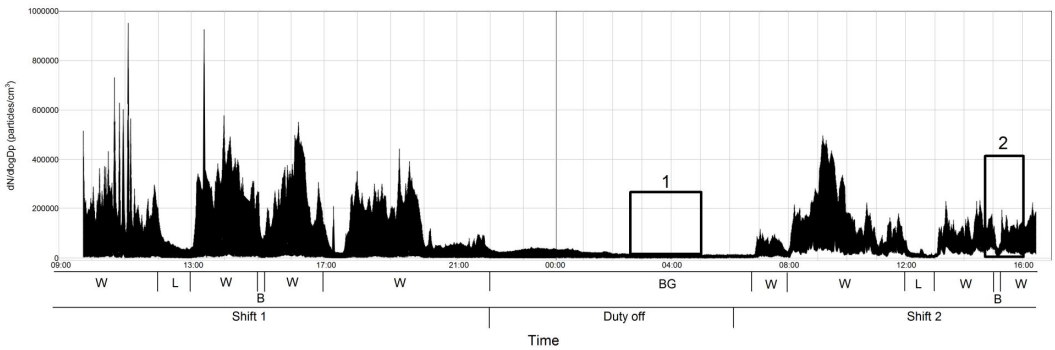

(a)

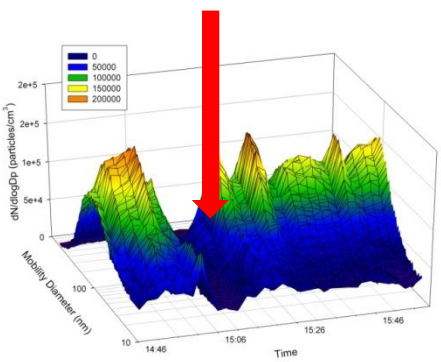

(b)

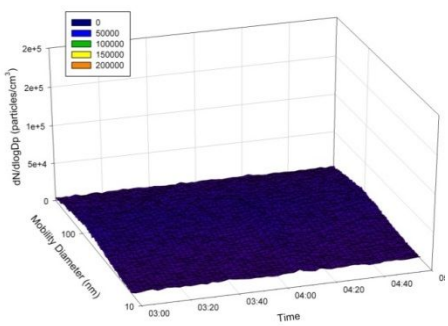

(c)

Figure 2-5. The results for the direct reading device (SMPS) in UNP-L: (a) concentration profile by time: 1, background; 2, working and break time; W, working; L, lunch; B, break; and BG, background, (b) the size distribution of nanoparticles from the welding process from Box 2 in Figure 2-5 (a), where the red arrow indicates the changes of size distribution during the break time and (c) the size distribution of nanoparticles from the background from Box 1 in Figure 2-5 (a) in UNP-L.

Figure 2-6 shows the concentration profile using SMPS from 13:21 to 19:51 in UNP-M. In this workplace, numerous fluctuations in the concentration, which depended on the generation of welding fumes, were observed. The work shift was from 13:30 to 17:23, and a break occurred from 15:20 to 15:45. The background concentration was determined after the working day was completed. The highest concentration was 151,623 particles/cm^3, whereas the background concentration was less than 10,000 particles/cm^3.

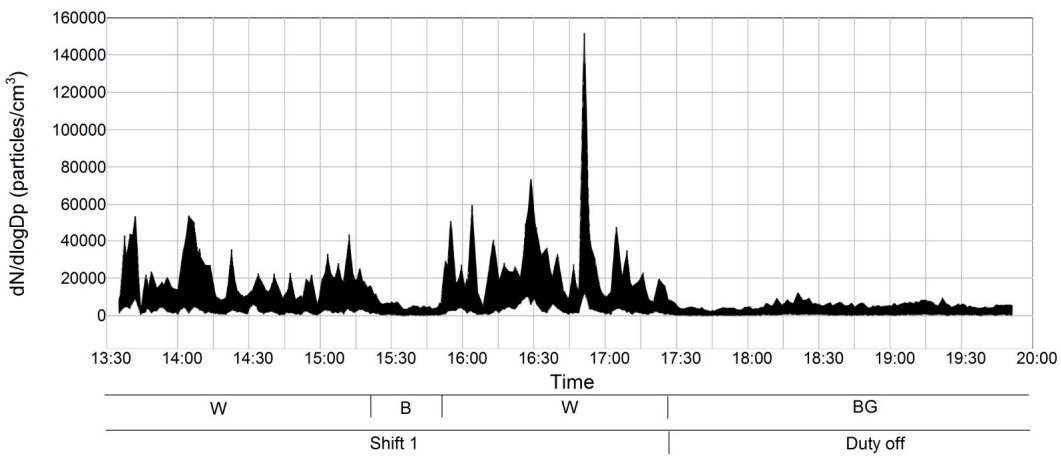

Figure 2-6. Number concentration profile in UNP-M.

The ratios between the task and the background concentrations for a standardized comparison in the workplaces are shown in Figure 2-7. The background concentrations were measured during periods when no work was being performed. Tasks such as an accidental spillage of TiO_2, moving the TiO_2 powder, mixing liquid TiO_2, pouring liquid phase TiO_2 into the reactor tank, Al nanoparticle grinding, and tobacco smoking produced concentrations higher than the background concentration in ENP-J. In ENP-K, except during the task of opening the door to collect manufactured nanoparticles from the facility, concentrations were similar to the background. For welding tasks at UNP-L and UNP-M, the concentrations were higher than during meals and break times. The concentrations were higher at UNP-L than at UNP-M. In the case of accidental spillages and moving TiO_2 powder, no significant differences between the concentrations measured were observed (p <0.05). Additionally, no significant differences in concentration were observed for the tasks of moving TiO_2 powder, mixing liquid phase TiO_2 and grinding Al powder (p <0.05). There were no significant differences between the tasks of mixing liquid phase TiO_2, grinding Al powder, and pouring liquid phase TiO_2 into tanks (p <0.05) in ENP-J. Sieving under the LEV and mixing nanoparticles in the fume hood produced no significant differences in concentrations (p <0.05). There were similar concentrations during breaks and at meal times in UNP-M (p <0.05). The descriptive statistics for concentrations of tasks/events at workplaces shows Table S 2-1 (Appendix).

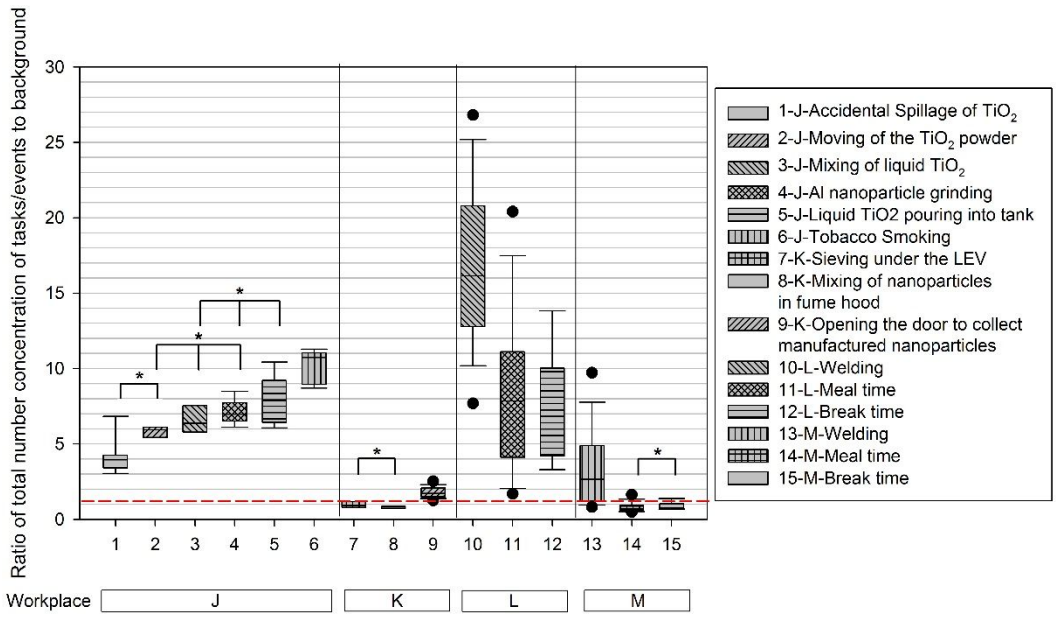

Figure 2-7. Comparison of the total number concentration ratios of tasks/events to background. Break time and meal time included to compare with background even these are not tasks. Upper and lower whiskers represent the 5th and 95th percentiles, respectively. The boxes show the 25th and 75th percentiles. The median is indicated by the solid line inside the box. The reference is indicated by the dashed line. The number concentrations were obtained from the SMPS with particle sizes less than 100 nm. The background concentrations were 215,137 particles/cm^3 in ENP-J, 85,020 particles/cm^3 in ENP-K, 412,805 particles/cm^3 in UNP-L, and 103,935 particles/cm^3 in UNP-M.

* Sheffe's post hoc test (p<0.05)

Discussion

In this study, nanoparticle exposure assessments were performed for two ENP companies and two UNP (welding fume)-generating workplaces.

Size-distribution differences depend on the task performed

Differences in size distributions and concentrations depended on the task being performed. As shown in Figures 2-1, 2-4 (a), 2-5 (a), and 2-6, particle concentrations also varied according to task. The exposure profiles differed between work shifts and background periods. Moreover, there were different ratios between the different task and background concentrations (Figure 2-7).

In this study, the task being performed was one of the most significant factors determining changes in the nanoparticle number concentrations. In ENP-J, the concentration peaked when the cover of the grinder containing aluminum nanoparticles was opened, and the concentrations measured from this task (99,984 particles/cm^3 with a diameter of 57.3 nm) were approximately three times higher than the concentration during the grinding process and 15 times higher than the background concentration (Figure 2-3 (a)). When the reactor was opened, the peak concentration reached 447,000 particles/cm^3, as measured by CPC. During the production of nanostructured materials used for the electronics industry, the concentration was 62,000 particles/cm^3, which was 30–50 times higher than the background of 5,500–15,000 particles/cm^3 (Plitzko 2009).

The concentration during the reaction of titanium dioxide was 45,889 particles/cm^3, whereas the background concentration was 11,418 particles/cm^3. After the reaction was completed, the particle number concentration decreased to 14,000 particles/cm^3 (Lee *et al.,* 2011). An aluminum nanopowder exposure experiment performed in a laboratory hood found that a more dynamic handling method resulted in significantly higher total particle concentrations than did a less energetic handling method (Tsai *et al.,* 2009).

Our results indicated that the size distributions differed when dealing with liquid-phase nanoparticles. For example, the same raw material (liquid-phase titanium dioxide) was involved in both the spillage accident and the regular pouring process in ENP-J. The size distribution changed after both the spillage accident and the pouring process. The median diameter increased, which may have been the result of the agglomeration or aggregation of nanoparticles. In a previous study, the size distribution of particles also increased from small to large. This increase, especially after production ceased, may be an influence of the background particle-size distribution (Demou *et al.,* 2008).

The regular pouring process (Figure 2-1-Box 3) generated higher nanoparticle concentrations than did the accidental spillage (Figure 2-1-Box 1). After the accidental spillage, a worker cleaned the floor using a wet towel. Cleaning may have reduced the number of released airborne nanoparticles. The National Institute for Occupational Safety and Health (NIOSH) (2009) defined an accidental spillage as an event that increases the risk of exposure to ENPs. Guidelines for handling nanoparticles (*The interim best practices for working with nanoparticles issued by the Center for High-rate*

Nanomanufacturing (CHN) laboratory) (Ellenbecker and Tsai 2008) require that laboratory staff have the use of barricade tape, gloves, N95 respirators, adsorbent material, wipes, sealable plastic bags, and a walk-off mat. For liquid-phase ENP spillages, absorbents were recommended for the clean-up in addition to the use of a barrier to minimize the spill area. To remove the nanomaterials, the use of a HEPA-filtered vacuum is required. After cleaning, all cleaning materials used should be treated as hazardous waste. Similar recommendations have also been published as guidelines for nanomaterial handling (BSI 2007; NIOSH 2009). Workers must also be aware that nanomaterial spill accidents can cause explosions (IRSST 2009). During the sampling, a worker in ENP-J smoked a cigarette on two different occasions, which affected the workplace nanoparticle concentrations (Figure 2-2 (c)). The maximum concentration of ultrafine particles larger than 0.02 μm, during cigarette smoking has been reported to be approximately 213,000 particles/cm^3 in a chamber experiment (Afshari *et al.,* 2005). This result suggests cigarette smoking should be prohibited in the workplace, not only because of the cancer risk but also because of the generation of unintended nanoparticles. However, the concentrations of airborne ENPs during the downtime overnight fluctuated rather than decreased in ENP-K, whereas the other workplaces showed clear reductions in nanoparticle concentration profiles during the downtime, as shown in Figures 2-1, 2-5 (a), and 2-6. One possible reason for the higher concentration of nanoparticles in the downtime of ENP-K is the flow of outdoor air into the workplace by the natural ventilation system. Another reason might be a concentration baseline drift resulting from

the long-term use of the SMPS.

In this study, concentration profiles varied according to the tasks being performed, and that task-based exposure assessments could be useful for predicting exposure and suggesting controls for emission sources.

The tasks being performed in the welding (UNP-L and UNP-M) were simpler than those being performed in the ENP companies. The tasks were divided into those that were work, breaks and meals and found significant differences in the results obtained for different tasks. The results indicated that totally different tasks were performed in the ENP companies and welding workplaces. Because a task-based approach can identify tasks with high exposure potential (Virji *et al.,* 2008), task definition is a crucial factor (Neitzel *et al.,* 2011).

As shown in Figure 2-7, the concentrations of nanoparticles between during periods when tasks were performed were found to differ from the background levels. ANOVA was used to compare the concentrations during various tasks, and the analysis revealed that concentration profiles varied among tasks as well as among workplaces. For ENP-J, all tasks produced concentrations higher than background levels. Tasks at ENP-K produced relatively lower concentrations. When comparing the two ENP workplaces, the concentrations were higher in ENP-J. This might be due to the effect of the LEV system, which would reduce the particle concentration. The concentrations were higher during welding than during breaks and mealtimes. Although breaks and mealtime were not tasks, they were included for comparison. The concentrations in UNP-L were higher than those

in UNP-M because there were 20 welders at UNP-L and two at UNP-M. Variations among tasks were observed at the ENP workplaces due to the irregular nature of tasks resulting from manufacturing taking place to order. Therefore, task-based sampling is required to accurately assess ENP workplaces.

Comparison of concentrations between ENP-generating and welding workplaces

There were differences in the concentrations and size distributions of ENP workplaces and welding fume-generating workplaces. With the exception of the SMPS results, the ranks of the metrics for concentration were comparable (Table 2-1). One unexpected observation was that the number concentrations measured by SMPS at welding UNP-M were lower than were those measured at ENP-J, whereas the other metrics such as surface number, fine particles, $PM_{1.0}$, and filter-based TWA concentrations were higher. For example, the number concentration measured by SMPS was 312,855 particles/cm^3 at UNP-M and 1,032,889 particles/cm^3 at ENP-J. In contrast, the surface area concentrations were 193.09 $\mu m^2/cm^3$ and 91.38 $\mu m^2/cm^3$ for UNP-M and ENP-J, respectively (Table 2-1). The concentrations of nanoparticles generated from welding were higher than those generated from the ENP workplace, excluding ENP-K. In ENP-K, there was a relatively controlled working environment. The GM of the number concentration was 8,471 particles/cm^3 (fifth and ninety-fifth percentiles, 4,532 particles/cm^3, 14,295 particles/cm^3) in ENP-K, which may be evidence of a better ventilation system. In ENP-J, the geometric mean for number concentration was 20,803 particles/cm^3 (fifth and ninety-fifth percentiles, 2,493 particles/cm^3, 68,061 particles/cm^3),

whereas the number concentrations were 54,476 particles/cm^3 (fifth and ninety-fifth percentiles, 2,778 particles/cm^3, 233,266 particles/cm^3) and 34,661 particles/cm^3 (fifth and ninety-fifth percentiles, 10,476 particles/cm^3, 137,333 particles/cm^3) in welding UNP-L and UNP-M, respectively. The outdoor number concentration has been reported to be 33,000 particles/cm^3, whereas values ranging from 69,000 to 230,000 particles/cm^3 have been reported during the welding processes in automotive plants (Buonanno *et al.,* 2011). Both the concentration profiles and size distributions differed between the ENP workplaces and the welding workplaces in this study.

Background measurement

The measurement of background levels in nanoparticle exposure assessments is controversial (Kuhlbusch *et al.,* 2011). Background aerosols, including engineered particles, can be natural occurring or incidental. Several methods can be used to estimate background levels; these include using the levels before or after the process or taking outdoor ambient concentrations (Ramachandran *et al.,* 2011). In this study, the background was determined during the downtime, after the work was finished. However, it was still difficult to set the background level because of fluctuations and the possibility of exposure from other emission sources, despite the lack of primary emission sources. It is necessary to distinguish ENPs from incidental nanoparticles in nanoparticle exposure assessments (Ono-Ogasawara *et al.,* 2009). Several strategies have been used to measure background concentrations; these include using concentrations measured at the same location before or after the tasks, using outdoor concentrations, and using concentration

measured during activity and subtracting the infiltration fraction (Brouwer *et al.,* 2009). Subtraction of the background concentration is an issue to consider in nanoparticle exposure assessments of a workplace with low levels because the final values can be negative. The assessment of background levels should also consider both real-time measurement as well as analysis by electron microscope or wet chemistry to identify morphology and composition. Therefore, further research regarding background differentiation is required.

Real-time monitoring and electron microscope

In this study, real-time monitoring of nanoparticles and electron microscope were used to identify sources of the nanoparticles. Real-time monitoring, providing temporal variations, depends on the task or location and the sources of the nanoparticles (Ramachandran *et al.,* 2011). An electron microscope was used to confirm the shape (i.e., size, morphology, and aggregation status) of the sampled particles. At present, no standard protocol for electron microscope and EDS exists, and preliminary recommendations for reporting electron microscope results have been proposed. The characteristics of the observed nanoparticles should be reported systemically (Brouwer *et al.,* 2012). As shown in Figures 2-3 (b) and 2-3(c), the SEM image and the EDS spectrum may provide evidence that the sampled nanoparticles originated from the aluminum grinding process when a peak concentration was measured by SMPS (Figure 2-3 (a)). In this case, a short-term sample was collected close to the source. Two or three measurement techniques used together provide a powerful sampling approach and

increase the quality of the data analysis (Maynard and Aitken 2007). The single nanoparticles were also aggregated with one another. Nanoparticles are not found as single particles but are typically present in significantly larger-sized aggregates (Baveye and Laba 2008). Use of SEM or TEM (Transmission Electron Microscope) is useful for compensating for the weak points in real-time monitoring because real-time monitoring cannot confirm the shapes of the captured particles. Therefore, both complementary methods (real-time monitoring and electron microscope analysis) were recommended (Peters *et al.,* 2008).

Time–activity diary recording

During this study, a researcher observed and recorded a time–activity diary (TAD) for all tasks during the sampling period with the exception of the off-duty period. The TAD was particularly important for task-based sampling because real-time monitoring data could provide data on only the airborne concentrations in the workplaces. Generalizing tasks is important to compare the exposure. In ENP workplaces, it is difficult to generalize because most of the manufacturing process were different by company due to the patent. In the ENP workplace, several tasks occurred during production; however, most tasks in the welding workplaces involved only welding. Because elimination of a TAD may result in analysis errors, it is necessary to maintain this record using either a researcher or a video exposure monitoring technique such as PIMEX (Picture Mix Exposure) to supplement real-time monitoring (Beurskens-Comuth *et al.,* 2011).

Effect of LEV and isolation systems on nanoparticle concentrations in ENP workplace

A number of different factors affect workplace nanoparticle concentrations, such as workplace volume, amount of material handled, manner of handling, and so on. The type of ventilation may be a key factor in determining concentration. There was a difference in the concentrations between the workplace with the LEV system (ENP-K) and that with no LEV (ENP-J). In the case of ENP-J, no LEV system minimized exposure, and much higher concentrations were observed during tasks such as pouring, accidental spillage, opening of the powder grinder cover, and cigarette smoking, as shown in Figures 2-2 and 2-3. Lower concentrations were observed in ENP-K because a LEV system and a system for containment of the manufacturing system were operating (Figure 2-4a). It appeared that no leakage occurred during the normal operation of ENP-K. However, during the collection of manufactured ENPs into a 2-L bottle after operation, some ENPs were released. During maintenance work or during cleaning between each operation when workers opened a side door, ENPs were emitted, even though a LEV system was operating. In most cases, it is necessary to minimize exposure using an engineering control such as isolation or ventilation. Adequate ventilation systems, such as a LEV or a fume hood, should be utilized to minimize exposure to nanoparticles. In a previous study of unintentionally generated nanoparticles (i.e., welding fumes), the effects of ventilation systems were evaluated during arc welding. The concentrations after a booth-type ventilation system was employed during arc welding decreased concentrations from 7.78

x 10^5 particles/cm^3 to 1.48 x 10^4 particles/cm^3 (Lee *et al.,* 2007). During testing in the laboratory with aluminum nanopowder, concentrations decreased when the face velocity of the fume hood was in the range of 0.4 to 0.6 m/s (Tsai *et al.,* 2009). However, nanoparticles could still escape from a traditional fume hood under certain conditions. One such condition involved the energetic movements of the workers because such movements were able induce the strong turbulence necessary to transfer nanoparticles to a worker's breathing zone (Tsai *et al.,* 2010). When the installation of adequate ventilation systems is not practical, the final measure is personal protective equipment (PPE) to reduce the inhalation exposure among workers (Maynard and Aitken 2007; Oberdörster *et al.,* 2005; Peters *et al.,* 2008). Thus, an adequate ventilation system may lead to a minimization of exposure to nanoparticles.

Current OELs (Occupational Exposure Limits)

Currently, no generally accepted standard OELs for nanoparticles exists (Schulte *et al.,* 2010). However, for particles with a density of >6,000 kg/m^3 and number concentrations that range from 1 to 100 nm, the IFA has recommended benchmark limits of 20,000 particles/cm^3 for metal oxides and other biopersistent granular nanomaterials. In the case of nanoparticles with densities below 6,000 kg/m^3, the limit is 40,000 particles/cm^3, which indicates that size and density were the important factors when workers were exposed to nanoparticles (IFA 2009). The containment of manufacturing systems may reduce exposure in the workplace according to the results for ENP-K. No concentration exceeded 20,000 particles/cm^3, which is the recommended benchmark

exposure limit recommended by the IFA. Therefore, the current OELs were not appropriate and, as a result, it is necessary to develop OELs for nanomaterials. The purpose of OELs is to minimize the possibility of the adverse health effects that may result from exposure to hazardous materials (Schulte *et al.,* 2010). Traditional mass-based (integrated) exposure assessments may miss the peak concentrations during the sampling time. Prior to the establishment of OELs for nanoparticles, it is necessary to set up a standardized sampling strategy, including metrics, background, and measurement devices. Thus, task-based exposure assessments may be important for determining a worker's nanoparticle exposure.

Limitations

This study had several limitations. First, area sampling was conducted. Area sampling is difficult to translate into personal exposure (Lee *et al.,* 2011). Second, this study was cross-sectional and did not reflect the entire exposure. Third, real-time data represent time-series data, which are known to be strongly correlated between samples. This can lead to an overestimation of statistical significance when using a *t*-test for statistical testing. This overestimation can be overcome using the autoregressive integrated moving average (ARIMA) model (Klein Entink *et al.,* 2011). Despite these limitations, this study may provide an understanding of nanoparticle sources, both engineered and unintended, because only limited data are currently available concerning nanoparticle exposure assessments in the workplace even though the number of workers handling nanoparticles continues to increase. Additionally, this study utilized a task-based approach to workplace

exposure assessment.

Conclusion

Standardization of ENP exposure monitoring is required prior to the risk assessment associated with nanoparticle management. A nanoparticle exposure assessment utilizing task-based sampling was performed in this study. The data were collected from two ENP workplaces and two welding workplaces using real-time measuring devices, gravimetric sampling analysis, and an electron microscope.

The nanoparticle concentrations varied depending on the tasks performed, metric adopted, and working status (working or off-duty). The data indicated differences in the concentration profiles between ENP workplace and the unintended nanoparticle generation in welding workplaces. Thus, task-based exposure assessments can provide useful information regarding nanoparticle exposure profiles and can be used as exposure assessment tools.

Chapter 3. Comparison of Data Analysis Procedures for Real-time Nanoparticle Sampling Data using Classical Regression, AR(1), and ARIMA Models

Introduction

Nanoparticle exposure assessment in the workplace has been performed by many research groups because of the rapid growth of nanotechnology and the probable risks of nanoparticle exposure. Measurement strategies, sampling devices, and data analysis methods vary among studies. Therefore, standardization of measurement strategies and data analysis is necessary for risk assessment, epidemiology, and exposure control measures as well as for determining compliance with occupational exposure limits in the near future (Brouwer *et al.,* 2012; Van Broekhuizen *et al.,* 2012). Sampling strategies have been published by many organizations and have been specified in detail (Asbach *et al.,* 2012; Brouwer 2012; Gomez *et al.,* 2014; Ham *et al.,* 2012; Honnert and Grzebyk 2013; Methner *et al.,* 2009; Neubauer *et al.,* 2013). However, insufficient guidelines regarding data processing have been formulated, and researchers are using their own methods for analysis (Klein Entink *et al.,* 2011; Van Duuren-Stuurman *et al.,* 2012).

Several methods are available for airborne nanoparticle sampling in the workplace. Among them, real-time monitoring is mainly used for nanoparticle exposure assessments. Real-time data constitute a time series, which is a sequence of observations taken sequentially in time. There are advantages using a concentration profile over time to determine the source of particles, their mobility and simplicity have advantages when employing a real-time monitor. However, the interpretation of time-series data requires caution because real-time data are highly correlated. This phenomenon, termed

autocorrelation, means that the set of measurement results are not independent, i.e., there is significant autocorrelation among samples in a series.

Due to the basic assumption of independence among data when employing statistics (Lin *et al.,* 2013), it is necessary to adjust for autocorrelation when interpreting time-series data in exposure assessments (Houseman *et al.,* 2002). Two methods are commonly used to control for autocorrelation. One entails modeling the autoregressive component of time series data, an approach adopted by the first-order autoregressive (AR(1)) and autoregressive integrated moving average (ARIMA) models, and the other is the use of a longer averaging time. AR(1) and ARIMA models are not very different. AR(1) could be one special case of ARIMA model. Several studies have accounted for autocorrelation using an AR(1) model (Fuller *et al.,* 2012; Levy *et al.,* 2002; Zwack *et al.,* 2011) in atmospheric environmental monitoring and modelling. When using an AR(1) model, the data should be stationary. Therefore, an artificial transformation of non-stationary data into stationary data is needed before data processing. In ARIMA(p, d, q) models (Box and Jenkins 1976), a differencing term (d) transforms stationary data, and its applicability to handling nanoparticle exposure assessment data has been suggested in recent studies (Brouwer *et al.,* 2012; Ham *et al.,* 2012; Klein Entink *et al.,* 2011). The use of a longer averaging time may lead to a reduction in the autocorrelation of real-time monitoring data, but it could lose specific events, especially sudden emissions, and thereby impair the results of statistical analysis (Houseman *et al.,* 2002; Levy *et al.,* 2002).

In the real-time monitoring of airborne nanoparticles, the time interval varies according to the principle of operation and type of instrument. For example, the P-trak (Model 8582, TSI Inc., USA) interval is 1 s to 30 min, whereas the TSI Optical Particle Sizer (OPS: Model 3330, TSI Inc., USA) interval is over 1 s. In the scanning mobility particle sizer (SMPS), the time interval is different from that of other real-time monitors because of its size bin. The sampling time varies according to the number of size bins, iteration, and range of measurements. One measurement cycle of a simple SMPS (Nanoscan Model 3910, TSI Inc., USA) is 1 min (fixed). The measurement interval for the full-size SMPS (Model 3936L75, TSI, Inc., USA) that used in a previous study was 135 s (120 s upscan, 15 s retrace time) for one cycle, for particles from small to large in size (14.6-661 nm) (Ham *et al.,* 2012) and one cycle of other SMPS was 406 s with 10 s of retrace time (SMPS+C, model 5.403, Grimm GmbH, Germany) for particles from large to small (11.1-1083.3 nm) (Asbach *et al.,* 2009).

Although autocorrelation should be considered first when handling real-time monitoring data, most previously reported studies of nanoparticle exposure assessment in the workplace have ignored it and used a central tendency (arithmetic mean, geometric mean, median), measure of dispersion (range, interquartile range, standard deviation, geometric standard deviation), or graphical presentation (Brouwer *et al.,* 2013; Heitbrink *et al.,* 2008; McGarry *et al.,* 2013; Methner *et al.,* 2012; Park *et al.,* 2010; Peters *et al.,* 2008; Tsai *et al.,* 2012).

The ARIMA model was introduced in a study that considered autocorrelation using simulations and provided three examples using real-time data (Klein Entink *et al.,* 2011). Therefore, the verification of statistical methods using real-time monitoring field data is necessary.

The aim of this study was to compare the results of (1) statistical methods (classical regression and the AR(1) and ARIMA models) and (2) to investigate the effect of different averaging times to account for autocorrelation using field data and suggest possible data interpretation methods for real-time nanoparticle monitoring data.

Materials and Methods

Sampling site information

Three workplaces, two fabricating engineered nanoparticles (LAB-N and ENP-O) and the other for incidental nanoparticles (UNP-P), were investigated to obtain real-time data and related information regarding nanoparticles. Table 3-1 shows that the basic characteristics of the investigated workplaces. LAB-N was a material research and development laboratory that handles engineered nanoparticles (Fe_2O_3, Ti). The floor area was 78 m^2. The main experimental procedures undertaken were weighing, sonication, reaction on a hot plate, centrifuging, and drying on a furnace. All experiments were performed using a small fan on the window for ventilation. For weighing, the powder was moved from a bottle to weighing paper on a micro balance with a spoon. The next step was a sonication procedure that disperses the powder in a liquid medium such as ethanol and distilled water. The reaction process was performed on a hot plate with a magnetic stirrer at a temperature of about 100 °C. In both steps, there was no wrapping on the beaker and no local exhaust ventilation system. In ENP-O, silver, aluminum, nickel, and copper nanoparticles were manufactured. During sampling, they produced nickel and copper nanoparticles. The area of the workplace was 97 m^2. The four workers wore only poly gloves to reduce their exposure. The manufacturing processes in the ENP facilities were enclosed with glass sashes and included a ventilation system. Additionally, a natural ventilation system was operated. The workplaces where different processes

were undertaken were separated by walls. Engineered nanoparticles (Ni and Cu) were generated by eight well-contained booth-type facilities that used a pulsed wire evaporation method. The metal wire was evaporated by a 30 kV pulse power and condensed into a cyclone, where particles were collected. During the process, all side walls were closed, and a flexible duct connected to the ceiling of the booth-type facilities was operated. On the sieving process, LEV was installed. UNP-P was a facility that assembled excavators, where welding is undertaken to bond the excavator parts during day and night shifts. The other processes undertaken were metal cutting, machining (drilling, tapping, and bending), and grinding, but focused on the welding process. Nanoparticles produced by CO_2 gas metal arc welding on mild steel were measured. Thirty of a total of 58 employees were responsible for welding, and measurement instruments were located in the welding area where the influence of the other processes was minimal. The area was 2,017 m^2, and natural ventilation was available through doors and windows.

Sampling strategy

In LAB-N, the sampling time was about 22 h due to the experimental schedule. The background level was determined during the period when workers were off duty. In ENP-O, daily working time was 7 hours. The lunch break period was selected to determine the background level of ENP-O because it was characterized by a lower, more stable concentration than other work periods. For UNP-P, a 32-h sampling was performed to assess shift work: two full day time shifts and the night shift between them. During the

night, there was break period when the background level could be determined.

The device used for measurement was a SMPS (Nanoscan Model 3910, TSI, Inc., USA). The inlets of each instrument were located within at least 30 cm of one another to reduce the measurement error. The height of the inlets was between 1.2 and 1.5 m (Ham *et al.,* 2012). The SMPS was used to compare the data analysis procedures for real-time nanoparticle sampling data. a time activity diary (TAD) was kept to record the activity of the workers, including break time, lunch time, and the start or end of work shifts, as well as a description of the process being undertaken and contextual information about the workplace. During the downtime at night in LAB-N, when no workplace activities occurred, the TAD was not kept. In ENP-O, the TAD was kept by a researcher. In UNP-P, the night working time schedule was obtained by interviewing staff before the sampling began. For data analysis, coding for work status and the tasks performed was determined. Coding was generated by using dummy variables to distinguish between tasks during statistical analysis. For portability, a sampling cart was used to move the sampling devices.

Real-time measurements

To determine the distribution of particle sizes, an SMPS with a detectable size range from 10 to 420 nm and a concentration range of 0 to 10^6 particles/cm^3 was used. The inlet flow rate was 0.75 l/min, and the sample flow rate was 0.25 l/min. A flow check was performed in the laboratory before any measurements. The sampling time of the SMPS

was one minute per averaging time, and it measured particle sizes from small to large with 13 sequence channels. A cyclone was used to remove the larger particles. The particles were collected from the inlet and passed through the aerosol neutralizer using a unipolar charger. Particles were separated by mobility diameter using a radial differential mobility analyzer (RDMA) before being counted using an isopropanol-based CPC. An external isopropyl reservoir was used.

Statistical analysis

Classical regression, AR(1) and ARIMA model were used to apply for analyzing real time monitored data which is time series in this study. AR(1) was used to perform for atmospheric research to account for autocorrelation (Fuller *et al.,* 2012; Houseman *et al.,* 2002; Levy *et al.,* 2002). ARIMA was recently suggested for nanoparticle exposure assessment data analysis (Brouwer *et al.,* 2012; Ham *et al.,* 2012; Klein Entink *et al.,* 2011).

The first step in any time-series data analysis is to plot the observed data with respect to time. This enables the determination of any trends, seasonality (in long-term data), discontinuities, and outliers in the data. Most of the theory regarding the analysis of time series considers stationary time series, and for this reason, the analysis requires the conversion of a non-stationary series into a stationary series. It is important to check whether the data are stationary because, in contrast to the ARIMA model, the data should be stationary for the AR(1) model. The ARIMA model should also use stationary data,

but the data do not need to be transformed by the researcher because they are transformed to stationary data using the differencing term I(d) during the ARIMA procedure. Several methods can be used to transform the data into stationary data, such as the use of logarithms, square roots, and differencing. To check that the data are stationary, a unit root test should be performed. A Kwiatkowski–Phillips–Schmidt–Shin (KPSS) tests is used to check for a stationary series in autoregressive models (Kwiatkowski *et al.,* 1992). Once the data are proven to be stationary, the following process can be followed. AR(1) and ARIMA models were separated because ARIMA model is appropriate for real time monitored data with relatively short sampling duration because it is difficult to get the stationary data and this model could be applied to both stationary and non-stationary.

AR(1) model

The AR(1) model is a special case of the ARIMA model. AR(1) is suitable for stationary data (little varied with the time) and is used as a simple model. An autocorrelation function (ACF) is independent of the scale of the measurement of the time series (Box and Jenkins 1976). To determine the ACF coefficient of an AR(1) model, acf( ) was used to calculate the first lag of the autocorrelation function for imputing the coefficient. The gls( ) function was used for Generalized Least Squares (GLS) regression. The estimation of GLS is commonly used in time-series regression (Fox and Weisberg 2011). The corAR1() function should be used to represent an autocorrelation structure of order 1 (Pinheiro *et al.,* 2013). As mentioned above, it is necessary to check that the data are stationary. Differencing was performed when the data were not stationary, but it was

impossible to obtain estimated values for each task. Therefore, in this study, checking for stationary data was ignored when comparing with the ARIMA model, in which the data are automatically checked to confirm stationary, and an estimated value is provided.

ARIMA model

ACF and the partial autocorrelation function (PACF) can be used to determine the AR and moving average (MA) terms. To determine the best ARIMA model according to the Akaike information criterion (AIC), the auto.arima() function conducts a search for all possible models. AIC is used to measure both the fit and unreliability of model (Ozaki 1977). Here, it was used to obtain the values of p, d, and q, which were the coefficients for ARIMA(p, d, q) model. The parameters for ARIMA model is classified where p is the order of Auto-Regressive model, d is for order of differencing and q is the order of Moving Average model. (Cowpertwait 2009; Hyndman 2013; Hyndman and Khandakar 2008). In this study, auto.arima() function was used to determine the order of those parameters for ARIMA model because it is difficult and ambiguous to determine the model using the ACF and PACF graphs for non-experts in ARIMA.

Data analysis was conducted using R (version 3.0.2; R Development Core Team, Vienna, Austria). An alpha level of 0.05 was used to determine statistical significance throughout the study. Classical regression analysis and the AR(1) and ARIMA models were used to examine differences among the work tasks or working statuses. For classical regression analysis, the lmtest package (version 0.9-32) was used. To run the AR(1) and

ARIMA models, nlme (version 3.1-113) and forecast (version 4.8) packages were used (Hothorn *et al.,* 2014; Hyndman 2013; Pinheiro *et al.,* 2013).

Results

Table 3-1 summarizes the characteristics of the workplaces investigated with respect to the type of particles and ventilation and the particle number concentrations.

Table 3-1. Summary of the workplace characteristics and sampling statistics in the three workplaces

	LAB-N	ENP-O	UNP-P
Primary particles	Engineered nano particles (Fe_2O_3, Ti)	Engineered nano particles (Cu, Ni)	Incidental particles (Welding fume)
Floor area (m^2)	78	97	2,017
Ventilation type	Natural ventilation	LEV and Isolation	Natural ventilation
No. of workers	7	6	30
Sampling duration	One shift + One off-duty time	One shift	Two day shifts + One night shift
Main Process	Weighing, sonication, reaction on a hot plate, centrifuging, and drying	Manipulation of facilities, collecting, and sieving	Welding
Time interval (min.)	1	1	1
Observations (n)	1,310	407	1,870
Mean ± SD ($particle/cm^3$)	10,488 ± 6,842	11,598 ± 2,164	131,349 ± 111,650
GM (GSD) ($particle/cm^3$)	8,480 (1.96)	11,386 (1.21)	88,550 (2.60)
Median ($particle/cm^3$)	9,843	11,952	110,463
5^{th} percentile ($particle/cm^3$)	2,945	8,230	16,717
95^{th} percentile ($particle/cm^3$)	21,745	14,793	336,827
Filter-based mass ($\mu g/m^3$)	63.00[a] 26.83[b]	130.00[c]	504.92[d] 216.51[e] 433.88[f] 44.87[g]

Sampling duration

N: Day1 working time ([a]323 min), day 1 off-duty time ([b]952 min), O: Day 1 working time ([c]509 min), P: Day 1 working time ([d]404 min), day 1 night shift ([e]914 min), day 2 working time ([f]524 min), day 2 lunch time ([g]52 min)

Time-series plots of LAB-N, ENP-O, and P are presented in Figures 3-1, 3-2, and 3-3, respectively. As shown in Figure 3-1, the number concentration of ENP measured by SMPS in LAB-N varied among processes and over time. Three processes were identified in LAB-N, indicated by the colored boxes with numbers. The uncolored part of Figure 3-1 shows the concentration profile for non-experimental periods. The profile fluctuated depending on the process being operated, with the highest concentration during reaction (peak 3 in Figure 3-1), followed by sonication (peak 2), and weighing (peak 1) of Fe_2O_3 and Ti particles. The reaction process was performed in an open space with no control measures. The boiling process proceeded at 100 °C using a magnetic stirrer and without wrapping. The sonication process was also performed without wrapping. The weighing process was performed with a vertical partition installed outside of microbalance. Part 4 of Figure 3-1 shows the number concentration measured during off-duty time when no experimental work was underway. There was an unexpected concentration drift from 20:30 to about 00:00, which sometimes occurs when a real-time monitor was used and cannot be easily explained. The uncolored areas show time periods when no experimental work was ongoing, but researchers were in the laboratory.

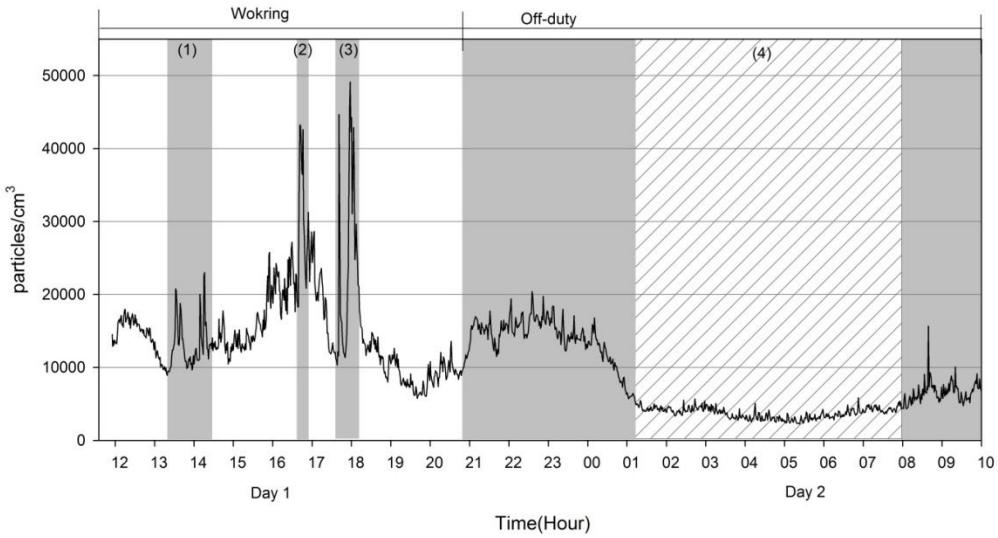

Figure 3-1. Time-series plot of the total concentration profile in LAB-N. (1) Weighing process for Fe_2O_3 and Ti. (2) Sonication. (3) Reaction. (4) Off duty (Background; shown in hatching region). Other sections are non-experimental periods.

Figure 3-2 shows a time-series plot of ENP-O during one workshift. Two processes were in operation. For one, a worker collected the ENP from a cyclone inside the manufacturing facility (Figure 3-2. (2)), and the other was a process that sieved the collected nanoparticles (Figure 3-2. (4)). The sieving process was performed automatically by vibrating equipment with an LEV system. Other periods in Figure 3-2 where the facilities were operated are labelled as (1). Part (3) of Figure 3-2 was the lunch time, during which there was a lower concentration than during the operation periods.

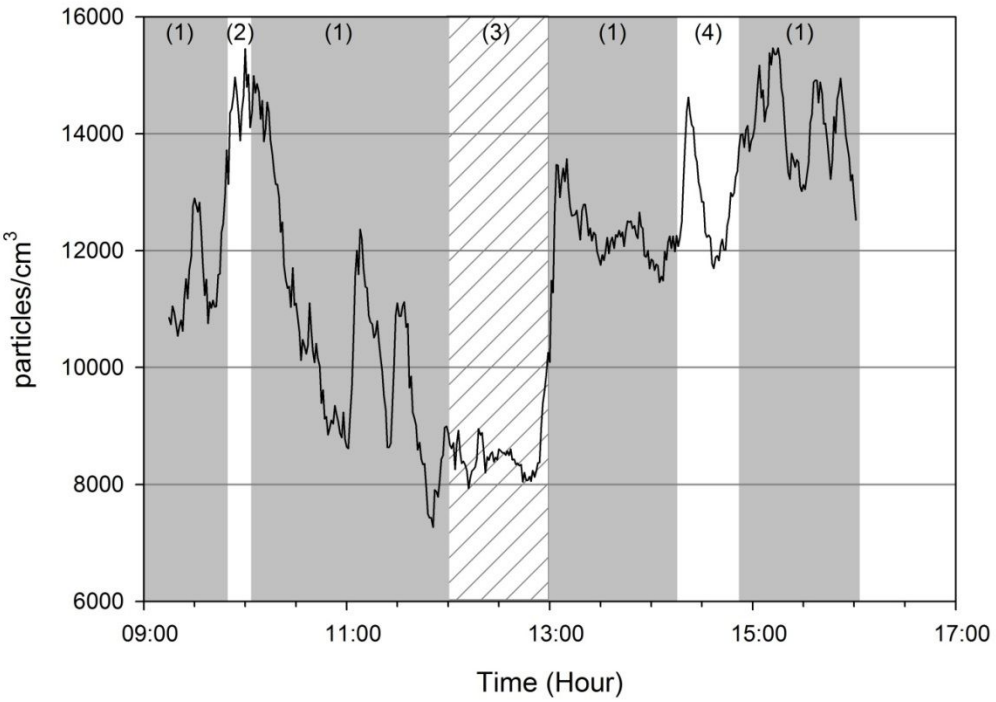

Figure 3-2. Time-series plot of the total concentration profile in ENP-O. (1) Work periods, (2) Collection of ENP, (3) Lunch (background; shown in hatching region), (4) Sieving process.

Figure 3-3 shows a time-series plot of the processes occurring in UNP-P. There were three work shifts (two day time and one at night). The colored boxes show the work process periods. The uncolored parts of Figure 3-3, (1), (2), (4) and (5), are break times such as lunch and dinner. The night shift started on the first day of sampling at 20:00 and ran to 08:00 on the morning of the second day. There was a long break time during the night (3) (shift 2) because of the flexible working conditions.

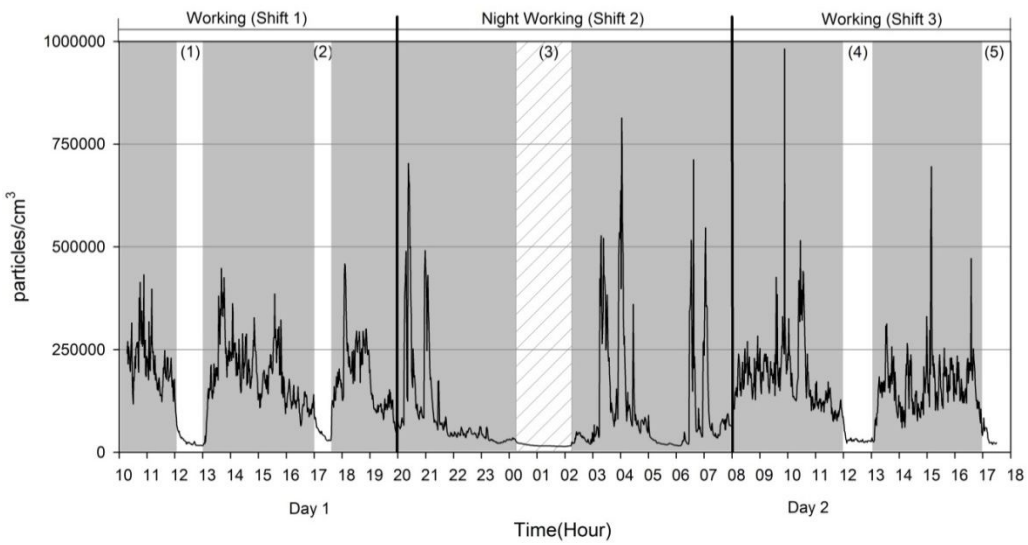

Figure 3-3. Time-series plot of the total concentration profile in UNP-P. Gray-boxes indicate work shifts during the day. Meal breaks (1), (2), (4), (5) are white; Background break time during the night shift (Ref.) is shown in hatching region (3).

Comparison of Statistical Approaches

To find the best model for data, the AIC values were compared (Table 3-2). The AIC values from classical regression were higher than AR(1) and ARIMA model. The AIC values for AR(1) and ARIMA were very similar. AIC values of 1 minute data for classical regression was 48,333 and for both AR(1) and ARIMA were 45,890 in LAB-N. For ENP-O, AIC values of 1 minute data of classical regression, AR(1) and ARIMA were 7,211, 5,855 and 5,856, respectively. AIC values for workplaces were 23,265 (classical regression), 21,116 (AR(1)) and 21,094 (ARIMA) by 1 minute data. In 5 minute and 10 minute averaging time data shows also the AIC values for classical regression were higher than AR(1) and ARIMA.

Table 3-2. Akaike Information Criteria (AIC) values for regression, AR(1), and ARIMA models and averaging times

Workplace		1 min.	5 min.	10 min.
LAB-N	Classical Regression	48,333	9,598	4,889
	AR(1)	45,890	9,255	4,788
	ARIMA	45,890	9,332	4,875
ENP-O	Classical Regression	7,211	1,452	733
	AR(1)	5,855	1,274	633
	ARIMA	5,856	1,296	660
UNP-P	Classical Regression	23,265	4,625	2,290
	AR(1)	21,116	4,312	2,060
	ARIMA	21,094	4,337	2,108

To compare the results of the AR(1) and ARIMA models for LAB-N, the estimated parameters are summarized in Table 3-3. The off-duty time during day 2 (from 1:00 to 8:00) was set as the background, because there was a stable concentration in LAB-N at this time. The data shows very high autocorrelation (autocorrelation coefficients for the first lag were 0.958 for 1 min, 0.898 for 5 min and 0.900 for 10 min data). In the classical regression analysis, all tasks (weighing, the reaction and sonication processes, and non-experimental intervals during the day) produced significantly different ($p<0.01$) results compared with the background. The AR(1) models showed no significant difference between the results obtained during the weighing process ($p = 0.06$) and the background values. The ARIMA model showed no significant difference between the results obtained during the weighing process ($p = 0.27$) and non-experimental time ($p = 0.07$) compared with the off-duty background period. There was no background estimate value in the ARIMA model due to the first-order differentiation that was used to make the data stationary. Therefore, a background estimate was not calculated, and the other estimated value was an absolute value.

Table 3-3 shows the results for the three different statistical models with different averaging times in LAB-N. The classical regression model found significant differences between the results for 1, 5, and 10 minutes. The results of the AR(1) and ARIMA models showed significantly higher values for the reaction and sonication processes than for the off-duty period at all averaging times. In contrast, there was no significant difference between the results obtained for the off-duty period and the weighing process

and non-experimental time according to the AR(1) and ARIMA models, with the exception of the result obtained from AR(1) for the 1-min average time period between the off-duty period and the non-experimental time ($p = 0.02$).

Table 3-3. The total concentration according to the AR(1), and ARIMA models using different averaging times in LAB-N

Classical regression									
	1-min average			**5-min average**			**10-min average**		
Parameter (Particle/cm^3)	**Estimate**	**SD**	***p*-value**	**Estimate**	**SD**	***p*-value**	**Estimate**	**SD**	***p*-value**
Off duty (4) (Ref.)	3,833	227	<0.01	4,724	408	<0.01	4,444	524	<0.01
Weighing (1)	8,895	566	<0.01	8,733	1,182	<0.01	8,312	1,460	<0.01
Non-exp.	7,649	292	<0.01	7,603	589	<0.01	8,052	749	<0.01
Reaction (3)	22,256	911	<0.01	21,631	1,801	<0.01	21,912	2,285	<0.01
Sonication (2)	34,715	1,665	<0.01	30,108	3,065	<0.01	30,388	3,888	<0.01
AR(1)									
	1-min average (ACC* = 0.958)			**5-min average (0.898)**			**10-min average (0.900)**		
Parameter (Particle/cm^3)	**Estimate**	**SD**	***p*-value**	**Estimate**	**SD**	***p*-value**	**Estimate**	**SD**	***p*-value**
Off duty (4)	7,408	1,550	<0.01	8,330	1738	<0.01	8,171	1,950	<0.01
Weighing (1)	3,498	1,817	0.06	1,844	1978	0.35	1,582	2,035	0.44
Non-exp.	2,913	1,247	0.02	1,850	1166	0.11	2,603	1,404	0.07
Reaction (3)	4,888	1,852	0.01	12,817	2247	<0.01	13,278	2,058	<0.01
Sonication (2)	12,221	1,866	<0.01	11,522	2039	<0.01	13,710	2,068	<0.01
ARIMA (p, d, q)									
	1-min average ARIMA (2, 1, 2)			**5-min average ARIMA (1, 1, 1)**			**10-min average ARIMA (0, 1, 2)**		
Parameter (Particle/cm^3)	**Estimate**	**SD**	**p-value**	**Estimate**	**SD**	**p-value**	**Estimate**	**SD**	**p-value**
Off duty (4)	-**	-	-	-**			-**		
Weighing (1)	1,822	1,639	0.27	1,507	1759	0.39	779	1,976	0.70
Non-exp.	2,073	1,160	0.07	673	1106	0.54	1,605	1,389	0.25
Reaction (3)	7,584	1,748	<0.01	11,957	1953	<0.01	10,821	2,454	<0.01
Sonication (2)	13,956	1,765	<0.01	11,982	2060	<0.01	13,093	2,041	<0.01

*** ACC: Autocorrelation coefficient for the first lag**

****A non-zero mean is allowed after the series has been differentiated. Therefore, the estimate from the ARIMA model might be an absolute term.**

(1) **13:10-14:30: Weighing; (2) 16:40-16:47: Sonication; (3) 17:40-18:07: Reaction; (4) 1:00-08:00: Off duty (Background level); Others: Non-experimental time**

Table 3-4 presents the results of three different analysis methods. For the classical regression, working, sieving, and collecting were significantly different compared with the lunch time period, which was used as the background reference. The data shows very high autocorrelation (autocorrelation coefficients for the first lag were 0.987 for 1 min, 0.925 for 5 min and 0.844 for 10 min data). The AR(1) model indicated no significant difference between the background and the results obtained during the sieving process (p = 0.19). In the ARIMA model, the results obtained during the sieving process (p = 0.50) and the working time (p = 0.07) were not significantly different from the lunchtime background values.

Table 3-4 shows the results for the three different statistical models with different averaging times in ENP-O. The results of the classical regression analysis for working time, the sieving process, and collecting ENP from facilities were significantly different from those for the lunch time period (p<0.01). However, in the AR(1) and ARIMA model results, only the collection of ENP was significantly different from the lunchtime results. The AR(1) and ARIMA model results for the lunch period were not significantly different from those for the sieving process. The results for the day shift from the AR(1) model were significantly different from those for lunch time (p = 0.02), unlike in the ARIMA model.

Table 3-4. The total concentration for AR(1), and ARIMA models with different averaging times in ENP-O

Classical regression									
	1-min average			5-min average			10-min average		
Parameter (Particle/cm^3)	**Estimate**	**SD**	***p*-value**	**Estimate**	**SD**	***p*-value**	**Estimate**	**SD**	**p-value**
Lunch (3) (Ref.)	8,585	215	<0.01	8,924	437	<0.01	9,391	625	<0.01
Working (1)	3,397	236	<0.01	2,847	491	<0.01	2,224	695	<0.01
Sieving (4)	4,273	361	<0.01	4,076	698	<0.01	3,758	993	<0.01
Colleting ENP from facilities (2)	6,105	604	<0.01	5,386	797	<0.01	4,041	1,088	<0.01
AR(1)									
	1-min average (ACC* = 0.987)			**5-min average (0.925)**			**10-min average (0.844)**		
Parameter (Particle/cm^3)	**Estimate**	**SD**	***p*-value**	**Estimate**	**SD**	***p*-value**	**Estimate**	**SD**	***p*-value**
Lunch (3) (Ref.)	11,262	1,122	<0.01	11,192	1067	<0.01	10,958	1,000	<0.01
Working (1)	472	198	0.02	506	460	0.28	788	513	0.13
Sieving (4)	408	313	0.19	409	728	0.58	1,228	920	0.19
Colleting ENP from facilities (2)	1,095	314	<0.01	1,990	730	<0.01	2,378	819	<0.01
ARIMA									
	1-min average ARIMA (1, 1, 2)			**5-min average ARIMA (0, 1, 1)**			**10-min average ARIMA (0, 1, 0)**		
Parameter (Particle/cm^3)	**Estimate**	**SD**	***p*-value**	**Estimate**	**SD**	***p*-value**	**Estimate**	**SD**	***p*-value**
Lunch (3) (Ref.)	-**	-	-	-**	-	-	-**	-	-
Working (1)	336	188	0.07	355	409	0.39	709	491	0.15
Sieving (4)	196	295	0.50	-388	667	0.56	1,079	886	0.22
Colleting ENP from facilities (2)	991	293	<0.01	1,296	635	0.04	2,313	777	<0.01

*** ACC: Autocorrelation coefficient for the first lag;**

**** A non-zero mean is allowed after the series has been differentiated. Therefore, the estimate from the ARIMA model might be an absolute term.**

(1) 9:15–9:54, 10:02–11:59, 13:01–14:17, 14:51–16:01 Working; (2) 9:54–10:02 Colleting ENP from facilities; (3) 12:00–13:00 Lunch; (4) 14:18–14:51 Sieving

To compare the results of the classical regression, and AR(1), and ARIMA in UNP-P, the estimated parameters are shown in Table 3-5. The data shows very high autocorrelation (autocorrelation coefficients for the first lag were 0.887 for 1 min, 0.797 for 5 min and 0.456 for 10 min data).

Four categories were determined for UNP-P: daytime shifts, meals (lunch, dinner), night shift, and the background (the non-working period during the night shift). From 00:32 to 2:12, there was no work activity in UNP-P. Therefore, this non-working period was used to set the background concentration in the analysis. Significant differences were found between the background and the results obtained during the working time (shifts 1, 3) in the classical regression and in the AR(1) and ARIMA (1, 1, 2) models (Figure 3-3). However, no significant differences were observed between the background and the results obtained during night working in the AR(1) and ARIMA models (p = 0.20, p = 0.22, respectively). There was a significant difference between the background and the results obtained during the night shift (p<0.01) in the classical regression model. All three analyses found no difference between the background and the results obtained during meal times.

Table 3-5 shows the results for the three different statistical models with different averaging times in UNP-P. Meal times were used as a background because no work was performed during that time. The results of the classical regression model were significantly different from the background for both night and daytime work periods. The results of the AR(1) and ARIMA models showed significantly higher values for working time than for the background However, the values derived by the AR(1) and ARIMA models were not significantly higher than the background for the night shift period at all-time intervals.

Table 3-5. The total concentration for AR(1), and ARIMA models using different averaging times in UNP-P

Classical regression									
	1-min average			**5-min average**			**10-min average**		
Parameter (Particle/cm^3)	**Estimate**	**SD**	***p*-value**	**Estimate**	**SD**	***p*-value**	**Estimate**	**SD**	***p*-value**
Night background (Ref.) (3)	15,854	9,580	0.09	16,100	18,923	0.40	15,876	33,387	0.63
Meal (1, 2, 4, 5)	17,373	11,923	0.14	16,930	23,579	0.47	16,427	41,248	0.69
Night shift	86,593	10,332	<0.01	86,891	20,475	<0.01	102,543	35,979	<0.01
Day shift	165,049	10,067	<0.01	165,582	19,926	<0.01	169,201	35,066	<0.01
AR(1)									
	1-min average (ACC* = 0.887)			**5-min average (0.797)**			**10-min average (0.456)**		
Parameter (Particle/cm^3)	**Estimate**	**SD**	***p*-value**	**Estimate**	**SD**	***p*-value**	**Estimate**	**SD**	***p*-value**
Night background (Ref.) (3)	65,652	30,756	0.03	71,203	45,138	0.09	38,336	52,305	0.46
Meal (1, 2, 4, 5)	55,376	36,229	0.13	30,854	49,257	0.53	26,168	62,692	0.68
Night shift	38,442	30,087	0.20	32,064	40,180	0.42	77,412	54,899	0.16
Day shift	92,243	32,871	<0.01	90,804	45,056	0.04	139,996	55,293	0.01
ARIMA									
	1-min average ARIMA (1, 1, 2)			**5-min average ARIMA (1, 0, 1)**			**10-min average ARIMA (2, 0, 2)**		
Parameter (Particle/cm^3)	**Estimate**	**SD**	***p*-value**	**Estimate**	**SD**	***p*-value**	**Estimate**	**SD**	***p*-value**
Night background (Ref.) (3)	*	-	-	51,769	34,494	0.13	37,466	47,994	0.44
Meal (1, 2, 4, 5)	52,418	35,777	0.14	40,364	40,321	0.31	15,636	56,101	0.78
Night shift	36,359	29,892	0.22	49,889	35,128	0.15	82,157	49,629	0.10
Day shift	90,254	33,418	<0.01	115,251	37,108	<0.01	141,152	51,384	<0.01

*** ACC: Autocorrelation coefficient for the first lag**

**** A non-zero mean is allowed after the series has been differentiated. Therefore, the estimate from the ARIMA model might be an absolute term.**

(1, 2, 4, 5) 12:01–13:00 for Lunch, 17:01–17:35 for Dinner; (3) 00:32–02:12: Night Background, 20:00–08:00: Night shift Others: Working time

Discussion

This study compared three different statistical methods using three averaging times (1, 5, and 10 minutes) to examine nanoparticle exposure assessment in workplaces based on real-time data while taking autocorrelation into account. Two methods were used to achieve this. The independence of observed samples is a basic assumption of regression analysis (Osborne and Waters 2002), but most of the data gathered from real-time monitoring are not independent. Hence, a classic regression analysis breaks this rule. Therefore the AR(1) and ARIMA models were used, which can process autocorrelated data. A longer averaging time is a further method used to reduce autocorrelation (Houseman *et al.,* 2002).

Comparison of Statistical Methods

The aim of the study was to compare three different statistical methods, namely classical regression, AR(1), and ARIMA models, for processing time-series data.

All of the results obtained from classical regression analysis showed significant differences from the background, except for the comparison of meal times in ENP-O with the background, where the difference in nanoparticle concentration was relatively small between background and meal time. Therefore, the use of a classical regression may result in erroneous conclusions as reported in previous study (Brouwer *et al.,* 2012). As seen in Tables 3-3, 3-4 and 3-5, classical regression model showed that all tasks were

significantly different from background because it ignored considering autocorrelation.

However, when the AR(1) and ARIMA models were used, the results for the reaction and sonication processes in LAB-N, the collection of ENP from facilities in ENP-O, and daytime working in UNP-P all revealed values that differed significantly from the background values which was reference in analysis. The results for the weighing process in LAB-N, the sieving process in ENP-O, and the night shift in UNP-P were not significantly different from the each background because it considered autocorrelation. In ENP-O, the sieving process was performed under an LEV system to capture particles, and in UNP-P, the work load during the night shift was lower than that during the day. For the non-experimental time in LAB-N, the AR(1) model indicated a significant difference compared with the background values, but the ARIMA model found none. This might be a result of the different principles underlying the two approaches.

The ARIMA model has more I(d) terms. All of the sampled data were not stationary. The ARIMA model could determine whether the data were stationary and make the necessary adjustments by estimating a value for each task using the initial data before comparisons were performed while using auto.arima( ) function in R. When the AR(1) model is used, it is necessary to differencing to make data stationary, but no estimated value which is intercept value is obtained after differencing. In the previous study, the AR(1) model was used for real-time monitoring data but without considering data stationary (Fuller *et al.,* 2012; Houseman *et al.,* 2002; Levy *et al.,* 2002; Zwack *et al.,* 2011). The use of the ARIMA model has been suggested in recent nanoparticle

monitoring studies (Brouwer *et al.,* 2012; Ham *et al.,* 2012; McGarry *et al.,* 2013), but has only been applied once (Klein Entink *et al.,* 2011). The ARIMA model could be used to real time monitoring data which is both highly autocorrelated and non-stationary data, but industrial hygienists are not familiar with its use. After checking for stationary data, an estimation of the autocorrelation procedure should be performed, especially for AR(1). The autocorrelation coefficients of first order for 1 minute were 0.958, 0.987, and 0.887 for LAB-N, ENP-O, and UNP-P, respectively.

To decide the parameters for the AR(1) and ARIMA models, the AIC can be used to search for the best-fit model (Klein Entink *et al.,* 2011). The AIC is a relative measure of model fit that balances improvement in model fit based on log-likelihood against the number of added model parameters. Thus, it can be used to compare two (or more) models, and the model with the lower AIC value is considered to provide to the data with better fit. To achieve the parsimony coefficient which means the lowest values for each parameter (p, d, q), the order of AR(p) and ARIMA (p, d, q) increases, and the complexity of the correlation structure increases and suggests the production of a parsimonious model to achieve better analysis results (Box and Jenkins 1976). Therefore, a lower parameter (p, d, q) is recommended for ARIMA(p, d, q) modeling.

Background concentration could be measure at different time such as meal time or off-duty time at same place (near-field) or other location which is not affected by certain nanoparticles (far-field) (Brouwer *et al.,* 2012). Determining the background (reference) is important. In this study, the near-field background concentration was used as

references because of the low values and stability of nanoparticle concentrations. This could be determined by an industrial hygienist. The measured nanoparticle concentrations during the off-duty period for LAB-N, lunch time for ENP-O, and during the non-working part of the night shift were used as background values for UNP-P.

When the results of the classical regression, which ignores the autocorrelation in the time-series data, were used to summarize the three workplaces, the concentration profiles among the processes were significantly different for the three workplaces (Tables 3-3, 3-4, and 3-5). A problem arises in that autocorrelation may lead to violations of the assumption underlying classical regression analysis, which dictates that data be independent. Furthermore, if the autocorrelation is ignored, a large degree of uncertainty ensues when considering predicted concentrations (Zwack *et al.,* 2011). When the mean differences are small or the autocorrelation between samples is high, incorrect results may be obtained (Klein Entink *et al.,* 2011). Therefore, the correct statistical methods should be used that correct for the autocorrelation effect. For nanoparticle exposure assessment, the ARIMA model is a more suitable method to compare the effects of a task using time-series data, because most real-time monitoring data are not stationary.

The effect of a longer averaging time

The second aim of the study was to investigate the changes in the results due to differences in the averaging time because a longer averaging time might reduce the autocorrelation for real-time monitoring data (Houseman *et al.,* 2002; Ott *et al.,* 1994). The ARIMA model is used for real-time data in the previous discussion. As a result, the averaging time did not directly affect the result when the ARIMA model was applied. A shorter averaging time could distinguish short term variations in the nanoparticle emissions. It should be noted that a longer averaging time could unite different tasks that are undertaken in sequence into one similar exposure pattern, and therefore differences in the exposure pattern might become obscured. An expert judgment is required to categorize the importance of a series of processes when transforming the averaging time.

Rather than reducing autocorrelation, the main goal was to determine an appropriate analysis method for processing real-time monitoring data. There are advantages and disadvantages of different averaging times in time-series data. Houseman et al. (2002) and Levy et al. (2002) reported that longer averaging times may be inappropriate in microenvironmental studies because they may impair variance estimation. However, elsewhere, longer averaging times were recommended to reduce autocorrelation between measurements (Ott *et al.,* 1994). When the averaging time was set to 10 min, the influence of some processes, such as sonication for 7 minutes (peak 3 in Figure 3-1) in LAB-N and the collection of ENP from facilities in ENP-O, could be ignored or diluted in the results.

However, when the interval of a monitoring device is more than one minute, i.e., 135 s for a full-scale SMPS (Ham *et al.,* 2012) or 230 s for a short DMA and 406 s for a long DMA with a GRIMM SMPS (Asbach *et al.,* 2009), a longer averaging time should be used to analyze the data with flexibility of time interval. Caution should be exercised in the categorization process because the averaging time can cause the impact of different processes to overlap.

Conclusion

Three different statistical methods were evaluated for processing highly autocorrelated real-time monitoring data. Classical regression was not an appropriate analysis method for time-series data due to the effects of autocorrelation. The AR(1) model could be used, but the data should be stationary. Therefore, the ARIMA model is most appropriate for the analysis of real-time monitoring data because it accounts for autocorrelation and stationary of data. When using the ARIMA model, averaging times of 1, 5, and 10 minutes produced the almost same results. Flexible time averaging is suggested because it can be used with a full-size SMPS, which has a sampling interval longer than one minute. An averaging time with flexible time interval would allow a series of tasks to be determined, and the exact time used should be determined by the investigator or industrial hygienist.

Chapter 4. Comparison of the real time nanoparticle monitoring instruments

Introduction

Traditionally, gravimetric sampling which collect the airborne particles on the filter has been used to assess the workplace. However, nanoparticles are difficult to evaluate by gravimetric sampling because nanoparticles are very small size to affect the mass concentration and difficult to find the source of emission during working time. Therefore, many real time monitoring devices are available to measure the airborne nanoparticles such as a scanning mobility particle sizer (SMPS), condensation particle counter (CPC) and surface area monitor (SAM). There is controversial issue in measurement metrics in exposure assessment as well as toxicity (Oberdörster *et al.,* 2005; Wittmaack 2007). For this reason, many researcher employed and suggest the combination of measurement devices for nanoparticle exposure assessment (Ham *et al.,* 2012; Heitbrink *et al.,* 2008; Kaminski *et al.,* 2014; Maynard and Aitken 2007; Park *et al.,* 2009; Tsai *et al.,* 2011).

SMPS, CPC and SAM are the most common combinations for nanoparticle exposure assessment at workplaces (Asbach *et al.,* 2012; Ham *et al.,* 2012). Research grade (RG)-SMPS such as Grimm 5.403+C and TSI Model 3936L75 remains the golden standard of aerosol instrumentation even 20 years after its invention. It measures aerosol size distributions with high accuracy, but low time resolution, and thus cannot be used to measure rapidly changing particle size distributions at workplace because scanning time is over 2 minutes (Fierz *et al.,* 2009). However, RG-SMPS is expensive and heavy to move to sampling site and portable (P)- SMPS (TSI Model 3910 with 1 minute time interval) is cheaper than RG-SMPS but, still expensive (Fierz *et al.,* 2009). It is necessary

to find the possible surrogate measurement device to measure nanoparticles. CPC and SAM are relatively cheaper than SMPS and portable. To compare and find relation among SMPS, CPC and SAM correlation analysis is necessary.

When the number concentration was measured, measurement devices have different size and concentration range by manufacturer. In exposure assessment studies, the potentially different results from different instruments are issues when results obtained simultaneously at the same location or different locations (Watson *et al.,* 2011). Two common RG-SMPSs are manufactured by Grimm and TSI (Wiedensohler *et al.,* 2012). They have a different technique to separate particles size. Grimm SMPS measures large particles to small particles in size and TSI SMPS measures particles from small particles to large particles. Also, sampling time is different between SMPS. It may occur differences in the concentration when nanoparticles at same location with different SMPS was measured. Therefore, harmonization and investigation of difference of devices is necessary and getting the relationships between same metric measurement devices is essential for use of exposure assessment data in the future (Asbach *et al.,* 2009). There are small number of studies to compare the nanoparticles measurement instruments in the well-controlled laboratories (Asbach *et al.,* 2009; Joshi *et al.,* 2012) and no studies at workplace with our knowledge.

The aims of this study were to determine relation among three monitoring devices of nanoparticle, such as SMPS, CPC, and SAM and compare two widely used RG-SMPS for harmonization.

Materials and Methods

Sampling Facility

Three types of workplace was categorized: laboratory (LAB), engineered nanoparticle (ENP) workplace, and UNP-emitting workplaces (Table 4-1). A total of 9 workplaces were participated. Three laboratories at a university were investigated. LAB-A was an earth environment laboratory, and the primary nanoparticle was Al_2O_3. Two workers performed experiments of transfer to the crucible, transfer from the crucible to a vial, and weighing. LAB-B was involved with development of new materials, with the primary nanoparticles used being Fe_2O_3 and TiO_2. Major experiments were weighing, sonication, and reaction. Seven workers performed the experiments. LAB-C dealt with graphene for space aviation. Dip-coating processes to fabricate graphene were the primary experiments performed; together with spraying the base of the DIP coater for cleaning by five workers. A natural ventilation system and a fume hood were installed in all laboratories. Three ENP manufacturing workplaces examined. ENP-D company fabricated Ti and Zn powder for cosmetic sunscreen. Reaction, dehydration, mixing, drying, and bagging were the major processes at ENP-D company. The reaction was operated at 120 °C and 3 atm, and dehydration was performed at 60 °C. There were a natural ventilation system and no local exhaust ventilation (LEV). ENP-E company dealt with metallic nano sized powders such as copper, nickel, and silver. Nano sized powders were fabricated by the high-voltage pulsed-wire evaporation (PWE) method, and the

main products were copper-nickel alloy and nickel nanopowders for use as additives in automobile engines. The main processes were collecting and sieving. Manufacturing equipment for PWE was isolated in a cabinet equipped with a LEV system. During the manufacturing process, the glass door was closed. Amorphous silica was manufactured at ENP-F company and automation system was installed for all processes. Amorphous silica was used for abrasive materials that were applied in the chemical mechanical polishing (CMP) process for the semiconductor industry. The main process was packaging of a 10-kg bag. A natural ventilation system and LEV were operated during the bagging process. In ENP-D company, titanium dioxide and aluminum ENPs were fabricated by a worker. Natural ventilation was operated during the measurement. The worker performed several tasks not frequently. TiO_2 was extracted from $TiCl_4$ for the photocatalyst material. The liquid-phase TiO_2 was synthesized using low-temperature (i.e., without any heat treatment) by precipitation methods using the hydrolysis process. Electrolysis was used to manufacture aluminum nanoparticles. Welding process was existed to next door, but the door was closed for most of the working duration. Three UNP workplaces were investigated. UNP-G produced steel structures and heat exchangers by the arc and stainless steel welding were the major processes and a total of 100 workers performed welding. The major product of UNP-H was bodyframes for the back hoe and forklift. Welding and grinding were the main processes at UNP-I. A total of 30 workers were active. UNP-G manufactured automobile engine by smelting and welding. There was natural ventilation system and no LEV was installed at the all of UNP workplaces.

Sampling devices for correlation of SMPS, CPC and SAM

For the distribution of particle sizes, a portable (P)-SMPS (Nanoscan, Model 3910, TSI Inc., USA) with a detectable size range from 10 to 420 nm and a concentration range of 0 to 10^6 particles/cm^3 was utilized. The flow rate of inlet was 0.75 L/min and the flow rate for sample was 0.25 L/min. The sampling time of the P-SMPS was one minute per averaging time, and particle sizes from small to large were measured by 13 sequence channels. The cyclone was attached to get lid of the larger particles. The particles were collected from the inlet and passed through the aerosol neutralizer (unipolar charger). Particles were separated by the mobility diameter with a RDMA (radial differential mobility analyzer) before being counted using a CPC. A CPC (P-Trak Model 8525, TSI Inc., USA) was utilized to measure the number concentration of particles of 20 to 1,000-nm diameter with a 0.1 lpm sample flow rate. The measurable concentration range was 0–500,000 particles/cm^3. Isopropyl alcohol was used for particle condensation, which increases the particle size of optical detection available. A sampling averaging time was fixed as 1 min in this study. The zero calibration was operated by a HEPA filter before sampling. For measurement of the surface area concentration, a surface area monitor (SAM) (AeroTrak Model 9000, TSI Inc., USA) was employed. An averaging time was 1 min. The measurable particle size range was 10–1,000 nm and the aerosol concentration ranged from 1–10,000 μm^2 /cm^3 for alveolar deposition mode. Cyclone was set on the inlet to avoid into the SAM of particles larger than 1 μm. The flow rate of sample was 1.5 lpm. Zero calibration of the electrometer was operated before each sampling.

Sampling devices for comparison between two different (Grimm vs. TSI) SMPSs

Table 4-4 shows the parameters of the RG-SMPSs used for comparison at ENP-E. To investigate the distribution of particle sizes, two research-grade SMPSs were used. One is RG-SMPS (Model 3936L75, TSI Inc., Shoreview, MN, USA) with a measurable size range from 14.6 to 661 nm and a concentration range of $0–10^7$ particles/cm^3 was used. The sample flow rate was 0.3 l/min, and the sheath flow rate was 3 l/min for the sample. The sampling time of the SMPS was 135 s per averaging time, and it measured the particle size from small to large (up-scan) with 107 sequence channels. The particles were collected from the inlet and passed through the aerosol neutralizer (krypton-85). Particles were separated by mobility diameter using a differential mobility analyzer before being counted using a CPC. The other is RG-SMPS (5.403+C, Grimm GmbH, Germany) with the detectable size range from 11.1 to 1,083.3 nm with down-scan and a concentration range of $0–10^7$ particles/cm^3 was used. The sample flow rate was 0.3 l/min, and the sheath flow rate was 3 l/min. The sampling time of the SMPS was 213 s per averaging time, and it measured the particle size from large to small with 44 sequence channels. The particles were collected from the inlet and passed through the aerosol neutralizer (americium-241). TSI SMPS data were analyzed using Aerosol Instrument Manager (version 7) and Grimm used SMPS version 1.35.

Statistical analysis

Descriptive statistics was performed to show correlation of the concentration levels by measurement device. For comparison among devices (P-SMPS, CPC, and SAM) are analyzed by Pearson correlation. The correlation such as good to excellent relationship (> 0.75), moderate to good relationship (0.50 to 0.75), fair degree of relationship (0.25 to 0.50) and little or no relationship (0.0 to 0.25) were categorized (Reiman and Manske 2009). Pearson correlation coefficient was calculated to investigate the relationship between Grimm and TSI SMPSs. The one cycle of SMPS was different. SMPS data were organized into five-minute averages. Data for comparison between two RG-SMPS were used with Grimm (5.403+C) and TSI (Model 3936L75) and for comparison between devices with many metrics are used with TSI P-SMPS (Model 3910). Normalized concentration dN/dlogDp was used to compare aerosol size distributions taken of the same aerosol using instruments of different resolutions. Data analysis was conducted using SPSS (Version 20.0, IBM, USA).

Results

Table 4-1 summarizes the general characteristics of workplaces investigated based on the type of workplace, emitted or source of nanoparticles, ventilation type, processes or tasks, size of workplaces, number of workers, and other possible sources. Two LABs were dealing with metal and one LAB handled graphene. Three ENPs manufactured metal nanoparticles and one ENP manufactured fumed silica. All UNP workplaces performed welding, and UNP-J also undertook smelting processes.

All LABs had natural ventilation (NV) and a fume hood. For ENP workplaces, ENP-D had NV. Local exhaust ventilation (LEV) and isolated cabinets for facilities were installed at ENP-E. NV and LEV were installed at the ENP-F workplace. Only NV was installed at the ENP-G and UNP workplaces in this study.

There were two, seven, and five workers at the LAB workplaces. One to twelve workers were engaged at the ENP workplaces. One hundred, thirty, and three welders were employed at the UNP-G, UNP-H, and UNP-I workplaces, respectively. At the UNP-H workplace a total of 30 workers participated in two shifts, each of which comprised 15 workers.

Table 4-1. The general characteristics of workplaces

Workplace		Emitted / source of nanoparticles	Ventilation type	Task****	Production rate	Workplace Area (m^2)	No. of workers / NP handling workers	Sampling duration
LAB*	A	Al_2O_3	NV, Fume hood	Transferred to crucible, Transferred from crucible to vial, Weighing	-	120	2	One shift + One off-duty time
	B	Fe_2O_3, TiO_2	NV, Fume hood	Weighing, Sonication, Reaction	-	78	7	One shift + One off-duty time
	C	Graphene	NV, Fume hood	Spraying air using compressor, DIP-coater	-	90	5	One shift + One off-duty time
ENP**	D	TiO_2, ZnO	NV	Reaction, Dehydration, Mixing, Drying, Bagging, Lunch	TiO2: 10 ton/year ZnO: 50 ton/year	1,400	10	Two day shifts + One night shift
	E	Cu-Ni alloy, Ni	LEV and Isolation	Collecting, Sieving, Lunch	Ni: 100 kg/year Cu-Ni: 100 kg/year	97	6	One shift
	F	Fumed silica	LEV, NV	Packaging, Meal (Lunch, dinner), Break time, Night shift - No works, Outdoor, Warehouse	9,000 ton/year	3,500	12	Two day shifts + One night shift
UNP***	G	Welding (Arc, SUS)	NV	Arc Welding, SUS Welding, Break time, Lunch	-	Arc: 10,000 SUS: 820	100	Two day shifts
	H	Welding (Arc)	NV	Arc Welding, grinding (Day shift, Night shift), Lunch	-	2,017	30	Two day shifts + One night shift
	I	Smelting process, Welding (Arc)	NV	Smelting, Welding, Break time, Lunch	-	11,000	Smelting: 15/shift * 2 Welding: 3	Two day shifts + One night shift

* Laboratory; ** ENP: Engineered nanoparticle manufacturing workplace; *** UNP: Unintended nanoparticle-emitting workplace

**** Contextual information such as meal (lunch, dinner) time, break time, no working, outdoor, and warehouse are not tasks.

Correlation of many metric devices (SMPS, CPC, SAM)

Table 4-2 shows descriptive statistics of three type workplaces measured by SMPS, CPC and SAM. LAB showed the lowest concentration among three different types of workplaces and UNP workplaces showed the highest concentration for all metrics. Also, there were significant differences among three types of workplaces which were LAB, ENP and UNP (p<0.01). For conversion equations among SMPS, CPC, and SAM were listed at equation (1) to (6) and SMPS result less than equal to 100 nm (equation (7) to (12)).

- Comparison of SMPS and CPC/SAM from 10 nm to 420 nm (full range)

$y_{SMPS\_LAB} = 1.073\, x_{CPC\ LAB} + 1634$ ---------- equation (1)

$y_{SMPS\ ENP} = 1.482\, x_{CPC\ ENP} + 2274$ ---------- equation (2)

$y_{SMPS\ UNP} = 1.589\, x_{CPC\ UNP} + 45178$ ---------- equation (3)

$y_{SMPS\_LAB} = 113.176\, x_{SAM\ LAB} + 3241$ ---------- equation (4)

$y_{SMPS\ ENP} = 190.160\, x_{SAM\ ENP} + 3569$ ---------- equation (5)

$y_{SMPS\ UNP} = 170.526\, x_{SAM\ UNP} + 37721$---------- equation (6)

- Comparison of SMPS and CPC/SAM from 10 nm to 100 nm

$y_{SMPS\ 100\_LAB} = 0.769 x_{CPC\ LAB} + 1253$ ---------- equation (7)

$y_{SMPS\ 100\_ENP} = 1.263\, x_{CPC\ ENP} + 737$ ---------- equation (8)

$y_{SMPS\ 100\_\ UNP} = 1.230\, x_{CPC\ UNP} + 31429$ ---------- equation (9)

$y_{SMPS\ 100\_LAB} = 74.936\, x_{SAM\ LAB} + 2702$ ---------- equation (10)

$y_{SMPS\ \ 100\_ENP} = 149.740\, x_{SAM\ ENP} + 3762$ ---------- equation (11)

$y_{SMPS\ 100\_\ UNP} = 121.296\, x_{SAM\ UNP} + 34179$---------- equation (12)

Table 4-2. The descriptive statistics of three type workplaces and total measured by SMPS, CPC, and SAM

Workplace*	GM (GSD) [5th-95th percentile]				
	P-SMPS (particles/cm^3)			CPC (particles/cm^3)	SAM (μm^2/cm^3)
	Total number concentration	≤ 100 nm	> 100 nm		
LAB (A, B, C)	8,458 (1.41) [3,695-16,668]	5,879 (1.49) [2,600-13,328]	2,521 (1.30) [665-4,196]	6,143 (1.45) [3,613-16,209]	32.79 (1.46) [7.94-98.51]
ENP (D, E, F)	19,612 (2.18) [5,152-54,428]	14,969 (2.18) [3,047-43,294]	4,643 (2.00) [1,421-12,089]	11,955 (2.42) [3,575-58,153]	93.68 (2.60) [24.57-549.09]
UNP (G, H, I)	84,172 (2.80) [14,249-369,765]	61,167 (2.94) [10,667-315,822]	16,539 (3.23) [2059-91,790]	38,886 (2.61) [6,039-134,751]	358.41 (2.74) [61.37-1,514.03]

*p<0.01

Table 4-3 shows Pearson correlation among measurement devices. Correlation coefficients for LAB and ENP showed the good correlation among SMPS, CPC and SAM (p<0.001). On the other hand, correlation coefficients in UNP workplaces, fair correlation was found for SMPS, CPC and SAM than LAB and ENP (p<0.001).

Table 4-3. Pearson correlation coefficient among measurement devices

	LAB (N=1,631)					ENP (N=1,539)					UNP (N=3,027)					Total (N=6,377)				
	SMPS Total	**≤100**	**>100**	**CPC***	**SAM****	**SMPS Total**	**≤100**	**>100**	**CPC**	**SAM**	**SMPS Total**	**≤100**	**>100**	**CPC**	**SAM**	**SMPS Total**	**≤100**	**>100**	**CPC**	**SAM**
SMPS Total	1					1					1					1				
≤100	0.963	1				0.992	1				0.962	1				0.970	1			
>100	0.830	0.650	1			0.829	0.753	1			0.671	0.445	1			0.742	0.558	1		
CPC	**0.869**	0.823	0.750	1		**0.925**	0.905	0.823	1		**0.457**	0.427	0.349	1		**0.623**	0.585	0.517	1	
SAM	**0.883**	0.766	0.908	**0.889**	1	**0.857**	0.825	0.824	**0.834**	1	**0. 648**	0.525	0.705	**0.538**	1	**0.745**	0.644	0.770	**0.694**	1

* CPC data was missed for LAB-C

**SAM data was missed for ENP-D

All results of Pearson correlation coefficient were $p<0.001$.

Figure 4-1 shows the concentrations for number concentration measured by SMPS (black line), CPC (red line) and surface area concentration measured by SAM (blue line) in the workplaces (a) LAB-A, (b) ENP-F, and (c) UNP-H on the same graph to investigate responses. Figure 4-1 (a) and (b) shows the similar response. On the other hands, response in Figure 4-1 (c) shows relatively poor responses compared to Figure 4-1 (a) and (b).

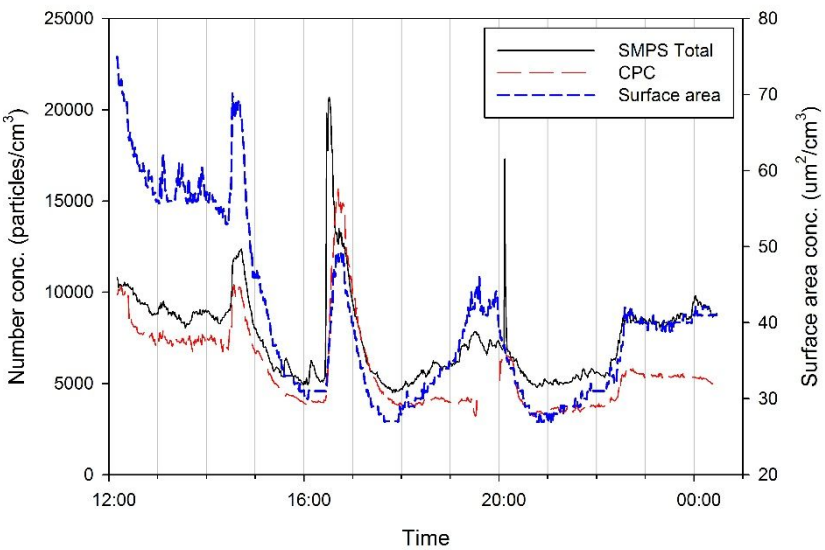

(a)

Figure 4-1. The concentration profiles measured by three sampling devices (SMPS, CPC, and SAM) at (a) LAB-A, (b) ENP-F, and (c) UNP-H (Continued).

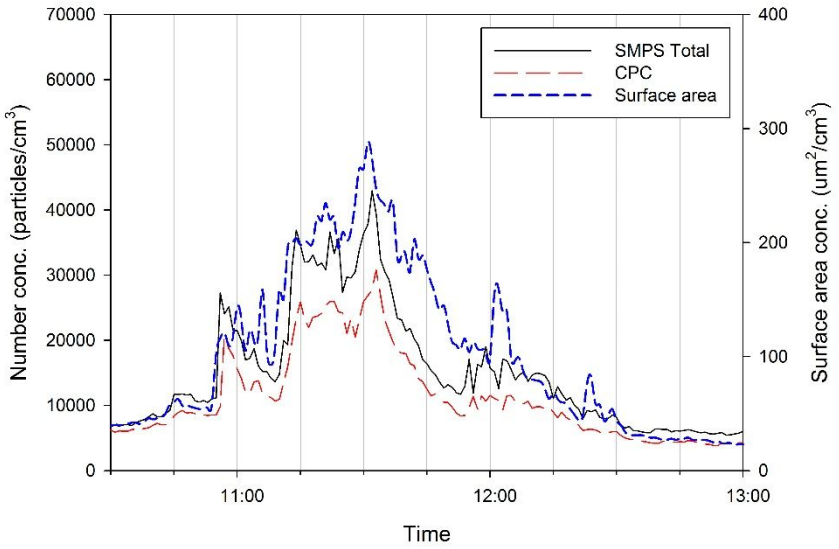

(b)

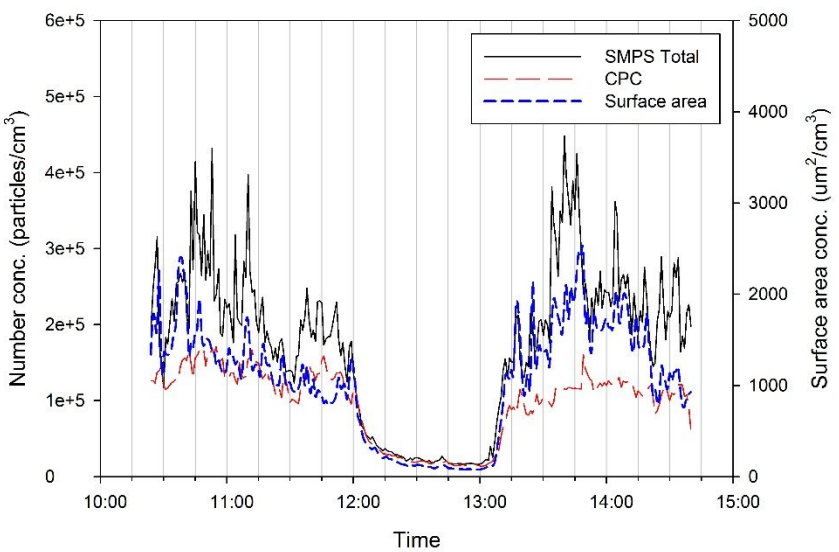

(c)

Figure 4-1. The concentration profiles measured by three sampling devices (SMPS, CPC, and SAM) at (a) LAB-A, (b) ENP-F, and (c) UNP-H.

Figure 4-2 shows the scanning electron microscopy (SEM) images magnified by 50,000 at (a) LAB-B, (b) ENP-E, (c) UNP-H. SEM images indicate that particles at LAB-C (Figure 4-2 (a)), ENP-E (Figure 4-2 (b)) with diameters of 50–60 nm and UNP (Figure 4-2 (c)) with diameters of 30–40 nm formed agglomerates/aggregates. Particles shape spherical at LAB-C and ENP-E. SEM image from UNP-H illustrates that the chain like form of particles (Figure 4-2 (c)).

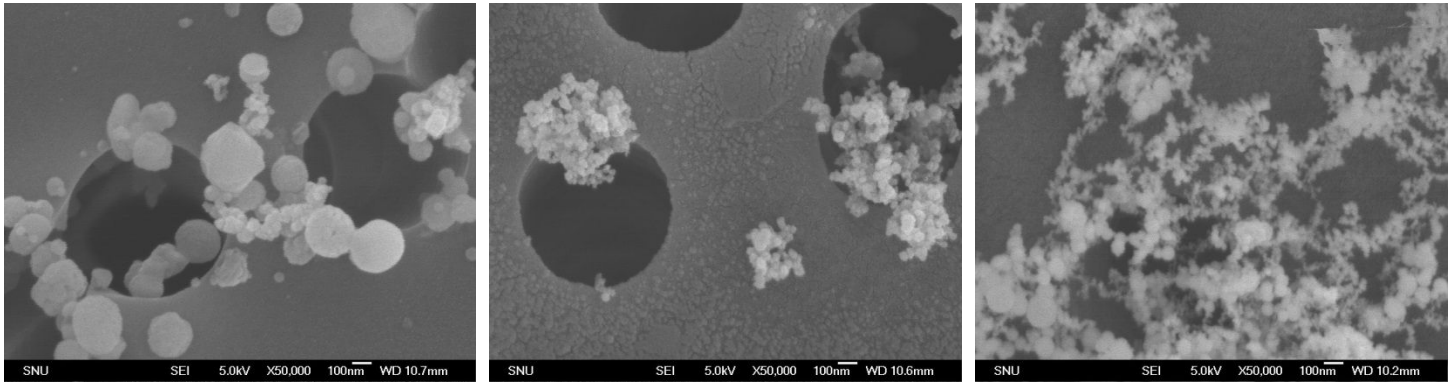

(a) (b) (c)

Figure 4-2. Scanning electron microscopy (SEM) images magnified by 50,000 at (a) LAB-C, (b) ENP-E, (c) UNP-H.

Comparison between two different (Grimm vs. TSI) SMPSs

Table 4-4 presents that specification of the SMPS that used to compare between two different SMPSs.

Table 4-4. Parameters of the SMPSs used for comparison at ENP-E

	Grimm-SMPS	**TSI-SMPS**
Model	5.403+C	3936L75
DMA	Vienna type (Larger to smaller) Long-DMA	TSI-3081
Scanning sequences	From larger particles to smaller particles	From smaller particles to larger particles
Neutralizer	AM^{241} (alpha emitter)	Kr^{85} (beta emitter)
Measurement range	11.1-1083.3 nm	14.6-661.1 nm
Aerosol sampling rate (L/min)	0.3	0.3
Sheath air flow rate (L/min)	3	3
Sampling interval	213 seconds	135 seconds
CPC type	Butanol based	Butanol based
CPC maximum concentration	10^7 particles/cm^3	10^7 particles/cm^3

Table 4-5 shows the descriptive statistics for comparison between Grimm and TSI SMPS at LAB-C, ENP-E and UNP-H. There were significant differences in total number concentration between SMPSs at LAB-C, ENP-E and UNP-H workplaces ($p<0.01$). Also, particle size of SMPS less than or equal to 100 nm and greater than 100 nm results show the significant differences ($p<0.01$).

Table 4-5. Nanoparticle concentrations measured by Grimm and TSI SMPS at ENP-E (unit: dN/dlogDp [particles/cm^3])

		Grimm SMPS			TSI SMPS		
		Total	**≤ 100 nm**	**> 100 nm**	**Total**	**≤ 100 nm**	**> 100 nm**
ENP-E (N=232)	Mean	122,429*	91,389*	31,040*	147,031	104,317	42,713
	SD	2,359	1,834	631	2,637	1,898	1,018
	Median	125,462	96,036	28,418	145,627	107,767	39,617
	Percentile [5th - 95th]	62,134-173,921	42,422-131,046	18,625-46,620	87,221-204,526	59,393-145,322	25,758-61,954

* $p<0.01$

Figure 4-3 shows correlation graph and coefficient values between Grimm and TSI SMPS by size ranges for number concentration at ENP-E. Figure 4-3 (a) shows the correlation during whole sampling time. Figure 4-3 (b) and (c) shows the relationship between Grimm SMPS and TSI SMPS for working time and background which has no working activities. The results of correlation analysis at ENP-E shows good relation between SMPSs for total concentration, greater than 100 nm, and less than or equal to 100 nm (ρ=0.791, 0.848, and 0.455; p<0.001, respectively). During working time, correlation coefficients were 0.791, 0.848, and 0.455, respectively (p<0.001). Background measurement data show the good to excellent correlation between two SMPS (ρ=0.916, 0.899, and 0.944; p<0.001, respectively).

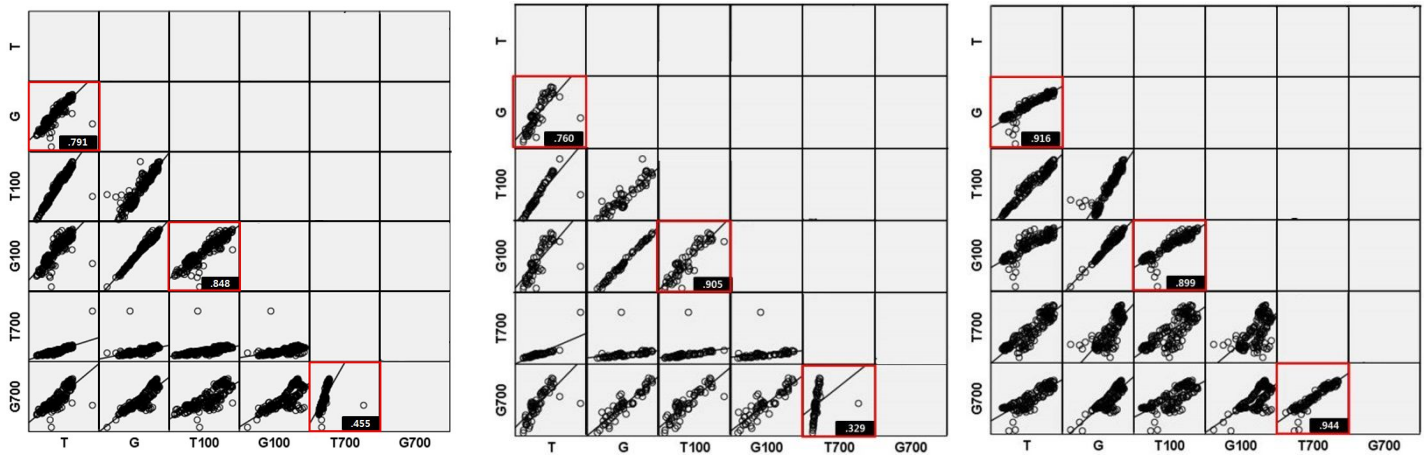

(a) (b) (c)

Figure 4-3. Correlation graph and coefficient values between TSI and Grimm SMPS by size ranges for number concentration at ENP-E (a) Total (b) Working and (c) Background.

Figure 4-4 shows size distributions for particles from workplaces, measured with the two different SMPSs in the test with same location at ENP-E. The results of TSI SMPS shows higher number concentration than Grimm SMPS.

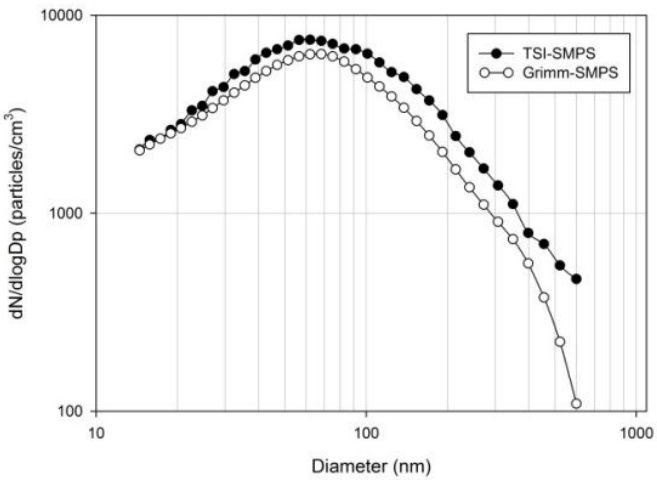

Figure 4-4. Size distributions for particles measured with the two different SMPSs in the test with same sampling location ENP-E.

Discussions

This study investigated two different objectives. The first objective was to performed comparison analysis for multi metric measurement devices such as SMPS (number concentration), CPC (number concentration) and SAM (surface area concentration). The concentration of nanoparticles at workplaces categorized by three different types of workplaces to examine relation of concentration based on real-time data. For the second objective, the relationship between two SMPSs were compared. This is the first challenge to compare two common SMPSs at workplaces which were real field.

Correlation among SMPS, CPC, and SAM

The RG-SMPS is the golden standard measurement devices for nanoparticle measurement because it could collect the number concentration in size distribution with many channels with high accuracy. But the research-grade SMPS is expensive and needs the longer time resolutions for one cycle to measure rapidly changing of exposure (Fierz *et al.,* 2009). P-SMPS that used in this study is one of verified measurement device with one minute sampling cycle (Tritscher *et al.,* 2013). Compare to the RG-SMPS, the number of channel of P-SMPS is smaller but it is portable and but expensive than CPC or SAM. Therefore, the alternative measurement device is necessary to use as a surrogate for nanoparticle exposure assessment.

Pearson correlation analysis was performed to measure relation of exposure profile

during sampling among three measurement devices (P-SMPS, CPC, and SAM). In the result of LAB and ENP showed the good correlation among P-SMPS, CPC and SAM (Table 4-3). The responses of P-SMPS, CPC and SAM were similar at LAB and ENP because of the particle shape which is similar to spherical in Figure 4-1 (a) and (b). On the other hand, correlation in UNP workplaces, lower correlation was found for P-SMPS, CPC and SAM. The responses of P-SMPS, CPC and SAM were similar during lunch time but had large variances during working time. It might be assumed that particles during lunch time were not from processes which is from outside of UNP workplace. P-SMPSs were usually calibrated by the manufactures only for spherical particles (Kinney and Pui 1991; Mulholland *et al.,* 2006) as well as CPC and SAM. However, the shape of particles in real world is not spherical as seen in Figure 4-2. Particles from UNP-H showed the chain like form of particles (Figure 4-2 (c)). It may occur errors in the results. Electron microscope image could useful to figure out the characteristics of nanoparticles at workplaces (Ham *et al.,* 2012).

Using equations (1) to (12), variations in the relationships of the P-SMPS with the CPC and SAM in the different workplaces were investigated. The intercept values were higher at ENP and UNP workplaces than LAB. Degree of increment for concentration was higher at ENP and UNP workplaces for P-SMPS versus CPC and SAM. It was difficult to verify the exact evidences of variations. The variations might be caused by the different measurement ranges of the sampling devices, as well as their response times and operating principles. The measurement range of the SMPS was to 10–420 nm with

13 channels. The CPC and SAM had measurement ranges of 20–1,000 nm and 10–1,000 nm, respectively. The measurement ranges among the devices overlapped but were not exactly matched. The response times were different. One cycle of P-SMPS was fixed at 1 minute (45 seconds of sampling and 15 seconds of retrace time), whereas the The CPC and SAM had flexible cycles ranging from 1 second to 1 minute. The principles of operation of both devices differed from those of the (P)-SMPS.

There are advantages and disadvantages of devices. Compare to the SAM, CPC is light weight to use portably (CPC: 1.7 kg and SAM: 8.2 kg with 2 battery packs). CPC is required to consume Isopropyl alcohol (IPA) inside the instrument and refill regularly. However, it is difficult to use in hot or warm conditions such as UNP workplaces (welding, smelting etc.) because the rate of consumption is very rapid. On the other hand, SAM is very robust to the hot and warm conditions but, it is difficult to compare with P-SMPS number concentration directly. P-SMPS consumes IPA for condensation but there is cooling fan inside the instrument and extension bottle is available to exhaust heat from condensation heater. Therefore, the instrument check should be done with shout term when temperature is over 35 °C for all measurement devices.

Comparison between two different (Grimm vs. TSI) SMPSs

In this study, Grimm SMPS showed lower concentration than TSI SMPS. However, Grimm SMPS showed higher concentration than TSI SMPS in other comparison studies (Asbach *et al.,* 2009; Watson *et al.,* 2011). Asbach *et al.,* (2009), in their study on laboratory comparisons with NaCl aerosols, obtained a factor of 1.42-1.7 with Grimm

SMPS showing higher number concentrations. Sodium chloride (NaCl), ammonium sulphate were tested in the laboratory and ambient exposure (Joshi *et al.,* 2012). They reported results from Grimm SMPS were found to be a factor of 1.25 higher than TSI SMPS at ambient air. In this study, size distributions were similar (Figure 4-3) but there are significant differences in concentrations (Table 4-5). There might be the cause of systemic errors between SMPSs.

Differences between SMPSs may be related to differences in particle charging efficiency due to the neutralized charge distribution (Am, Kr), diffusion loss, CPC responses, DMA transfer function (Joshi *et al.,* 2012; Watson *et al.,* 2011; Wiedensohler *et al.,* 2012), effect of aerosol flow changes and insufficient neutralization on the differences between SMPS (Liu and Deshler 2003). In this study, correlation coefficients were higher during background which was no working at ENP-E (Figure 4-2). During working time, variations of nanoparticle emission are fluctuating. Instabilities in the aerosol are likely to cause of uncertainties in the particle number concentration and sizing (Wiedensohler *et al.,* 2012). For background measurement during no working at workplaces, results showed very good relationship between two SMPS even there are significant differences in concentration because air might be stable (Figure 4-2 (c)). However, during working time, fair relationship was investigated due the fluctuation of aerosol.

Also, sampling time is different between SMPS. The sampling intervals for Grimm SMPS are 213 seconds for one cycle, and TSI SMPS is 135 second. It might lose the

emissions of nanoparticles during certain tasks because the task might be short duration. The other source of differences in the principle is transfer to DMA between SMPSs (Wiedensohler *et al.,* 2012). They have a different technique to separate particles size. Grimm SMPS measures large particles to small particles (down-scan) in size and TSI SMPS measures small particles to large particles (up-scan) because the electrical polarity of rod voltage in the DMA is positive (+) for Grimm and opposite polarity (-) for TSI DMA rod.

Data gathered by real time monitor are highly correlated. This problem can be overcome using the concordance correlation coefficient (CCC) (Lawrence and Lin 1989). CCC could measures the agreement between two variables with same metric for highly correlated data such as two different blood pressure measurement devices for same person. Despite these limitations, this study may provide an understanding of nanoparticle sources, both engineered and unintended, because only limited data are currently available concerning nanoparticle exposure assessments in the workplace even though the number of workers handling nanoparticles continues to increase.

Conclusions

This is the first study that compared measurement devices, specialized on nanoparticles in the workplace. Two parts were performed: 1) investigation of correlation among P-SMPS, CPC, and SAM which are widely using nanoparticle measurement devices and 2) comparison between two commercial SMPSs to assess the comparability in an engineered nanoparticle manufacturing workplace.

There are good relationship among P-SMPS, CPC and SAM at LAB and ENP workplaces. However, fair relationship was investigated at UNP workplaces. Therefore, CPC and SAM with electron microscope image may be the good alternative instruments for nanoparticle exposure assessment instead of SMPS which is relatively expensive instrument.

There are significant differences between two different widely using SMPSs. Caution would be necessary and interpretation with understand to compare the exposure monitoring data gathered from real-field such as workplaces when using different SMPSs.

Chapter 5. Summary

Nanotechnology is developing rapidly and the number of people working with this technology is increasing. Reliable exposure assessment data are important in the field of industrial hygiene to effectively protect the health of workers. The development of new methods for assessing nanoparticle exposure is necessary because nanoparticles behave differently to larger particles. The purpose of this study was to investigate the appropriate methods for nanoparticle assessment in the workplace. This is the first study to compare nanoparticle exposure by workplace type; a task-based approach was applied in the analysis of field data using ARIMA and a comparison of nanoparticle sampling devices using data collected at the workplace. The study contributes to the development of effective methods to assess nanoparticle exposure.

First, a comparison of the concentration and characteristics of nanoparticles at three different types of workplace was performed. UNP workplaces showed the highest concentration for all measured metrics. The nanoparticle concentration at LAB workplaces was lower than those at other workplaces. Certain tasks at LAB workplaces showed higher concentrations than at ENP or UNP workplaces, even for a short exposure time. The LEV system could be appropriate for reducing exposure to nanoparticles at ENP workplaces. The characteristics of exposure differed among LAB, ENP and UNP workplaces; hence, different control strategies are necessary.

Second, a nanoparticle exposure assessment utilizing task-based sampling was performed. Real-time measuring devices, gravimetric sampling analysis, and an electron microscope were utilized to assess four workplaces (two ENPs and two UNPs). The nanoparticle concentrations varied depending on the tasks performed and working status (working or off-duty). The results indicated differences in the concentration profiles between the ENP and UNP (welding) workplaces. Thus, task-based exposure assessments can provide useful information regarding nanoparticle exposure profiles and could be used as nanoparticle exposure assessment tools.

Third, three statistical methods were used to analyze real-time monitoring data that were highly autocorrelated. Classical regression was inappropriate for the time-series data due to the effects of autocorrelation. To use the AR(1) model, the data should be stationary. Thus, the ARIMA model was most suitable for the analysis of real-time monitored data because it accounts for autocorrelation and the stationary nature of the data. Using the ARIMA model, averaging times of 1, 5, and 10 minutes gave almost identical results. Flexible time averaging is suggested because it can be used with a research-grade sampling device, which in this study was a full-size SMPS that had a sampling interval longer than one minute. An averaging time with flexible time interval allows a series of tasks to be determined, and the time selected should be determined by the investigator or industrial hygienist.

Finally, an investigation of correlations among the SMPS, CPC, and SAM, which are widely used nanoparticle sampling devices, and a comparison between two commercial SMPS to assess performance in the workplace, were performed. There was a high correlation among the SMPS, CPC and SAM at LAB and ENP workplaces. However, only a moderate correlation was found at the UNP workplaces. Therefore, the CPC and SAM are suitable alternative instruments for nanoparticle exposure assessment, rather than the SMPS, which is a relatively expensive and heavy instrument. There were significant differences between the two SMPSs, which are widely used devices. Therefore, caution is required when interpreting the results and comparing exposure monitoring field data using different SMPSs.

References

Afshari, A., U. Matson and L. E. Ekberg (2005). "Characterization of indoor sources of fine and ultrafine particles: A study conducted in a full-scale chamber." *Indoor Air* 15(2): 141-150.

Antonini, J. M., S. Stone, J. R. Roberts, B. Chen, D. Schwegler-Berry*, et al.* (2007). "Effect of short-term stainless steel welding fume inhalation exposure on lung inflammation, injury, and defense responses in rats." *Toxicology and Applied Pharmacology* 223(3): 234-245.

Asbach, C., H. Kaminski, H. Fissan, C. Monz, D. Dahmann*, et al.* (2009). "Comparison of four mobility particle sizers with different time resolution for stationary exposure measurements." *Journal of Nanoparticle Research* 11(7): 1593-1609.

Asbach, C., H. Kaminski, D. Von barany, T. A. J. Kuhlbusch, C. Monz*, et al.* (2012). "Comparability of portable nanoparticle exposure monitors." *Annals of Occupational Hygiene* 56(5): 606-621.

Asbach, C., T. Kuhlbusch, H. Kaminski, B. Stahlmecke, S. Plitzko*, et al.* (2012). Standard operation procedures: For assessing exposure to nanomaterials, following a tiered approach, NanoGEM. **7708:** 1006-1015.

Ashby, H. S. (2002). "Welding fume in the workplace." *Professional Safety* 47(4): 55-63.

Baveye, P. and M. Laba (2008). "Aggregation and toxicology of titanium dioxide nanoparticles." *Environ Health Perspect* 116(4): A152.

Bello, D., B. Wardle, N. Yamamoto, R. Guzman deVilloria, E. Garcia*, et al.* (2009). "Exposure to nanoscale particles and fibers during machining of hybrid advanced composites containing carbon nanotubes." *Journal of Nanoparticle Research* 11(1): 231-249.

Beurskens-Comuth, P. A. W. V., K. Verbist and D. Brouwer (2011). "Video exposure monitoring as part of a strategy to assess exposure to nanoparticles." *Annals of Occupational Hygiene* 55(8): 937-945.

Box, G. E. and G. M. Jenkins (1976). Time series analysis, control, and forecasting, San Francisco, CA: Holden Day.

Brouwer, D., M. Berges, M. A. Virji, W. Fransman, D. Bello*, et al.* (2012). "Harmonization of measurement strategies for exposure to manufactured nano-objects; report of a workshop." *Annals of Occupational Hygiene* 56(1): 1-9.

Brouwer, D., B. van Duuren-Stuurman, M. Berges, E. Jankowska, D. Bard, *et al.* (2009). "From workplace air measurement results toward estimates of exposure? Development of a strategy to assess exposure to manufactured nano-objects." *Journal of Nanoparticle Research* 11(8): 1867-1881.

Brouwer, D. H. (2012). "Control banding approaches for nanomaterials." *Annals of Occupational Hygiene* 56(5): 506-514.

Brouwer, D. H., B. van Duuren-Stuurman, M. Berges, D. Bard, E. Jankowska, *et al.* (2013). "Workplace air measurements and likelihood of exposure to manufactured nano-objects, agglomerates, and aggregates." *Journal of Nanoparticle Research* 15(11): 1-14.

BSI (2007). Nanotechnologies–part 2: Guide to safe handling and disposal of manufactured nanomaterials. PD 6699-2, British Standards Institution.

Buonanno, G., L. Morawska and L. Stabile (2011). "Exposure to welding particles in automotive plants." *Journal of Aerosol Science* 42(5): 295-304.

Cena, L. G. and T. M. Peters (2011). "Characterization and control of airborne particles emitted during production of epoxy/carbon nanotube nanocomposites." *Journal of Occupational and Environmental Hygiene* 8(2): 86-92.

Chung, G. (1990). De morbis artificum diatriba, Dongmyungsa.

Cowpertwait, P. S. P., Metcalfe, A V. (2009). Introductory time series with r, Springer.

Dasch, J. and J. D'Arcy (2008). "Physical and chemical characterization of airborne particles from welding operations in automotive plants." *Journal of Occupational and Environmental Hygiene* 5(7): 444-454.

Debia, M., S. Weichenthal, R. Tardif and A. Dufresne (2012). "Ultrafine particle (ufp) exposures in an aluminium smelter: Soderberg vs. Prebake potrooms." *Environment and Pollution* 1(1): p2.

Demou, E., P. Peter and S. Hellweg (2008). "Exposure to manufactured nanostructured particles in an industrial pilot plant." *Annals of Occupational Hygiene* 52(8): 695-706.

Demou, E., W. J. Stark and S. Hellweg (2009). "Particle emission and exposure during nanoparticle synthesis in research laboratories." *Annals of Occupational Hygiene* 53(8): 829-838.

Donaldson, K., L. Tran, L. A. Jimenez, R. Duffin, D. E. Newby, *et al.* (2005). "Combustion-derived nanoparticles: A review of their toxicology following inhalation exposure." *Particle and Fibre Toxicology* 2(1): 10.

Ellenbecker, M. and S. Tsai (2008). "Interim best practices for working with nanoparticles." *Center for High-Rate Nanomanufacturing*.
Fierz, M., S. Weimer and H. Burtscher (2009). "Design and performance of an optimized electrical diffusion battery." *Journal of Aerosol Science* 40(2): 152-163.
Fox, J. and S. Weisberg (2011). An r companion to applied regression, Sage.
Fuller, C. H., D. Brugge, P. L. Williams, M. A. Mittleman, J. L. Durant*, et al.* (2012). "Estimation of ultrafine particle concentrations at near-highway residences using data from local and central monitors." *Atmospheric Environment* 57: 257-265.
Gomez, V., M. Levin, A. T. Saber, S. Irusta, M. Dal Maso*, et al.* (2014). "Comparison of dust release from epoxy and paint nanocomposites and conventional products during sanding and sawing." *Annals of Occupational Hygiene*.
Halperin, W. E. (1996). "The role of surveillance in the hierarchy of prevention." *American journal of industrial medicine* 29(4): 321-323.
Ham, S., C. Yoon, E. Lee, K. Lee, D. Park*, et al.* (2012). "Task-based exposure assessment of nanoparticles in the workplace." *Journal of Nanoparticle Research* 14(9): 1-17.
Heitbrink, W. A., D. E. Evans, B. K. Ku, A. D. Maynard, T. J. Slavin*, et al.* (2008). "Relationships among particle number, surface area, and respirable mass concentrations in automotive engine manufacturing." *Journal of Occupational and Environmental Hygiene* 6(1): 19-31.
Heitbrink, W. A., D. E. Evans, B. K. Ku, A. D. Maynard, T. J. Slavin*, et al.* (2009). "Relationships among particle number, surface area, and respirable mass concentrations in automotive engine manufacturing." *Journal of Occupational and Environmental Hygiene* 6(1): 19-31.
Honnert, B. and M. Grzebyk (2013). "Manufactured nano-objects: An occupational survey in five industries in france." *Annals of Occupational Hygiene* 58(1): 121-135.
Hothorn, T., A. Zeileis and M. A. Zeileis. (2014). "Package 'lmtest'." Retrieved 30 Sep 2014, from http://cran.r-project.org/web/packages/lmtest/lmtest.pdf.
Houseman, E. A., L. Ryan, J. I. Levy and J. D. Spengler (2002). "Autocorrelation in real-time continuous monitoring of microenvironments." *Journal of Applied Statistics* 29(6): 855-872.
Hyndman, R. J. (2013). "Package 'forecast'." Retrieved 30 Sep 2014, from http://cran.r-project.org/web/packages/forecast/forecast.pdf.

Hyndman, R. J. and Y. Khandakar (2008). "Automatic time series for forecasting: The forecast package for r." *Journal of Statistical Software* 27(3).

IFA. (2009). "Criteria for assessment of the effectiveness of protective measures." Retrieved 18 July, 2012, from http://www.dguv.de/ifa/en/fac/nanopartikel/beurteilungsmassstaebe/index.jsp.

IRSST (2009). Best practices guide to synthetic nanoparticle risk management, Institut de recherche Robert-Sauvé en santé et en sécurité du travail.

ISO (2008). "27687." *Nanotechnologies–Terminology and definitions for nano-objects–Nanoparticle, nanofiber and nanoplate*.

Joshi, M., B. Sapra, A. Khan, S. Tripathi, P. Shamjad, *et al.* (2012). "Harmonisation of nanoparticle concentration measurements using grimm and tsi scanning mobility particle sizers." *Journal of Nanoparticle Research* 14(12): 1-14.

Kaminski, H., M. Beyer, H. Fissan, C. Asbach and T. A. Kuhlbusch (2014). "Measurements of nanoscale tio2 and al2o3 in industrial workplace environments–methodology and results."

Kinney, P. D. and D. Y. Pui (1991). "Use of the elecftrostatic classification method to 0.1 tm srm particles-a feasibiiiy study." *Journal of Research of the National Institute of Standards and Technology* 96(2).

Klein Entink, R., W. Fransman and D. Brouwer (2011). "How to statistically analyze nano exposure measurement results: Using an arima time series approach." *Journal of Nanoparticle Research* 13(12): 6991-7004.

Kuhlbusch, T., C. Asbach, H. Fissan, D. Gohler and M. Stintz (2011). "Nanoparticle exposure at nanotechnology workplaces: A review." *Particle and Fibre Toxicology* 8(1): 22.

Kwiatkowski, D., P. C. B. Phillips, P. Schmidt and Y. Shin (1992). "Testing the null hypothesis of stationarity against the alternative of a unit root: How sure are we that economic time series have a unit root?" *Journal of Econometrics* 54(1–3): 159-178.

Lawrence, I. and K. Lin (1989). "A concordance correlation coefficient to evaluate reproducibility." *Biometrics*: 255-268.

Lee, J. H., M. Kwon and J. H. Ji (2011). "Exposure assessment of workplaces manufacturing nanosized tio2 and silver." *Inhalation Toxicology* 23(4): 226-237.

Lee, M.-H., W. McClellan, J. Candela, D. Andrews and P. Biswas (2007). "Reduction of nanoparticle exposure to welding aerosols by modification of the ventilation system in a workplace." *Journal of Nanoparticle Research* 9(1): 127-136.

Lehnert, M., B. Pesch, A. Lotz, J. Pelzer, B. Kendzia*, et al.* (2012). "Exposure to inhalable, respirable, and ultrafine particles in welding fume." *Annals of Occupational Hygiene* 56(5): 557-567.

Levy, J. I., T. Dumyahn and J. D. Spengler (2002). "Particulate matter and polycyclic aromatic hydrocarbon concentrations in indoor and outdoor microenvironments in boston, massachusetts." *J Expo Anal Environ Epidemiol* 12(2): 104-114.

Lin, M., H. C. Lucas Jr and G. Shmueli (2013). "Research commentary-too big to fail: Large samples and the p-value problem." *Information Systems Research* 24(4): 906-917.

Liu, P. S. and T. Deshler (2003). "Causes of concentration differences between a scanning mobility particle sizer and a condensation particle counter." *Aerosol Science & Technology* 37(11): 916-923.

Maynard, A. D. and R. J. Aitken (2007). "Assessing exposure to airborne nanomaterials: Current abilities and future requirements." *Nanotoxicology* 1(1): 26-41.

McGarry, P., L. Morawska, L. D. Knibbs and H. Morris (2013). "Excursion guidance criteria to guide control of peak emission and exposure to airborne engineered particles." *Journal of Occupational and Environmental Hygiene* 10(11): 640-651.

Meeker, J. D., P. Susi and M. R. Flynn (2007). "Manganese and welding fume exposure and control in construction." *Journal of Occupational and Environmental Hygiene* 4(12): 943-951.

Methner, M., C. Beaucham, C. Crawford, L. Hodson and C. Geraci (2012). "Field application of the nanoparticle emission assessment technique (neat): Task-based air monitoring during the processing of engineered nanomaterials (enm) at four facilities." *Journal of Occupational and Environmental Hygiene* 9(9): 543-555.

Methner, M., L. Hodson, A. Dames and C. Geraci (2010). "Nanoparticle emission assessment technique (neat) for the identification and measurement of potential inhalation exposure to engineered nanomaterials—part b: Results from 12 field studies." *Journal of Occupational and Environmental Hygiene* 7(3): 163-176.

Methner, M., L. Hodson and C. Geraci (2009). "Nanoparticle emission assessment technique (neat) for the identification and measurement of potential inhalation exposure to engineered nanomaterials — part a." *Journal of Occupational and Environmental Hygiene* 7(3): 127-132.

Mulholland, G. W., M. K. Donnelly, C. R. Hagwood, S. R. Kukuck, V. A. Hackley*, et al.* (2006). "Measurement of 100 nm and 60 nm particle standards by differential mobility analysis." *Journal of Research-National Institute of Standards and Technology* 111(4): 257.

Neitzel, R., W. Daniell, L. Sheppard, H. Davies and N. Seixas (2011). "Evaluation and comparison of three exposure assessment techniques." *Journal of Occupational and Environmental Hygiene* 8(5): 310-323.

Neubauer, N., M. Seipenbusch and G. Kasper (2013). "Functionality based detection of airborne engineered nanoparticles in quasi real time: A new type of detector and a new metric." *Annals of Occupational Hygiene* 57(7): 842-852.

NIOSH (2009) Approaches to safe nanotechnology

Oberdörster, G. (2010). "Safety assessment for nanotechnology and nanomedicine: Concepts of nanotoxicology." *Journal of Internal Medicine* 267(1): 89-105.

Oberdörster, G., J. Ferin and B. Lehnert (1994). "Correlation between particle size, in vivo particle persistence, and lung injury." *Environ Health Perspect* 102: 173-179.

Oberdörster, G., E. Oberdörster and J. Oberdörster (2005). "Nanotoxicology: An emerging discipline evolving from studies of ultrafine particles." *Environmental Health Perspectives* 113(7): 823-839.

Oberdörster, G., E. Oberdörster and J. Oberdörster (2007). "Concepts of nanoparticle dose metric and response metric." *Environmental Health Perspectives* 115(6): A290-A290.

Olanow, C. W. (2004). "Manganese-induced parkinsonism and parkinson's disease." *Annals of the New York Academy of Sciences* 1012(1): 209-223.

Ono-Ogasawara, M., F. Serita and M. Takaya (2009). "Distinguishing nanomaterial particles from background airborne particulate matter for quantitative exposure assessment." *Journal of Nanoparticle Research* 11(7): 1651-1659.

Osborne, J. and E. Waters (2002). "Four assumptions of multiple regression that researchers should always test." *Practical assessment, research & evaluation* 8(2): 1-9.

Ott, W., P. Switzer and N. Willits (1994). "Carbon monoxide exposures inside an automobile traveling on an urban arterial highway." *Air & waste* 44(8): 1012-1018.

Ozaki, T. (1977). "On the order determination of arima models." *Journal of the Royal Statistical Society. Series C (Applied Statistics)* 26(3): 290-301.

Paik, S. Y., D. M. Zalk and P. Swuste (2008). "Application of a pilot control banding tool for risk level assessment and control of nanoparticle exposures." *Annals of Occupational Hygiene* 52(6): 419-428.

Park, J. Y., G. Ramachandran, P. C. Raynor and G. M. Olson (2010). "Determination of particle concentration rankings by spatial mapping of particle surface area, number, and mass concentrations in a restaurant and a die casting plant." *Journal of Occupational and Environmental Hygiene* 7(8): 466-476.

Park, J. Y., P. C. Raynor, A. D. Maynard, L. E. Eberly and G. Ramachandran (2009). "Comparison of two estimation methods for surface area concentration using number concentration and mass concentration of combustion-related ultrafine particles." *Atmospheric Environment* 43(3): 502-509.

Peters, T. M., S. Elzey, R. Johnson, H. Park, V. H. Grassian*, et al.* (2008). "Airborne monitoring to distinguish engineered nanomaterials from incidental particles for environmental health and safety." *Journal of Occupational and Environmental Hygiene* 6(2): 73-81.

Peters, T. M., W. A. Heitbrink, D. E. Evans, T. J. Slavin and A. D. Maynard (2006). "The mapping of fine and ultrafine particle concentrations in an engine machining and assembly facility." *Annals of Occupational Hygiene* 50(3): 249-257.

Pfefferkorn, F. E., D. Bello, G. Haddad, J.-Y. Park, M. Powell*, et al.* (2010). "Characterization of exposures to airborne nanoscale particles during friction stir welding of aluminum." *Annals of Occupational Hygiene* 54(5): 486-503.

Pinheiro, J., D. Bates and R. Maintainer. (2013). "Package 'nlme'." Retrieved 30 Sep 2014, from http://cran.r-project.org/web/packages/nlme/nlme.pdf.

Plitzko, S. (2009). "Workplace exposure to engineered nanoparticles." *Inhalation Toxicology* 21(s1): 25-29.

Ramachandran, G., M. Ostraat, D. E. Evans, M. M. Methner, P. O'Shaughnessy*, et al.* (2011). "A strategy for assessing workplace exposures to nanomaterials." *Journal of Occupational and Environmental Hygiene* 8(11): 673-685.

Reiman, M. P. and R. C. Manske (2009). Functional testing in human performance, Human kinetics.
Søyseth, V., H. L. Johnsen and J. Kongerud (2013). "Respiratory hazards of metal smelting." *Current Opinion in Pulmonary Medicine* 19(2): 158-162.
Schmoll, L. H., T. M. Peters and P. T. O'Shaughnessy (2010). "Use of a condensation particle counter and an optical particle counter to assess the number concentration of engineered nanoparticles." *Journal of Occupational and Environmental Hygiene* 7(9): 535-545.
Schulte, P., C. Geraci, R. Zumwalde, M. Hoover and E. Kuempel (2008). "Occupational risk management of engineered nanoparticles." *Journal of Occupational and Environmental Hygiene* 5(4): 239-249.
Schulte, P., V. Murashov, R. Zumwalde, E. Kuempel and C. Geraci (2010). "Occupational exposure limits for nanomaterials: State of the art." *Journal of Nanoparticle Research* 12(6): 1971-1987.
Seixas, N. S., L. Sheppard and R. Neitzel (2003). "Comparison of task-based estimates with full-shift measurements of noise exposure." *AIHA Journal* 64(6): 823-829.
Tritscher, T., M. Beeston, A. F. Zerrath, S. Elzey, T. J. Krinke*, et al.* (2013). "Nanoscan smps–a novel, portable nanoparticle sizing and counting instrument." *Journal of Physics: Conference Series* 429(1): 012061.
Tsai, C.-J., C.-Y. Huang, S.-C. Chen, C.-E. Ho, C.-H. Huang*, et al.* (2011). "Exposure assessment of nano-sized and respirable particles at different workplaces." *Journal of Nanoparticle Research*: 1-12.
Tsai, C.-J., C.-Y. Huang, S.-C. Chen, C.-E. Ho, C.-H. Huang*, et al.* (2011). "Exposure assessment of nano-sized and respirable particles at different workplaces." *Journal of Nanoparticle Research* 13(9): 4161-4172.
Tsai, C. S.-J., D. White, H. Rodriguez, C. E. Munoz, C.-Y. Huang*, et al.* (2012). "Exposure assessment and engineering control strategies for airborne nanoparticles: An application to emissions from nanocomposite compounding processes." *Journal of Nanoparticle Research* 14(7): 1-14.
Tsai, S.-J., E. Ada, J. Isaacs and M. Ellenbecker (2009). "Airborne nanoparticle exposures associated with the manual handling of nanoalumina and nanosilver in fume hoods." *Journal of Nanoparticle Research* 11(1): 147-161.
Tsai, S.-J., R. F. Huang and M. J. Ellenbecker (2010). "Airborne nanoparticle exposures while using constant-flow, constant-velocity, and air-curtain-isolated fume hoods." *Annals of Occupational Hygiene* 54(1): 78-87.

Van Broekhuizen, P., W. Van Veelen, W.-H. Streekstra, P. Schulte and L. Reijnders (2012). "Exposure limits for nanoparticles: Report of an international workshop on nano reference values." *Annals of Occupational Hygiene* 56(5): 515-524.

Van Duuren-Stuurman, B., S. R. Vink, K. J. Verbist, H. G. Heussen, D. H. Brouwer*, et al.* (2012). "Stoffenmanager nano version 1.0: A web-based tool for risk prioritization of airborne manufactured nano objects." *Annals of Occupational Hygiene* 56(5): 525-541.

Virji, M. A., S. R. Woskie and L. D. Pepper (2008). "Task-based lead exposures and work site characteristics of bridge surface preparation and painting contractors." *Journal of Occupational and Environmental Hygiene* 6(2): 99-112.

Virji, M. A., S. R. Woskie, M. Waters, S. Brueck, D. Stancescu*, et al.* (2009). "Agreement between task-based estimates of the full-shift noise exposure and the full-shift noise dosimetry." *Annals of Occupational Hygiene* 53(3): 201-214.

Watson, J. G., J. C. Chow, D. A. Sodeman, D. H. Lowenthal, M.-C. O. Chang*, et al.* (2011). "Comparison of four scanning mobility particle sizers at the fresno supersite." *Particuology* 9(3): 204-209.

Wiedensohler, A., W. Birmili, A. Nowak, A. Sonntag, K. Weinhold*, et al.* (2012). "Mobility particle size spectrometers: Harmonization of technical standards and data structure to facilitate high quality long-term observations of atmospheric particle number size distributions." *Atmospheric Measurement Techniques* 5: 657-685.

Wittmaack, K. (2007). "In search of the most relevant parameter for quantifying lung inflammatory response to nanoparticle exposure: Particle number, surface area, or what?" *Environmental Health Perspectives* 115(2): 187-194.

Yoon, C. S., N. W. Paik and J. H. Kim (2003). "Fume generation and content of total chromium and hexavalent chromium in flux-cored arc welding." *Annals of Occupational Hygiene* 47(8): 671-680.

Zhang, M., L. Jian, P. Bin, M. Xing, J. Lou*, et al.* (2013). "Workplace exposure to nanoparticles from gas metal arc welding process." *Journal of Nanoparticle Research* 15(11): 1-14.

Zimmer, A. T. (2002). "The influence of metallurgy on the formation of welding aerosols." *Journal of Environmental Monitoring* 4(5): 628-632.

Zimmer, A. T., P. A. Baron and P. Biswas (2002). "The influence of operating parameters on number-weighted aerosol size distribution generated from a gas metal arc welding process." *Journal of Aerosol Science* 33(3): 519-531.

Zimmer, A. T. and P. Biswas (2001). "Characterization of the aerosols resulting from arc welding processes." *Journal of Aerosol Science* 32(8): 993-1008.

Zwack, L. M., C. J. Paciorek, J. D. Spengler and J. I. Levy (2011). "Modeling spatial patterns of traffic-related air pollutants in complex urban terrain." *Environmental Health Perspectives* 119(6): 852-859.

Appendix

Table S 2-1. Descriptive statistics for concentrations of tasks/events at Workplace J, K, L, and M (Chapter 2)

Tasks/Event	GM (GSD)
1-ENP-J-Accidental Spillage of TiO2	882,014 (1.32)
2-ENP-J-Moving of the TiO2 powder	1,246,607 (1.06)
3-ENP-J-Mixing of liquid TiO2	1,401,831 (1.13)
4-ENP-J-Al nanoparticle grinding	1,525,918 (1.11)
5-ENP-J-Liquid TiO2 pouring into tank	1,711,732 (1.24)
6-ENP-J-Tobacco Smoking	2,181,460 (1.10)
7-ENP-K-Sieving under the LEV	80,596 (1.20)
8-ENP-K-Mixing of nanoparticles in fume hood	68,297 (1.10)
9-ENP-K-Opening the door to collect manufactured nanoparticles	156,809 (1.20)
10-UNP-L-Welding	6,555,739 (1.46)
11-UNP-L-Meal time	1,146,594 (1.73)
12-UNP-L-Break time	2,793,726 (1.60)
13-UNP-M-Welding	251,459 (2.63)
14-UNP-M-Meal time	78,357 (1.39)
15-UNP-M-Break time	88,604 (1.26)

국문 초록

작업장에서의 나노입자 노출평가의 새로운 방법 개발

나노기술(Nanotechnology: NT) 개발은 우리나라의 전략기술산업이며, 세계 NT 4대 강국 중 하나이다. 기하급수적으로 NT산업이 발전하고 있고, 국내에서 나노물질의 생산량 및 사용량이 증가하고 있기 때문에 근로자의 노출 현황 파악, 노출평가에 대한 연구가 필요하다. 나노입자는 크기가 작아짐에 따라 다른 특성을 보이기 때문에 다양한 형태로 만들어 사용하고 있고, 그에 따라 독성이 달라질 수 있음이 보고되고 있다. 그럼에도 불구하고 우리나라에서 나노입자를 생산, 취급, 사용하는 사업장에서 근로자에게 얼마나 어떻게 노출되는지 노출 모니터링 및 평가, 분석방법 그리고 취급근로자들의 노출감소(작업장 관리방법)에 대한 연구가 매우 미비한 실정이다. 따라서 본 연구에서는 사업장 규모에 따른 노출 특성, 사업장 측정에 있어서 작업기반 노출평가방법, 실시간 나노입자 측정기를 이용한 분석방법 그리고 측정 기기간 상관성에 대하여 연구하였다.

근로자가 나노입자에 노출될 수 있는 사업장은 다양하다. 실험실, 제조사

업장, 비의도적 발생 등 다양한 상황에서의 노출이 가능하다. 상황이 다양한 만큼, 노출특성도 다르기 때문에 이에 대한 규명이 필요하다. 따라서 본 연구에서는 각 3개 형태 (실험실, 나노입자제조 사업장, 비의도 나노입자 발생 사업장)으로 나누어, 각 형태별 3개 사업장을 측정하였다. 총 9개의 사업장에서 나노입자 측정을 하였고, 특성을 평가 하였다. 비의도 나노입자 발생사업장이 모든 측정 단위에서 가장 높은 농도를 보였다. 실험실에서 가장 낮은 농도를 보였다. 그러나 실험실에서 나노입자의 분포를 보면 특정 작업에서는 짧은 시간 동안 이지만 나노입자제조 사업장이나 비의도 나노입자 발생 사업장 보다 높은 농도를 보이기도 하였다. 국소배기장치가 나노입자제조 사업장에서는 농도를 낮추는 효과가 있어 근로자 노출저감에 도움이 될 것이라고 생각한다. 따라서 본 연구에서는 실험실, 나노입자제조 사업장, 비의도 나노입자 발생 사업장의 노출 농도나 특성이 다름을 밝혀 내었고, 사업장 특성에 따라 각기 다른 노출 저감 전략을 세워야 한다고 제안한다.

기존에는 입자상물질 측정 시 필터에 포집을 하는 시간가중평균농도(질량농도)를 사용하여 사업장을 평가 하였다. 기존의 산업은 작업의 특성이 근로자가 특정 작업을 일정시간 동안 지속적으로 해왔으나, 나노입자의 제조의 경우 공정이 지속적이지 않고 간헐적으로 있는 경우가 많아 기존의 방법인 시간가중평균농도를 사용하게 되면 과소평가의 가능성이 있다. 또한 질량농도를 사용할 경우 무게가 너무 적어 중량농도 측정이 어렵기 때문에 제대로 된 평가가 어렵다. 따라서 본 연구에서는 시간에 따른 변이를 관찰 할

수 없다는 점을 보완하고자 실시간 측정기기를 이용하여 시간의 따른 변이를 관찰 하였다. 총 4 개의 사업장 (나노입자제조 사업장 2 개, 비의도 나노입자 발생 사업장 2 개)에 대하여 측정을 하였고 작업기반 (Task-based) 노출평가를 실시하였다. 나노입자의 농도는 작업별로 변이가 있었고, 작업상태 (작업중, 작업이 없을 때)에 따라 달라짐을 알 수 있었다. 또한 나노입자제조 사업장, 비의도 나노입자 발생 사업장간에도 특성이 다름을 알 수 있었다. 따라서 작업기반 노출평가 방법은 나노입자 노출평가에 있어서 유용한 측정방법임을 알 수 있었고, 나노입자 노출평가에는 실시간 나노입자 측정기기와 작업기반 노출평가를 실시해야 한다고 제안한다.

나노입자는 실시간 측정기기를 사용하여 측정을 한다. 측정간격이 매우 짧아 측정된 데이터간에 자기상관성 (Autocorrelation)이 매우 강해서 t-test나 회귀분석 등의 통계분석을 실시할 경우 과소평가를 하는 문제가 있다. 자기상관성을 고려하는 방법은 두 가지 이며, 자기상관성을 고려한 통계적 처리 방법과 측정된 데이터의 평균을 길게 하여 분석하는 방법이 있다. 기존의 방법인 회귀분석과 자기상관성을 고려한 통계적 처리방법 2가지 (AR(1): First order Autoegressive, ARIMA: autoregressive integrated moving average 모델)을 이용하여 높은 자기상관성이 있는 실시간 나노입자 측정 자료를 비교, 평가 하였다. 기존에 사용되던 회귀분석은 자기상관성이 매우 높아 결과에 있어서 과소평가를 하기 때문에 적합하지 않음을 알 수 있었다. AR(1) model은 자기상관성을 고려하여 분석이 가능하고, 자료가 안정적 (stationary)일 때 사용이 가능하다. 하지만, 사업장에서의 자료는 농도의 변이가 크기 때문에 안정적이지 못하다

는 점을 발견하였다. 따라서, 자기상관성을 고려하고, 안정적이지 않은 자료가 많은 사업장에서의 실시간 나노입자 측정 자료에는 ARIMA 모델이 가장 적합하다고 제안을 한다. 평균시간을 길게 하는 방법에서는 실시간 측정기기를 사용하여 생성된 1분간격의 자료를 1분, 5분, 10분으로 평균을 내어 비교하였다. 결과에 있어서는 차이가 없었으나 평균시간을 길게 할수록 자기상관성은 줄어듦을 알 수 있었다. 본 연구에서 사용한 SMPS는 측정간격이 1분이었지만 대부분의 SMPS의 경우 1분 이상의 측정간격을 가지고 있고, 각 기기마다 다른 측정간격을 가지고 있다. 시간을 길게 하면 자기상관성은 줄어 들지만, 그 사이에 있던 노출을 희석시킨다는 점이 있어 과소평가의 가능성이 있기 때문에 평균시간을 산업위생 전문가의 판단에 의해 조정하여 사용하는 것을 제안한다.

나노입자 노출평가에는 연구자 마다 다양한 측정기기가 사용된다. 각기 다른 원리로 다양한 제조회사에서 만들기 때문에 같은 단위의 측정 결과일지라도 각 측정기기의 관계에 대한 연구가 필요하다. SMPS (Scanning mobility particle sizer)는 공기 중 나노입자의 분포를 측정하는데 주로 사용되는 실시간 나노입자 측정기기이다. 연구용 SMPS 는 무겁고 가격이 매우 비싸기 때문에 현장에서 사용이 가능한 휴대용 (portable (P)-) SMPS 가 개발되어 사용되고 있다. 그러나 휴대용 SMPS 도 아직 무겁고 가격이 높기 때문에 이를 대신 할

수 있는 기기의 제안이 필요하다. 또한 SMPS 간에도 원리, 결과의 차이가 있어 이들간의 상관관계의 규명이 필요하다. 다양한 측정단위 기기 간 (P-SMPS, CPC, SAM) 상관성 비교 연구에서는 각 3 개 형태 (실험실, 나노입자제조 사업장, 비의도 나노입자 발생 사업장)으로 나누어, 각 형태별 3 개 사업장을 측정하였다. 총 9 개의 사업장에서 나노입자 측정을 하였고, 상관성을 평가 하였다. SMPS 간의 비교 연구에서는 ENP-E 사업장에 대하여 평가 하였다.

실험실과 나노입자제조 사업장에서는 P-SMPS, CPC, SAM 간의 상관성에 매우 좋았다. 반면에 비의도적 나노입자 발생사업장의 경우에는 비교적 낮은 상관성을 보였다. 그 이유로는 입자의 형태가 체인형태 (Chain like form)으로 이루어져 있어서 구형으로 보정을 하는 실시간 측정기기와 상관성이 잘 맞지 않았을 것으로 판단된다. 따라서 실험실과 나노입자제조 사업장에서는 기기의 특성을 잘 이해하여 사용한다면, 무겁고 비싼 P-SMPS 를 대신하여 CPC, SAM 을 사용할 수도 있다고 제안한다. 제조사가 다른 두개의 SMPS 의 비교연구결과 TSI SMPS 가 Grimm SMPS 에 비하여 약 20% 높은 농도를 보임을 알 수 있었다. 그 이유는 사업장 공기중 나노입자의 변이에 따른 차이, 측정기기의 원리, 측정간격, 입자중성화장치의 상이 등을 들 수 있다. 따라서 이와 같은 기기의 특성을 잘 파악하고 사용을 해야 한다.

결론적으로 본 연구에서는 실험실, 나노입자제조 사업장, 비의도 나노입자 발생 사업장의 노출 농도나 특성이 다름을 밝혀 내었고, 사업장 특성에 따라 각기 다른 노출 저감 전략을 세우고, 나노입자 노출평가에는 실시간 나노입자 측정기기와 작업기반 노출평가를 실시해야 하며, 실시간 측정기기 사용시 자기상관성을 고려하고, 안정적이지 않은 자료가 많은 사업장에서는 ARIMA 모델이 가장 적합하며, 측정간격에 대한 평균시간을 산업위생 전문가의 판단에 의해 조정하여 사용하는 것을 제안한다. 또한 실험실과 나노입자제조 사업장에서는 기기의 특성을 잘 이해하여 사용한다면 무겁고 비싼 P-SMPS를 대신하여 CPC, SAM을 사용할 수 있고, TSI SMPS가 Grimm SMPS에 비하여 약 20% 높은 농도를 보이기 때문에 자료를 해석 시에 이러한 부분을 고려하여 노출평가 자료를 해석해야 한다.

주요어: 공학적 나노입자, 나노입자 노출평가, 비의도적, 산업보건, SMPS, 자기상관성

학번: 2010-30681